UNIVERSIDADE DE BRASÍLIA
PROGRAMA DE PÓS-GRADUAÇÃO EM PATOLOGIA MOLECULAR

ATIVIDADES ANTIBACTERIANA E ANTIBIOFILME DE DOIS PEPTÍDEOS HELICOIDAIS: *PA*-MAP 1.9 E ECDBS1R5

Autor: Marlon Henrique e Silva Cardoso

Orientador: Prof. Dr. Octávio Luiz Franco

Brasília – DF

Março de 2019

UNIVERSIDADE DE BRASÍLIA
PROGRAMA DE PÓS-GRADUAÇÃO EM PATOLOGIA MOLECULAR

ATIVIDADES ANTIBACTERIANA E ANTIBIOFILME DE DOIS PEPTÍDEOS HELICOIDAIS: *PA*-MAP 1.9 E ECDBS1R5

Autor: Marlon Henrique e Silva Cardoso

Orientador: Prof. Dr. Octávio Luiz Franco

Tese apresentada como requisito para a obtenção do Título de Doutor em Patologia Molecular pelo Programa de Pós-Graduação em Patologia Molecular - Universidade de Brasília.

Área de Concentração: Bioquímica/Biofísica

Brasília – DF

Março de 2019

“Que as palavras que falo não sejam ouvidas como prece

nem repetidas com fervor. Apenas respeitadas.”

Oswaldo Montenegro

Dedico este trabalho ao(a) meu(minha) filho(a), Dan/Hinata, por representar o que há de mais importante em minha vida, sendo meu motivo diário de motivação pessoal e profissional.

AGRADECIMENTOS

À minha companheira que escolhi para a vida, Dra. Elizabete Cândido, por todo o amor prestado, pela imensa compreensão mesmo nos momentos mais difíceis e, acima de tudo, por estar carregando o fruto do nosso relacionamento, nosso(a) filho(a) Dan/Hinata;

Ao meu orientador, Prof. Dr. Octávio Luiz Franco, por ser meu maior exemplo de pesquisador, por seu dinamismo e oportunidades que tem me oferecido ao longo dos anos. Conte sempre comigo;

Aos meus orientadores do Institute for Molecular Bioscience (IMB) na Austrália, Dra. Lai (Angeline) Chan e Dr. David J. Craik, por terem me acolhido em seu laboratório, pelos ensinamentos e, principalmente, por terem comprado minhas ideias de forma prestativa e humilde;

Às minhas filhas de quatro patas, Luna, Frida, Amora e Sunny, por serem parte essencial de nossas vidas e por tornarem mais leve a rotina diária;

À meu pai, Paulo Henrique, por todo o suporte emocional e financeiro, sempre compreendendo minhas escolhas e sendo meu porto seguro;

Aos meus avós, Dora e José, por serem, sem dúvidas, aqueles que mais estiveram presentes em todas as fases da minha vida e por quem tenho imenso afeto;

As minhas tias, Magda e Adriana, as quais foram minhas mães de criação, sempre me dando suporte no que fosse necessário;

Aos meus primos, Gabriel e Júlia, com os quais cresci e espero poder continuar acompanhando seu desenvolvimento;

À pessoa mais guerreira que já conheci até então, minha irmã, Laís Marina, meu exemplo de conquista e perseverança;

À minha mãe, Edna Maria, e minha vó, Nina, por todo o carinho maternal;

À meu amigo e colaborador, Dr. Nelson Gomes, por ter sido aquele que inicialmente apostou no meu potencial, me oferecendo oportunidades enquanto pesquisador, e a quem devo grande parte de meu conhecimento;

Às alunas de iniciação científica, mestrado e doutorado que tenho o orgulho de coorientar, MSc. Karen Oshiro, BSc. Samilla Rezende, MSc. Beatriz Meneguetti, MSc. Gislaine de Oliveira e BSc. Raquel Orozco, por todo o esforço e, principalmente, por depositarem sua confiança em mim enquanto pesquisador;

Às amizades que, felizmente, surgiram em minha vida, MSc. Karen Oshiro, MSc. Esther Carvalho, MSc. Sílvia Gomes, BSc. Elizangela Barros e BSc. Samilla Rezende;

À banca avaliadora, a qual é composta por pesquisadores que fizeram grande diferença na minha vida profissional ao longo da minha iniciação científica e doutorado;

À todos os integrantes do S-Inova Biotech, CAPB e IMB;

Aos meus colaboradores, Dr. César de la Fuente-Núñez, Dr. Marcelo Torres, Dr. Nuno Santos, MSc. Mário Felício, Dra. Sónia Gonçalves e Dr. Luciano Lião por todo o auxilio para que eu pudesse finalizar meus projetos;

À CAPES, CNPq, UnB, UCDB, UCB e FAP-DF por todo o suporte financeiro.

RESUMO

Os peptídeos antimicrobianos (PAMs) vêm sendo amplamente investigados, representando uma estratégia promissora no combate a células planctônicas e biofilmes bacterianos multirresistentes. Assim, o presente trabalho teve como objetivo a caracterização funcional e estrutural de dois PAMs helicoidais com potencial antibacteriano, antibiofilme e anti-infeccioso, denominados *Pa*-MAP 1.9 e EcDBS1R5. Inicialmente, foi observado que ambos os peptídeos de estudo apresentam atividades contra cepas Gram-negativas e Gram-positivas, susceptíveis e resistentes, sem causar hemólise ou comprometer a viabilidade de linhagens celulares saudáveis proveniente de mamíferos. Em adição, o peptídeo *Pa*-MAP 1.9 demonstrou atividade deletéria contra biofilmes a baixas concentrações (1,1-3,0 μM), resultando não somente na inibição da formação de biofilmes, como também na erradicação de biofilmes pré-formados por *E. coli* e *Klebsiella pneumoniae* KpC+. A atividade antibiofilme para EcDBS1R5 foi também confirmada, uma vez que este peptídeo reduziu o volume e altura de biofilmes de *P. aeruginosa* pré-formados, comprometendo também a viabilidade de células bacterianas nos biofilmes. Ademais, o potencial anti-infeccioso de EcDBS1R5 foi avaliado, resultando em uma redução de 100 vezes na carga de *P. aeruginosa* em infecções cutâneas. Ensaios *in vivo* com o peptídeo *Pa*-MAP 1.9 ainda estão em andamento. Em contrapartida, o mecanismo de ação de *Pa*-MAP 1.9 frente a cepas de *E. coli* foi aqui investigado, sugerindo sua atuação em alvos intracelulares. Além disso, estudos biofísicos mostram que *Pa*-MAP 1.9 foi mais eficiente na interação com vesículas e membranas aniônicas (bactérias Gram-negativas), em comparação àquelas enriquecidas com colesterol (células de mamíferos). Estruturalmente, ambos os peptídeos foram submetidos a experimentos de dicroísmo circular (DC), revelando a presença de altos conteúdos de α-hélice em ambientes hidrofóbicos e aniônicos, contrário à conformações em *random coil* observadas em ambientes aquosos. As estruturas tridimensionais desses peptídeos foram detalhadamente estudadas e corroboram os dados de DC, reforçando a preferência conformacional em α-hélice anfipática com regiões terminais flexíveis tanto para *Pa*-MAP 1.9 quanto para EcDBS1R5 em ambientes que mimetizam membranas bacterianas. Dessa forma, os PAMs helicoidais aqui estudados se mostram promissores candidatos no desenvolvimento de novas ferramentas biotecnológicas contra infecções causadas por células platônicas e biofilmes bacterianos.

Palavras chave: Peptídeos antimicrobianos; Desenho racional; Biofilmes; Biofísica estrutural.

ABSTRACT

Antimicrobial peptides (AMPs) have been largely investigated, representing a promising strategy in the combat of multidrug resistant planktonic bacteria and biofilms. Thus, the present study focused on the functional and structural characterization of two helical AMPs with antibacterial, antibiofilm and anti-infective potential, denominated *Pa*-MAP 1.9 and EcDBS1R5. Initially, it was observed that both peptides present activities against Gram-negative and Gram-positive, susceptible and resistant strains, without causing hemolysis or compromising healthy mammalian cell lines viability. Moreover, the peptide *Pa*-MAP 1.9 demonstrated deleterious activities against biofilms at low concentrations (1.1-3.0 μM), resulting not only in the inhibition of biofilm formation, but also in the eradication of *E. coli* and *K. pneumoniae* KpC+ pre-formed biofilms. The antibiofilm activity for EcDBS1R5 was also confirmed, as this peptide decreased both the volume and height of pre-formed *P. aeruginosa* biofilms, also compromising the viability of bacterial cells within biofilms. Moreover, the anti-infective potential of EcDBS1R5 was evaluated, reducing 100-times *P. aeruginosa* counts in cutaneous infections. *In vivo* assays for *Pa*-MAP 1.9 are in progress. In contrast, the mechanism of action of *Pa*-MAP 1.9 toward *E. coli* was here investigated, suggesting its action on intracellular targets. Moreover, biophysical studies showed that *Pa*-MAP 1.9 was more efficient in interacting with anionic vesicles and membranes (Gram-negative bacteria), in comparison to those enriched with cholesterol (mammalian cells). Structurally, both peptides were submitted to circular dichroism (CD) experiments, revealing the presence of high α-helical contents in hydrophobic and anionic environments, in contrary to random coil conformations observed in hydrophilic environment. The tridimensional structures of these peptides were studied in detail and corroborate the CD data, reinforcing the conformational preference in amphipathic α-helix with flexible termini for both *Pa*-MAP 1.9 and EcDBS1R5 in environments that mimic bacterial membranes. Thus, the helical AMPs here studied appear as promising candidates in the development of biotechnological tools against infections caused by bacterial planktonic cells and biofilms.

Keywords: Antimicrobial peptides; Rational design; Biofilms; Structural biophysics.

LISTA DE ILUSTRAÇÕES

Figura 1. Esquema demonstrando alguns dos mecanismos de resistência bacteriana a antibióticos mais comumente relatados em cepas Gram-negativas, incluindo a atuação de β-lactamases na hidrólise do anel β-lactâmico de antibióticos, superexpressão de bombas de efluxo, redução na expressão de porinas, modificação do alvo por meio de mutações em genes específicos, bem como modificações nas propriedades físico-químicas da superfície celular. Figura do autor.....15

Figura 2. Desenvolvimento de biofilmes bacterianos destacando os estágios de adesão, crescimento séssil, maturação e dispersão. Figura do autor. 19

Figura 3. Distribuição de 135 PAMs depositados no Antimicrobial Peptides Database (APD) (http://aps.unmc.edu/AP/main.php) de acordo com seus ângulos de torsão *phi* e *psi*. Todas as estruturas foram resolvidas por ressonância magnética nuclear. Adaptado de Fjell *et al.* (2011).....22

Figura 4. Mecanismos de ação propostos para PAMs com potencial antibiofilme, incluindo a regulação de genes envolvidos na comunicação e motilidade celular, desestabilização da membrana de bactérias que constituem os biofilmes, dispersão de biofilmes por meio da interação com a matriz extracelular e, por fim, interação/degradação de guanosina 5' – difosfato 3' – difosfato (ppGpp). PAM: peptídeos antimicrobianos; QS: quorum sensing. 25

Figura 5. Diagramas de hélice para *Pa*-MAP (A) e *Pa*-MAP 1.9 (B). O vetor de momento hidrofóbico está representado por setas a partir do centro dos diagramas, enquanto que o valor estimado do momento hidrofóbico resultante é proporcional ao tamanho das setas.....32

Figura 6. Diagramas de hélice para o fragmento de MerP utilizado como peptídeo parental (A) e EcDBS1R5 (B). O vetor de momento hidrofóbico está representado por setas a partir do centro dos diagramas, enquanto que o valor estimado do momento hidrofóbico resultante é proporcional ao tamanho das setas. 35

LISTA DE TABELAS

Tabela 1. Sequência de aminoácidos, carga, hidrofobicidade e momento hidrofóbicos para os peptídeos de primeira e segunda geração derivados de *Pleuronectes americanus*..... 33
Tabela 2. Sequência de aminoácidos carga, hidrofobicidade e momento hidrofóbico para os peptídeos desenhados por meio do algoritmo Joker e derivados do fragmento de MerP..... 35

LISTA DE ABREVIATURAS

ESKAPE – ***E****nterococcus faecium*, ***S****taphylococcus aureus*, ***K****lebsiella pneumoniae*, ***A****cinetobacter baumannii*, ***P****seudomonas aeruginosa* e ***E****nterobacter spp.*

OMS – Organização Mundial da Saúde

MRSA – *Staphylococcus aureus* resistente a meticilina

SccMec – cassete cromossômico estafilocócico mec (do inglês *staphylococcal cassette chromosome mec*)

ABC – Transportadores de cassetes de ligação de ATP (do inglês *adenosine triphosphate (ATP)-binding cassette (ABC) transporters*)

ATP – adenosina trifosfato

MFS – Superfamília dos facilitadores principais

SMR – Família de baixa resistência a múltiplos fármacos

RND – Família resistência-nodulação-divisão

MATE – Família de extrusão de múltiplos fármacos e compostos tóxicos

NDM – Nova Dehli metalo-β-lactamase

QS – *Quorum-sensing*

CIM – Concentração inibitória mínima

EPS – Substâncias extracelulares poliméricas

PAM – Peptídeos antimicrobianos

ppGpp - guanosina 5'- difosfato 3'- difosfato

HTS – Prospecção de alto desempenho (do inglês *high-throughput screening*)

SVM – Máquina de vetores de suporte

ANN – Rede neural artificial

DA – Análise discriminante

RF – Floresta randômica (do inglês *random forest*)

QSAR – Relação quantitativa estrutura-atividade (do inglês *Quantitative Structure- Activity Relationship*)

DC – Dicroísmo circular

SDS – Dodecil sulfato de sódio

DPC – dodecilfosfocolina

LPG – lisofosfatidilglicerol

RMN – Ressonância magnética nuclear

POPC – 1-palmitoil-2-oleoil-sn-glicero-3-fosfocolina

APD – *Antimicrobial peptide database*

NCBI – *National Center for Biotechnology Information*

TFE – 2,2,2-trifluoroetanol

DPPC – dipalmitoilfosfatidilcolina

DPPG – dipalmitoilfosfatidilglicerol

DPPE – dipalmitoil-3-fosfatidil-etanolamina

KpC – *K. pneumoniae* produtoras de carbapenemase

LPS – lipopolissacarídeo

SUMÁRIO

1. INTRODUÇÃO 14
1.1. Resistência bacteriana 14
1.2. Biofilmes bacterianos 18
1.3. Peptídeos antimicrobianos (PAMs) 21
1.4. PAMs com potencial antibiofilme 23
1.5. Estratégias de desenho de PAMs 27
1.6. O peptídeos polialanina *Pa*-MAP 1.9 30
1.7. O peptídeo desenhado computacionalmente EcDBS1R5 34
2. JUSTIFICATIVA 37
3. OBJETIVOS 38
3.1. Objetivos específicos 38
4. ARTIGO CIENTÍFICO PUBLICADO NA SCIENTIFIC REPORTS 40
5. ARTIGO CIENTÍFICO PUBLICADO NA AMERICAN CHEMICAL SOCIETY (ACS) INFECTIOUS DISEASES 55
6. DISCUSSÃO GERAL 68
7. CONCLUSÕES 78
8. PERSPECTIVAS 78
9. ANEXOS 80
10. REFERÊNCIA BIBLIOGRÁFICAS 103

1. INTRODUÇÃO

1.1. Resistência bacteriana

Nas últimas décadas, o investimento na prevenção e tratamento de doenças infecciosas causadas por bactérias patogênicas por meio do desenvolvimento de novos antibióticos têm influenciado, significativamente, no aumento da qualidade e expectativa de vida da população (Afacan *et al.*, 2012; Marcone *et al.*, 2018). Contudo, mesmo levando-se em consideração seu saldo positivo na saúde pública, o uso indiscriminado dessa classe de fármacos tem gerado grande alarme visto os crescentes adventos de resistência, intrínseca ou adquirida, a partir da seleção positiva de patógenos multirresistentes (Ventola, 2015). Bactérias patogênicas pertencentes ao grupo "ESKAPE" (acrônimo para "habilidade de escapar"), incluindo ***E****nterococcus faecium*, ***S****taphylococcus aureus*, ***K****lebsiella pneumoniae*, ***A****cinetobacter baumannii*, ***P****seudomonas aeruginosa* e ***E****nterobacter spp.* estão associadas aos maiores índices de infecções multirresistentes em ambiente hospitalar, resultando em altas taxas de mortalidade, especialmente, em pacientes imunossuprimidos (Smith *et al.*, 2018).

Em termos globais, tem sido estimado que ~700 mil mortes sejam atribuídas a infecções por bactérias resistentes anualmente (Jee *et al.*, 2018). Do ponto de vista econômico, foi projetado um impacto de U$100 trilhões de dólares até 2050 (Jee *et al.*, 2018). Recentemente (2017), a Organização Mundial da Saúde (OMS) publicou uma lista global de bactérias resistentes a antibióticos, na qual *Acinetobacter baumannii* e *P. aeruginosa*, assim como cepas da família Enterobactereaceae resistentes a cefalosporina e antibióticos carbapenêmicos foram classificadas como prioridade crítica; enquanto cepas de *S. aure*us resistentes a meticilina (MRSA) foram classificadas como prioridade alta/crítica (WHO, 2017). Infecções bacterianas causadas por essas cepas podem persistir no hospedeiro por longos períodos de tempo devido a imunossupressão, evasão do patógeno ao sistema imune e/ou ação pouco eficaz do antibiótico administrado (Fisher *et al.*, 2017).

Dentre os mecanismos de resistência mais comumente relatados podem ser citados a ação direta de β-lactamases, bem como a modificação de enzimas bacterianas para a inativação de diversas classes de antibióticos como as cefalosporinas, penicilina, aminoglicosidades, gentamicina e estreptomicina (Levy e Marshall, 2004). Além disso, estudos têm mostrado mecanismos relacionados às vias pelas quais os antibióticos são transportados, incluindo a ação seletiva de porinas, o bloqueio da penetração do fármaco,

como também a atuação de bombas de efluxo (Levy, 1992; Llarrull *et al.*, 2010). Ademais, a existência de regiões multirresistentes compostas de elementos móveis como integrons e transposons tem sido relatada em cepas bacterianas, os quais, uma vez combinados, podem contribuir ativamente para eventos de resistência (Osborn e Boltner, 2002; Wellington *et al.*, 2013). Por fim, estudos mostram ainda que a formação de biofilmes aumenta as barreiras físicas e químicas aos antibióticos (Drenkard e Ausubel, 2002).

A modificação de antibióticos mediada pela ação de enzimas bacterianas está diretamente relacionada a eventos de resistência a antibióticos (Jacoby e Munoz-Price, 2005). De fato, a atuação dessas enzimas, como por exemplo as β-lactamases (Figura 1), tem mostrado sua relevância desde o uso dos primeiros antibióticos, com o descobrimento da penicilinase em meados de 1940 (Abraham e Chain, 1988). Desde então, centenas de β-lactamases vêm sendo identificadas e caracterizadas, sendo em sua maioria codificadas por genes localizados em plasmídeos e transposons, bem como em regiões cromossomais e, assim, proporcionando resistência intrínseca (Alekshun e Levy, 2007). De maneira geral, as β-lactamases são divididas em enzimas contendo um resíduo de serina em seu sítio ativo (serino-β-lactamases, incluindo as classes A, C e D) e aquelas que necessitam de íons metálicos como cofatores (membros da classe B) (Jacoby e Munoz-Price, 2005). Interessantemente, estudos vem mostrando que as primeiras β-lactamases descobertas, as quais eram efetivas na hidrólise de β-lactâmicos de primeira geração, foram sucedidas por β-lactamases com amplo espectro de atividade (Blair *et al.*, 2015). Dessa forma, bactérias Gram-negativas como *K. pneumoniae*, *E. coli*, *P. aeruginosa* e *A. baumannii* produtoras de diferentes β-lactamases de amplo espectro têm contribuído efetivamente para a emergência de cepas resistentes a diversos antibióticos utilizados na clínica (Lynch *et al.*, 2013).

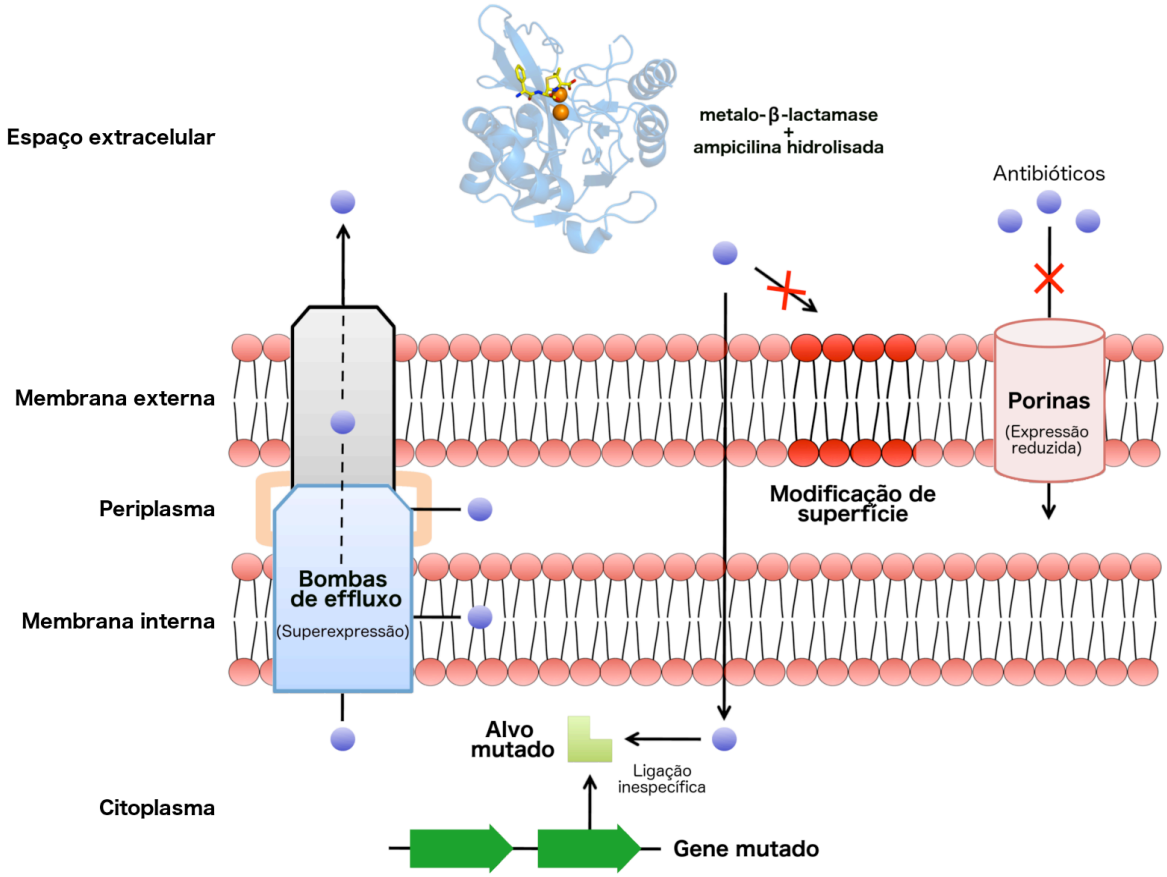

Figura 1. Esquema demonstrando alguns dos mecanismos de resistência bacteriana a antibióticos mais comumente relatados em cepas Gram-negativas, incluindo a atuação de β-lactamases na hidrólise do anel β-lactâmico de antibióticos, superexpressão de bombas de efluxo, redução na expressão de porinas, modificação do alvo por meio de mutações em genes específicos, bem como modificações nas propriedades físico-químicas da superfície celular. Figura do autor.

Em adição a hidrólise de antibióticos, bactérias resistentes podem realizar modificações nos sítios de ligação ao fármaco evitando, assim, o reconhecimento do agente antimicrobiano pelo alvo (Figura 1) (Blair *et al.*, 2015). Genes que codificam alvos para antibióticos, em sua maioria, existem em múltiplas cópias em cepas patogênicas. Ademais, mutações pontuais em uma dessas cópias podem conferir resistência a determinados antibióticos. Dentre os exemplos de resistência bacteriana pela modificação do alvo, podemos citar a resistência a linezolida, sendo este o primeiro antibiótico da classe das oxazolidonas que vem sendo utilizado na clínica na última década (Billal *et al.*, 2011). O uso clínico deste antibiótico tem selecionado cepas resistentes de *Streptococcus pneumoniae* e *S. aureus* por meio da modificação de uma das múltiplas cópias de genes que codificam o alvo da linezolida (subunidade 23S – RNA ribossomal) (Billal *et al.*, 2011). Em outros casos, a modificação do

alvo pode se dar também através da aquisição de genes homólogos ao alvo original, como por exemplo em MRSA, na qual essa resistência pode ser conferida pela aquisição de um elemento móvel denominado SCC*mec* (*staphylococcal cassette chromosome mec*) (Katayama *et al.*, 2000). Além disso, cepas de *E. faecium* e *Enterococcus faecalis* têm mostrado resistência a glicopeptídeos utilizados na clínica, incluindo vancomicina e teicoplanina, por meio da modificação de D-alanil-D-alanina por D-alanil-D-lactato ou D-alanil-D-serina impedindo, assim, a inibição da formação de parede celular pelos antibióticos supracitados (Giedraitiene *et al.*, 2011). Em alguns casos, onde não há a ocorrência de mutações nos genes que codificam os alvos dos antibióticos, estes podem ainda ser protegidos por modificações químicas, incluindo metilação (Kumar *et al.*, 2014).

Cepas bacterianas Gram-negativas são intrinsicamente menos permeáveis aos antibióticos quando comparadas a cepas Gram-positivas devido a presença de membrana externa, a qual atua como uma barreira de permeabilidade (Kojima e Nikaido, 2013). Dessa forma, antibióticos hidrofílicos atravessam membranas externas em cepas Gram-negativas por difusão através de porinas. Portanto, um dos mecanismos de resistência intrínseca comumente relatado em bactérias, em especial Enterobactereaceae, consiste na redução da expressão de porinas de membrana externa, ou a substituição destas por canais de maior seletividade, limitando a entrada de antibióticos na célula (Figura 1) (Kojima e Nikaido, 2013). Estudos apontam ainda que a alteração na expressão de porinas em Enterobactereaceae contribui significantemente para eventos de resistência a outras classes de antibióticos, incluindo carbapenêmicos e cefalosporinas, cuja resistência está usualmente associada a degradação enzimática (Lavigne *et al.*, 2013; Poulou *et al.*, 2013).

Associado a redução de permeabilidade celular, a superexpressão de bombas de efluxo em cepas patogênicas resulta no transporte ativo de diversos antibióticos para fora da célula, sendo este mecanismo um dos maiores responsáveis pela resistência intrínseca em cepas Gram-negativas (Figura 1) (Blair *et al.*, 2015). O efluxo de antibióticos pelas bombas de efluxo ocorre em altas taxas, o que se traduz em uma baixa concentração de antibióticos que não é suficientemente capaz de desencadear um efeito antibacteriano (Santajit e Indrawattana, 2016). Essencialmente, cinco famílias de bombas de efluxo vem sendo descritas na literatura, incluindo os transportadores de cassetes (ABC) de ligação de adenosina trifosfato (ATP), a superfamília dos facilitadores principais (MFS, do inglês *Major Facilitator Superfamily*), a família de baixa resistência a múltiplos fármacos (SMR, do inglês *Small Drug Resistance*

Family), a família resistência-nodulação-divisão (RND, do inglês *Resistance Nodulation Division Family*) e a família de extrusão de múltiplos fármacos e compostos tóxicos (MATE, do inglês *Multidrug and Toxic Compounds Extrusion Family*) (Cardoso *et al.*, 2018). Membros dessas famílias são codificados por múltiplos genes cromossomais em bactérias; contudo, estes genes podem ainda ser incorporados a plasmídeos e, consequentemente, disseminar resistência para outras cepas em um microambiente (por exemplo, sítios de infecção). Dolejska et al. (2013), por exemplo, identificaram genes de um membro da família RND em um plasmídeo IncH1 isolado de *Citrobacter freundii* (responsável por um grande espectro de infecções em humanos), a qual também carregava genes de resistência NDM-1 demonstrando, assim, o alto risco da disseminação de um ou mais mecanismos de resistência.

Juntamente aos mecanismos citados acima, a formação de biofilmes bacterianos representa, atualmente, um dos maiores desafios em ambiente hospitalar haja vista a alta resistência química e mecânica desses consórcios bacterianos sob diferentes situações de estresse.

1.2. Biofilmes bacterianos

A ocorrência e o tratamento de biofilmes bacterianos têm emergido como um dos maiores desafios dentro das ciências médicas visto as escassas opções de tratamento em infecções protagonizadas por esses consórcios bacterianos. De maneira geral, o desenvolvimento dos biofilmes inicia-se a partir de cepas bacterianas livre-nadantes que se aderem à superfícies bióticas ou abióticas formando microcolônias, as quais, com o passar do tempo, desenvolvem-se em biofilmes maduros (Figura 2) (Kostakioti *et al.*, 2013). Os biofilmes maduros são definidos como um consórcio estruturado de microrganismos, podendo ser uni ou polimicrobiano, conectados por uma complexa matriz composta de polissacarídeo (s), proteínas e DNA (de la Fuente-Nunez *et al.*, 2013).

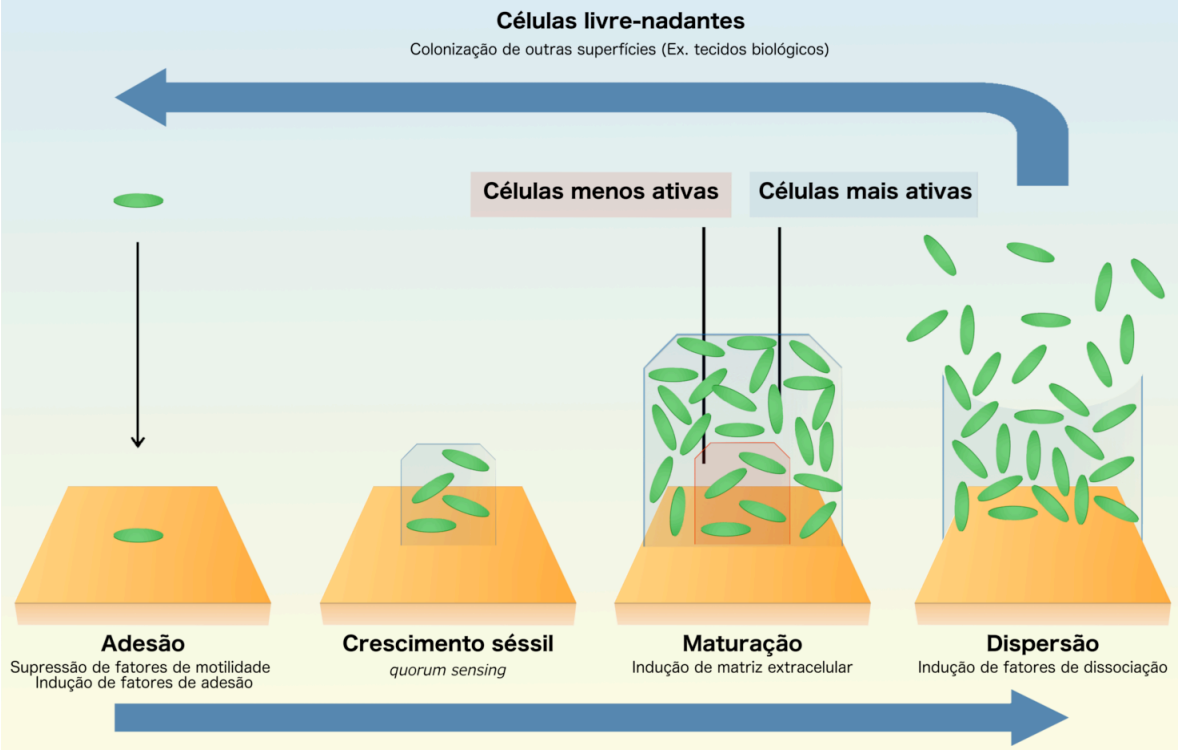

Figura 2. Desenvolvimento de biofilmes bacterianos destacando os estágios de adesão, crescimento séssil, maturação e dispersão. Figura do autor.

Avanços recentes em relação a comunicação célula-célula em bactérias, também conhecido como *quorum sensing* (QS), tem demonstrado o papel das sinalizações químicas na formação e manutenção de biofilmes (Davies, 2003). O QS pode ser controlado em nível molecular pela ação de auto-indutores, os quais são capazes de regular a expressão de genes e, assim, afetar a motilidade celular, adesão, produção de matriz extracelular e transferência de genes, fatores estes envolvidos intrinsicamente na formação de biofilmes (Bhardwaj *et al.*, 2013; Ribeiro *et al.*, 2016). Ademais, sabe-se que a expressão de fatores de virulência podem também ser regulados por mecanismos de QS sendo este, portanto, de grande interesse no campo farmacológico (Balestrino *et al.*, 2005).

Uma das características mais significantes dos biofilmes consiste na sua elevada resistência a condições de estresse, incluindo a administração de biocidas e antibióticos utilizados na indústria e na clínica, condições anaeróbicas, exposição a ácidos, gradientes de pH, entre outros (de la Fuente-Nunez *et al.*, 2013; Kostakioti *et al.*, 2013). Ademais, a proteção física estabelecida pela matriz dos biofilmes, em associação a proximidade das

células bacterianas nesse microambiente, representam uma condição ideal para a transferência horizontal de genes de resistência (Baker-Austin *et al.*, 2006). Estudos sugerem ainda que cepas bacterianas em biofilmes são capazes de tolerar níveis de antibióticos que estão em uma ordem de magnitude acima das concentrações inibitórias mínimas (CIM) obtidas para cepas resistentes em seu estágio planctônico (Jefferson *et al.*, 2005).

Em adição aos mecanismos de resistência bacteriana listados no tópico anterior, a matriz extracelular dos biofilmes pode ainda sequestrar os antibióticos utilizados no tratamento de infecções o que, somado a presença de uma pequena população de células persistentes, contribui diretamente para uma tolerância tempo-dependente aos antibióticos (Harrison *et al.*, 2005). Dessa forma, estima-se que os biofilmes sejam de 10 a 1.000 vezes mais resistentes aos antibióticos convencionais quando comparados com cepas de bactérias resistentes em seu estado planctônico (livre-nadante) (Van Acker *et al.*, 2014). Somado a isso, atualmente, têm sido estabelecidos que bactérias patogênicas encontram-se predominantemente organizadas em biofilmes, sendo responsáveis por cerca de 70 a 80% de todas as infecções bacterianas em seres humanos (de la Fuente-Nunez *et al.*, 2013; Van Acker *et al.*, 2014).

Biofilmes em ambiente hospitalar podem colonizar superfícies biológicas (bióticas) e não-biológicas (abióticas). No caso das superfícies abióticas, estudos vem mostrando que os biofilmes podem colonizar cateteres intravenosos e endotraqueais, assim como válvulas cardíacas e marca-passos, aparelhos ortopédicos, implantes dentários, dentre outros (Hall-Stoodley *et al.*, 2004; Romling e Balsalobre, 2012). Infecções relacionadas a aparelhos médicos foram as primeiras infecções clínicas a serem identificadas como tendo uma etiologia de biofilme, mostrando ainda que a formação desses consórcios pode ser facilitada pela resposta inflamatória do hospedeiro (Hall-Stoodley *et al.*, 2004). Ainda no contexto da colonização de superfícies abióticas, as cepas mais relatadas em ambiente hospitalar incluem *S. aureus*, *Staphylococcus epidermidis* e *P. aeruginosa*. Bactérias do gênero *Staphylococcus* apresentam características notáveis na colonização de implantes médicos por meio da expressão de diversas cópias de substâncias extracelulares poliméricas (EPS). Ademais, dados da literatura mostram que o estágio de adesão em *S. aureus* e *S. epidermidis* é multifatorial, sendo diretamente relacionado as propriedades físico-químicas do polímero utilizado no material biomédico infectado (Hall-Stoodley *et al.*, 2004).

Os biofilmes podem se associar também a superfícies bióticas, incluindo tecidos biológicos. Na clínica, os biofilmes estão amplamente associados a infecções recalcitrantes causadas por *P. aeruginosa*, *K. pneumoniae* e *S. epidermidis* (Baker-Austin *et al.*, 2006). Biofilmes de *P. aeruginosa*, por exemplo, vêm sendo comumente relatados em casos de infecção pulmonar crônica em pacientes com fibrose cística o que, em diversos casos, leva o paciente já imunocomprometido a óbito (Kovach *et al.*, 2017). Além disso, infecções associadas a biofilmes de *P. aeruginosa* e *S. aureus* vêm sendo observadas em pacientes com doenças pulmonares obstrutivas crônicas (Martinez-Solano *et al.*, 2008), otite e sinusite crônica (Wessman *et al.*, 2015), bem como em infecções crônicas em feridas, principalmente em pacientes com diabetes (Percival *et al.*, 2012). Neste cenário, a investigação e melhoramento de compostos naturais e sintéticos tem sido de grande interesse na busca por alternativas promissoras aos medicamentos convencionais.

1.3. Peptídeos antimicrobianos (PAMs)

Uma das estratégias propostas para o controle de bactérias resistentes inclui o uso de peptídeos catiônicos anfipáticos, mais conhecidos por peptídeos antimicrobianos (PAMs). Tais moléculas de caráter multifuncional vêm sendo largamente isoladas de diversos organismos como animais vertebrados e invertebrados, plantas e bactérias, também atuando como moléculas molde para estratégias de desenho racional (Cândido *et al.*, 2014; Cardoso *et al.*, 2016). A maioria dos PAMs consiste em L-aminoácidos, os quais estão organizados em estruturas secundárias com a presença de α-hélice e folhas-β ou mesmo por uma mistura de ambos (Figura 3). Contudo, crescentes relatos vêm descrevendo a descoberta, bem como construção de pequenos PAMs de estrutura altamente instável, com inúmeros estados de transição ambiente dependente (Hilpert *et al.*, 2005; Fjell *et al.*, 2012). Os PAMs são ainda conhecidos por apresentarem uma estrutura anfipática com conjuntos de regiões hidrofóbicas e carregadas positivamente, contendo cerca de 10 a 50 resíduos de aminoácidos arranjados, por exemplo, de forma linear ou cíclica (Sirtori *et al.*, 2008). A hidrofobicidade em PAMs varia, na maioria dos casos, de 40% a 60%, uma vez que estudos têm mostrado que o aumento excessivo desse percentual pode levar a perda do potencial antimicrobiano, além de aumentar os efeitos hemolíticos dos PAMs (Strempel *et al.*, 2015).

Devido a tais características físico-químicas, os PAMs são capazes de realizar interações eletrostáticas com superfícies microbianas carregadas negativamente (Baltzer e

Brown, 2011). Os peptídeos ativos na superfície, tais como aqueles que se ligam e afetam superfícies anfifílicas como membranas e receptores, têm sido estudados extensivamente nos últimos anos sendo alguns deles extremamente representativos em processos citolíticos como as defensinas de mamíferos, as melitinas e cecropinas de insetos (Chernysh *et al.*, 2015), bem como as magaininas de anfíbios (Sirtori *et al.*, 2008). Outra característica que torna os PAMs moléculas bastante atraentes quando se pensa em seu uso terapêutico consiste na seletividade de alvos para exercerem suas funções. A presença de colesterol na membrana de mamíferos, por exemplo, consiste em um fator conhecido por, na maior parte das vezes, reduzir a atividade dos PAMs, uma vez que auxilia na estabilização da bicamada lipídica (Nicolas, 2009). Evidências mostram ainda que podem haver interações entre o colesterol e os PAMs sem ocorrer o rompimento da membrana (Sirtori *et al.*, 2008; Nguyen *et al.*, 2011).

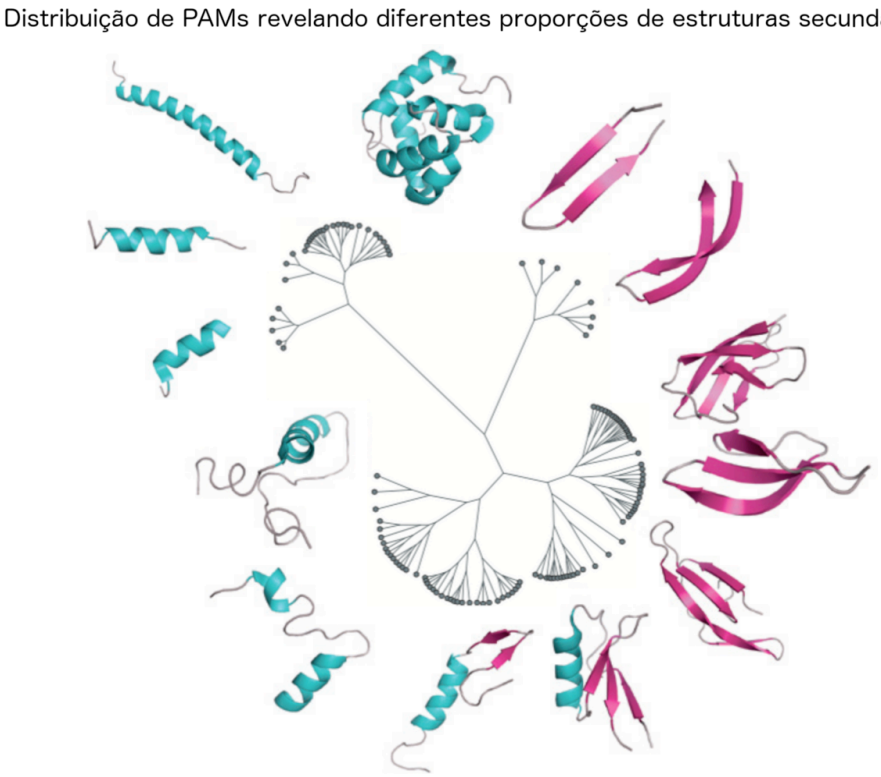

Figura 3. Distribuição de 135 PAMs depositados no *Antimicrobial Peptides Database* (APD) (http://aps.unmc.edu/AP/main.php) de acordo com seus ângulos de torsão *phi* e *psi.* Todas as estruturas foram resolvidas por ressonância magnética nuclear. Adaptado de Fjell *et al.* (2011).

Dentre seus mecanismos de ação mais bem descritos encontra-se a formação de poros em membranas biológicas, resultando na saída de íons e metabólitos do meio intracelular para

o extracelular, despolarização de membrana, interrupção de processos respiratórios, bem como morte celular (Pelegrini *et al.*, 2011). Assim, quando agem diretamente em membranas lipídicas, os PAMs podem atuar segundo três modelos principais, sendo eles conhecidos por modelo barril, poro toroidal e modelo carpete. No mecanismo de barril ocorre a oligomerização dos PAMs de forma que seus resíduos hidrofóbicos realizem interações com a bicamada lipídica, enquanto que seus resíduos hidrofílicos configuram a superfície do lúmen do poro recém-formado. No mecanismo de poro toroidal, durante o evento de agregação, os peptídeos se reorientam na membrana através de interações eletrostáticas, as quais ocorrem entre as regiões hidrofílicas dos fosfolipídios e os resíduos hidrofílicos dos peptídeos. Como consequência, a membrana sofre uma curvatura, caracterizando o poro toroidal. No modelo de carpete os PAMs, estando organizados em monômeros ou oligômeros, atuam como detergentes, se estendendo ao longo da membrana por meio de interações eletrostáticas (Pelegrini *et al.*, 2011). Este "carpete" constituído de moléculas anfipáticas causa o desarranjo da bicamada lipídica, alterando as propriedades da membrana, bem como levando ao seu rompimento. Além desses, são ainda conhecidos outros mecanismos de ação como o modelo "*sinking raft*", no qual os peptídeos são capazes de se inserir na bicamada e atravessá-la (Yandek *et al.*, 2007).

Em adição aos mecanismos relacionados a permeabilização/rompimento de membranas biológica, trabalhos vêm relatando a influência dos PAMs em processos macromoleculares, incluindo sua interferência na biossíntese de parede celular, bem como divisão celular, além de outras atividades cujos alvos são a síntese de RNA e proteínas (Fjell *et al.*, 2012). Evidências sugerem que a habilidade dos PAMs em atuar sobre alvos intracelulares pode ocorrer tanto como seu principal mecanismo de ação, uma vez ultrapassadas as barreiras físicas bacterianas sem causar a desestabilização destas, quanto como um mecanismo de ação secundário e/ou associado ao rompimento de membranas (Hale e Hancock, 2007). Tal diversidade dos PAMs em relação aos seus modos de ação, ao contrário do que se observa para os antibióticos convencionais, tem sido proposta como uma das razões para sua menor propensão em selecionar cepas bacterianas resistentes.

1.4. PAMs com potencial antibiofilme

Como descrito nos tópicos anteriores, a maioria das infecções persistentes em humanos são causadas por biofilmes, os quais prevalecem em infecções associadas a

aparelhos médicos, infecções crônicas e infecções em superfícies corporais, incluindo pele e pulmões (de la Fuente-Nunez *et al.*, 2013). Ademais, as células bacterianas em biofilmes são capazes de resistir à resposta imune do hospedeiro, tanto inata quanto adquirida, sendo ainda particularmente resistentes a eventos de fagocitose (de la Fuente-Nunez *et al.*, 2016). Dessa forma, os biofilmes bacterianos desempenham um papel fundamental em doenças infecciosas uma vez que podem se estabelecer em diversos tecidos biológicos e até mesmo implantes médicos (Costerton *et al.*, 1999). Curiosamente, mesmo levando-se em consideração o cenário alarmante representado por infecções persistentes causadas por biofilmes, ainda não há antibióticos disponíveis para uso clínico que tenham sido desenvolvidos com foco nesses consórcios bacterianos multirresistentes (Bjarnsholt *et al.*, 2013; De La Fuente-Nunez *et al.*, 2016).

Interessantemente, estudos recentes têm mostrado que o potencial antibiofilme de alguns PAMs independe de suas atividades frente a cepas patogênicas em seu estágio planctônico (Haney *et al.*, 2015). Como exemplo, podemos citar a catelicidina humana LL-37, a qual apresenta baixa atividade antibacteriana quando comparada a outras classes de PAMs, mas que é capaz de inibir de forma eficaz a formação de biofilmes de *P. aeruginosa* (Overhage *et al.*, 2008). Dessa forma, há um interesse crescente no uso de PAMs como agentes antibiofilme e, em alguns casos, estas moléculas têm sido avaliadas como agentes profiláticos e/ou terapêuticos para o controle de infecções causadas por biofilmes tanto *in vitro* como *in vivo* (Di Luca *et al.*, 2014).

Atualmente (última visualização em 26/02/2019), um total de 221 peptídeos antibiofilme estão depositados no banco de dados de PAMs ativos contra biofilmes (BaAMPs: do inglês *biofilm-active antimicrobial peptides*) (Di Luca *et al.*, 2015). Ademais, estes peptídeos vêm demonstrando atividade antibiofilme contra um total de 116 espécies de microrganismos. Dentre os peptídeos depositados nessa plataforma, vários têm sido capazes de não somente inibir a formação de biofilmes, como também erradicar biofilmes pré-formados (de la Fuente-Nunez *et al.*, 2015; Cardoso *et al.*, 2016). Além disso, alguns mecanismos pelos quais os PAMs inibem a formação ou eliminam biofilmes já vem sendo estudados, incluindo a interferência na adesão da célula microbiana planctônica no substrato biótico ou abiótico, influência no aumento da expressão de genes relacionados a motilidade celular, interferência na produção e liberação de matriz extracelular, bem como a morte de células bacterianas que constituem os biofilmes através de mecanismos já citados

anteriormente, como a formação de modelos carpete e poros (Figura 4) (Brancatisano *et al.*, 2014).

Mecanismos associados a regulação da expressão de genes de formação e manutenção de biofilmes, por exemplo, podem incluir alterações na produção de *pili* do tipo IV e flagelos interferindo, indiretamente, no ancoramento de bactérias planctônicas em diferentes substratos (Figura 4) (Overhage *et al.*, 2008). Além disso, PAMs podem influenciar na redução de expressão de genes responsáveis pelo QS. Dessa forma, há o comprometimento da expressão coordenada de autoindutores responsáveis pela comunicação célula-célula dentro dos biofilmes e, consequentemente, a redução da densidade celular nesses consórcios bacterianos (Figura 4) (Brackman e Coenye, 2015).

Quando em situações de estresse, como aquelas que levam à formação de biofilmes, bactérias planctônicas são capazes de ativar a chamada "reposta estringente", a qual pode ser mediada pelo nucleotídeo guanosina 5'- difosfato 3'- difosfato (ppGpp) (Pletzer *et al.*, 2016). Estudos têm demonstrado que a sinalização mediada por ppGpp tem papel crucial na resistência a antibióticos, virulência e formação de biofilmes através da modulação da maquinaria bacteriana (Chua *et al.*, 2015). Dessa forma, têm sido proposto a inativação da resposta estringente em bactérias planctônicas através da degradação de ppGpp por PAMs. De la Fuente-Nunez *et al.* (2014), por exemplo, têm mostrado que os peptídeos antibiofilme IDR-1018, DJK-5 e DJK-6 são capazes de se ligar e, posteriormente, desencadear a degradação de ppGpp. Dessa forma, seria prevenido o acúmulo intracelular desse nucleotídeo levando, assim, a inibição da formação de biofilmes em múltiplos patógenos Gram-positivos e Gram-negativos (Figura 4) (de la Fuente-Nunez *et al.*, 2014). Interessantemente, contudo, este mecanismo de ação está em processo de revisão. Estudos propõem que a interação PAM/ppGpp, seguido da degradação deste nucleotídeo, pode não ser um fator crucial para a inibição de biofilmes, uma vez que o ppGpp pode ser degradado por hidrolases bacterianas devido a tratamento com antibióticos, como por exemplo o cloranfenicol (Andresen *et al.*, 2016).

Considerando as características físico-químicas dos PAMs, bem como suas atividades antimicrobianas de amplo espectro, um crescente número de estudos vem destacando ainda a aplicação de PAMs no revestimento de biomateriais, com foco na inibição da formação de biofilmes bacterianos em dispositivos médicos utilizados na clínica. Essa estratégia, a qual se dá por meio da imobilização covalente dessa classe de peptídeos nas superfícies alvo permite,

por exemplo, que alguns obstáculos em relação ao uso dos PAMs sejam ultrapassados, incluindo sua curta meia-vida, biodisponibilidade e citotoxicidade devido a altas concentrações de peptídeos (Costa *et al.*, 2011). A imobilização de PAMs em superfícies poliméricas pode ocorrer por meio da adição de resíduos de cisteína na porção N-terminal dos peptídeos alvo, como tem sido demonstrado para PAMs ricos em arginina e triptofano com potencial antibiofilme (Lim *et al.*, 2013). Ademais, estudos mostram ainda que a conjugação de PAMs com as cadeias hidrofílicas de polímeros representa uma estratégia promissora na inibição da formação de biofilmes por cepas resistentes de *P. aeruginosa* (Gao *et al.*, 2011).

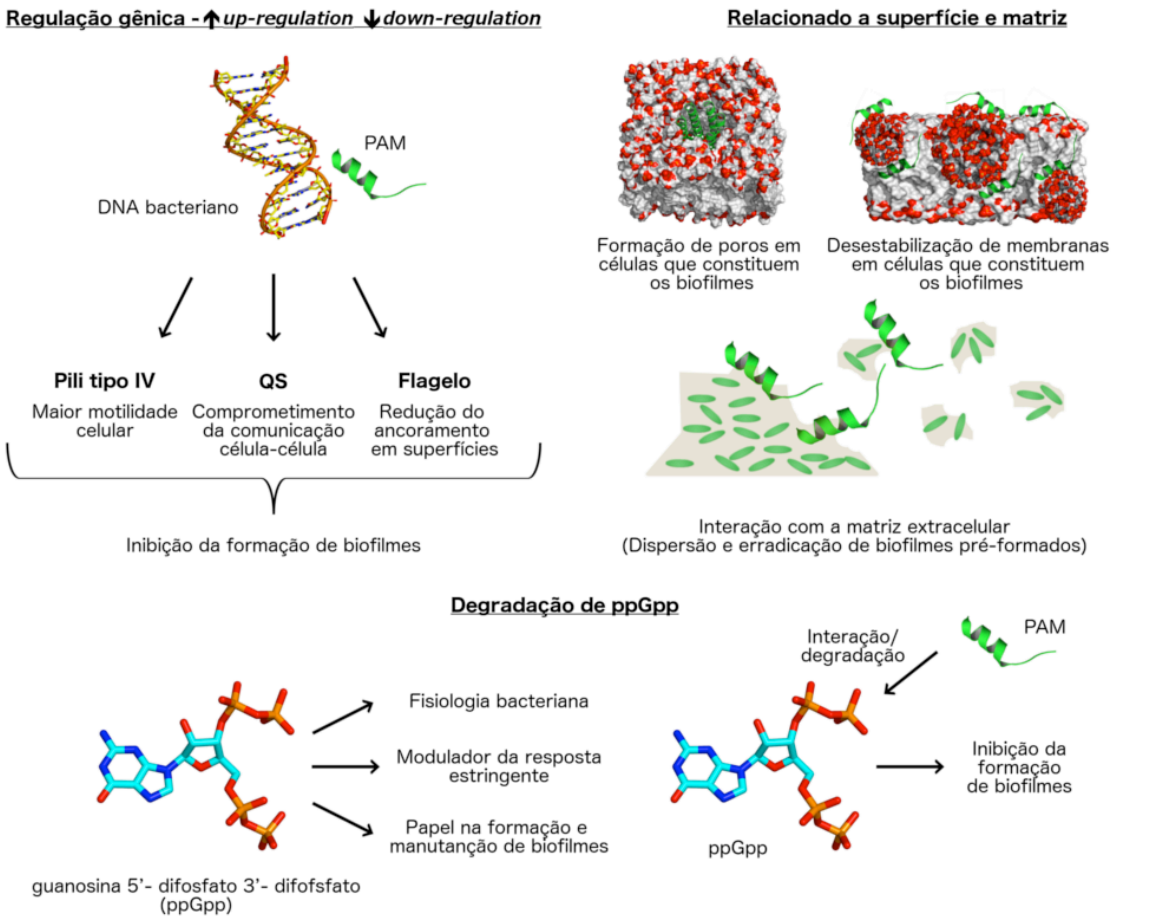

Figura 4. Mecanismos de ação propostos para PAMs com potencial antibiofilme, incluindo a regulação de genes envolvidos na comunicação e motilidade celular, desestabilização da membrana de bactérias que constituem os biofilmes, dispersão de biofilmes por meio da interação com a matriz extracelular e, por fim, interação/degradação de guanosina 5' – difosfato 3' – difosfato (ppGpp). PAM: peptídeos antimicrobianos; QS: *quorum sensing*.

Embora as estratégias de revestimentos (recobrimento – *coating*) citadas acima tenham demonstrado seu potencial no contexto farmacológico, PAMs imobilizados de forma covalente, com o tempo, podem perder sua funcionalidade. Como possíveis soluções, estudos têm mostrado a incorporação de PAMs com potencial antibiofilme em hidrogéis degradáveis, nanopartículas, bem como outras arquiteturas que possibilitem a liberação controlada e tempo-dependente de PAMs nos sítios de infecção (D'angelo *et al.*, 2015).

1.5. Estratégias de desenho de PAMs

A necessidade de novos compostos antimicrobianos, a qual ultrapassa a rápida ascensão de microrganismos resistentes aos medicamentos, vem encorajando pesquisadores de diversas áreas a investir no desenvolvimento e aplicação de tecnologias de alta capacidade para o desenho de novos fármacos. Historicamente, o processo de descobrimento de novos medicamentos tem se baseado na prospecção de alto desempenho (do inglês *high-throughput screening* - HTS) para a identificação de compostos biologicamente ativos (Congreve *et al.*, 2005). Esta técnica proporciona uma avaliação *in vitro* de milhares de moléculas contra uma proteína alvo ou um sistema celular (Lombardino e Lowe, 2004). Em adição ao HTS, metodologias *in silico*, como o desenho de fármacos baseado em estruturas, vem possibilitando identificar e selecionar marcadores moleculares, estudar a base molecular de interações proteína-ligante e caracterizar sítios de ligação. Tais estratégias podem ser utilizadas para racionalizar, melhorar a eficiência, bem como acelerar e reduzir os custos de produção para o desenvolvimento de novos fármacos (Anderson, 2003). Dessa forma, métodos de prospecção virtual (*in silico*) associados ao HTS podem ser empregados para a determinação de propriedades quantificáveis de peptídeos, tais como carga, hidrofobicidade, estrutura primária e outras características para correlacionar tais propriedades com suas respectivas atividades biológicas (Blondelle e Lohner, 2010; Fjell *et al.*, 2011).

O desenho racional consiste em uma estratégia que vem sendo amplamente utilizada no melhoramento de moléculas candidatas a fármacos. Como visto anteriormente, alguns obstáculos já têm sido bem definidos em relação ao uso de PAMs de origem natural como novas alternativas aos antibióticos convencionais. A principal barreira consiste na toxicidade dos PAMs perante células de mamíferos, visto que suas atividades são principalmente mediadas pelo rompimento e permeabilização de membranas. Além disso, os PAMs são altamente sujeitos a eventos proteolíticos já que são, em sua maioria, estruturalmente

formados por L-aminoácidos, os quais são mais sensíveis à degradação (Chen *et al.*, 2005). Para superação desses impasses, estratégias de desenho racional vêm sendo aplicadas de forma a, por exemplo, promover a substituição de resíduos de L-aminoácidos por D-aminoácidos, fazendo com que esses PAMs se tornem menos susceptíveis a degradação proteolítica. Além disso, tais mudanças poderiam gerar alterações na anfipaticidade e hidrofobicidade da molécula, levando a uma redução do seu efeito citotóxico quando em contato com células de mamíferos, sem alterar sua atividade antimicrobiana (Chen *et al.*, 2005). Estudos recentes mostram ainda que, em casos onde se tem um PAM promissor, mas susceptível à proteólise, a construção de um análogo retro-inverso se mostra atrativa, visto que este seria um peptídeo composto por D-aminoácidos, porém que preserva a orientação espacial de seu PAM parental, mantendo suas funções (de la Fuente-Nunez *et al.*, 2015).

Os primeiros estudos de desenho racional de PAMs foram responsáveis por gerar diversos análogos a PAMs já conhecidos como as catelicidinas, cecropinas, defensinas e magaininas. De fato, esses estudos desempenham um papel crucial na identificação de propriedades físico-químicas de PAMs, como momento hidrofóbico, carga e arranjo estrutural, os quais estão diretamente relacionados às suas atividades antimicrobianas. Baseado neste modelo físico-químico surgiram os modelos linguísticos, os quais tem por base não só levar em consideração as propriedades físico-químicas dos peptídeos, mas também otimizar a disposição dos aminoácidos dentro da sequência primária, de maneira a dar sentido "a frase" (Loose *et al.*, 2006). Dessa forma, cada vez mais essas propriedades têm sido alvo de estudos a fim de serem utilizadas como base para o desenvolvimento de metodologias de predição de PAMs por diferentes métodos (Jenssen *et al.*, 2007).

De forma geral, os métodos de desenho racional têm por objetivo criar novos peptídeos com melhores atividades antimicrobianas, baixa toxicidade às células humanas e tamanhos reduzidos. Em outras palavras, o desenho racional vem com a proposta de elaborar fármacos cada vez mais específicos aos seus alvos biológicos, evitando possíveis efeitos colaterais. Além disso, pode-se classificar os métodos de desenho racional em duas maiores classes, sendo elas a baseada em um modelo (*template*) e os métodos *de novo*. O primeiro método faz uso de um modelo estrutural de PAM previamente descrito. Assim, enquanto os métodos físico-químicos geram uma grande gama de análogos com diferentes propriedades, os métodos baseados em moldes visam à redução de tamanho, adicionando seletividade e/ou

atividade às sequências conhecidas. Além deste, os métodos *de novo* geram PAMs sem utilizar sequências *template*, usando apenas frequências e padrões (Porto *et al.*, 2010).

Diversos algoritmos vêm sendo utilizados para predizer a estrutura e função peptídeos (Morgenstern *et al.*, 2006). Algoritmos baseados em métodos empíricos são qualitativos, e funcionam baseados na probabilidade de uma sequência de entrada (*input*) comparada com sequências de PAMs conhecidos em bases de dados para prever uma possível função (Wang *et al.*, 2008). Os algoritmos de aprendizado de máquina (*machine learning*) são baseados em inteligência artificial, buscando reconhecimento de padrões (Kotsiantis *et al.*, 2007). Sendo assim, estes algoritmos são fundamentados em um conjunto de informações conhecidas que pode prever a informação de saída com base na informação de entrada (Davies e Shamu, 2014).

Dentre os métodos empíricos para predição de PAMs podemos citar o de classificação, bem como de busca em série de dados desenvolvido por Fernandes e colaboradores, denominada "*fuzzy modelling*" (Fernandes *et al.*, 2009). Aliado a este, há também o método de assinaturas multidimensionais desenvolvido por Yount e Yeaman (2004), no qual foi possível realizar o reconhecimento de sequências padrões e motivos em estruturas tridimensionais para correlacioná-las a atividades antimicrobianas (Yount e Yeaman, 2004). Ademais, Lata e colaboradores (Lata *et al.*, 2007) foram os responsáveis por desenvolver os primeiros métodos de aprendizagem de máquina supervisionados para a predição de atividade antimicrobiana, onde foram testados três algoritmos: máquinas de vetores de suporte (SVM), rede neural artificial (ANN) e matrizes quantitativas (QM) (Lata *et al.*, 2007). Anos mais tarde, Thomas e colaboradores (Thomas *et al.*, 2010), aliando o algoritmo SMV aos métodos de análise discriminante (DA) e floresta aleatória (*random forest*) (RF), implementaram um modelo de melhor acurácia para a predição de atividades antimicrobianas (Thomas *et al.*, 2010).

Outra técnica que vem sendo utilizada consiste na de abordagem estocástica, a qual visa à otimização de peptídeos através de processos aleatórios para realizar alterações. Com exemplo, podemos citar os algoritmos evolutivos, os quais realizam sucessivas gerações de mutações e deleções na sequência alvo buscando aprimorar suas características que lhe conferem atividade (Hiss *et al.*, 2010; Kliger, 2010). Os algoritmos evolutivos são chamados assim, pois sua otimização pode ser inspirada na natureza, como uma estratégia de evolução propriamente dita (Holland e Goldberg, 1989). Em sua maioria, estes métodos compartilham

o conceito de variação e seleção *in silico* onde, através de um conjunto de informações (genes ou sequências), busca pontualmente por um "indivíduo" mais apto. Dessa forma, através da variação é possível produzir descendentes (homólogos) com caráteres melhorados ou que favoreçam uma ação específica (Hiss *et al.*, 2010).

Mais recentemente, Haney *et al.* (2018) construíram uma biblioteca de peptídeos derivados do peptídeo imunomodulatório e antibiofilme, IDR-1018. Neste trabalho os autores objetivaram o desenho computacional em larga escala de peptídeos que tivessem, exclusivamente, atividade antibiofilme. Para isso, foi utilizado o modelo de relação quantitativa estrutura-atividade (QSAR – do inglês *Quantitative Structure- Activity Relationship*) para investigar a atividade antibiofilme de uma biblioteca de 96 peptídeos derivados de IDR-1018 de acordo com seus "descritores" químicos, os quais foram posteriormente utilizados para modelar essa atividade antibiofilme em novos análogos. O modelo QSAR tridimensional desenvolvido foi então utilizado para predizer a probabilidade de um peptídeo possuir atividade antibiofilme a partir de uma biblioteca virtual de 100 mil peptídeos. Após ensaios antibiofilme em larga escala, foi observado que a aplicação desse modelo resultou em uma acurácia de ~85% na predição de atividade. Um dos peptídeos gerados (IDR-3002), por exemplo, mostrou-se 8 vezes mais potente contra biofilmes bacterianos resistentes quando comparado ao peptídeo modelo IDR-1018 demonstrando, assim, o potencial dessa ferramenta para o desenvolvimento de peptídeos com potencial antibiofilme (Haney *et al.*, 2018).

1.6. O peptídeo polialanina Pa-MAP 1.9

Dentre as classes de PAMs descritas atualmente encontram-se as polialaninas (Cardoso *et al.*, 2016). Esta classe, embora ainda pouco estudada, vem ganhando atenção, visto a sua diversidade estrutural ambiente dependente. Na maior parte das escalas de hidrofobicidade, como a de Kyte e Doolittle (1982), a alanina é considerada moderadamente apolar. Assim, estudos acerca das propensões de hélice de peptídeos polialaninas na presença de membranas parecem confirmar que resíduos de alanina excedem seus limites hidrofóbicos para mecanismos de inserção em bicamadas lipídicas (Liu *et al.*, 1996; Liu e Deber, 1998). Em particular, análises biofísicas de peptídeos polialaninas por dicroísmo circular (DC) em ambientes miméticos como dodecil sulfato de sódio (SDS), lisofosfatidilglicerol (LPG) e dodecilfosfocolina (DPC), têm como padrão espectros característicos de peptídeos de alto

conteúdo de hélice, com elipicidades acima de 60% (Liu *et al.*, 1996). Estudos mais aprofundados a partir do uso de ressonância magnética nuclear (RMN) de fase sólida revelam ainda que peptídeos polialaninas, quando em contato com bicamadas lipídicas constituídas de 1-palmitoil-2-oleoil-sn-glicero-3-fosfocolina (POPC), apresentam ressonâncias correspondentes a orientações espaciais de peptídeos que se organizam sobre a membrana, bem como daqueles que adotam orientações transmembrana (Bechinger, 2001). Interessantemente, estudos adicionais de RMN mostram que os peptídeos polialaninas, em sua maioria, são capazes de interagir superficialmente e se inserir nas membranas sem causar grandes deslocamentos nas posições dos fosfolipídios mantendo, assim, a integridade da bicamada (Bechinger, 2001). Tal observação tem sido de extrema importância para estudos de elucidação dos mecanismos de ação destes peptídeos contra cepas bacterianas, onde sugere-se que as polialaninas poderiam transpassar as barreiras físicas bacterianas (parede e membranas celulares) e atuar diretamente em alvos intracelulares, interferindo em inúmeras vias biossintéticas (Liu *et al.*, 1996; Cardoso *et al.*, 2016).

Contudo, mesmo considerando sua diversidade estrutural relacionada ao ambiente, bem como habilidade de se aderir e inserir em membranas biológicas, os peptídeos polialaninas podem adquirir algumas configurações pouco desejadas em se tratando de PAMs. Algumas dessas configurações consistem na formação de agregados como pequenos complexos multiméricos, os quais não são capazes de se ancorar e inserir eficazmente em bicamadas lipídicas (Liu *et al.*, 1996; Bechinger, 2001). Tais eventos de agregação podem ainda levar a precipitação do complexo multimérico, assim reduzindo a concentração dos peptídeos no microambiente bacteriano.

A substituição ou adição de resíduos de leucina em peptídeos polialaninas, por exemplo, vem sendo proposta de forma a superar este obstáculo pelo aumento da estabilidade desses peptídeos em orientações transmembrana. Além disso, levando-se em consideração que a transferência de energia da alanina partindo de solventes hidrofílicos para solventes hidrofóbicos é de + 2,1 e + 0,7 $kJ.mol^{-1}$, respectivamente; enquanto os valores correspondentes para leucina são -5,2 e -2,3 $kJ.mol^{-1}$, respectivamente; infere-se que a substituição de resíduos alaninas por leucinas em peptídeos polialaninas pode aumentar esta energia de transferência em ~5 – 7,5 $kJ.mol^{-1}$, favorecendo a inserção desses peptídeos em membranas biológicas e, consequentemente, seus mecanismos de ação (White e Wimley, 1999). Esta estratégia, dentre muitas outras, tem sido aplicada para o desenho racional de

peptídeos polialaninas visando o aproveitamento de suas principais características acima descritas e já bem relatadas para outras classes de PAMs, aliado ao aumento de seu potencial biotecnológico e farmacológico para o controle de cepas e biofilmes patogênicos (Migliolo *et al.*, 2012; Teixeira *et al.*, 2013; Cardoso *et al.*, 2016; Migliolo *et al.*, 2016).

Com base nas propriedades citadas acima, Migliolo e colaboradores (2012) realizaram o desenho racional de peptídeos multifuncionais baseados em peptídeos anticongelantes isolados de *Pleuronectes americanus.* Como resultado, dez peptídeos polialaninas foram sintetizados, em que quatro deles foram separados em uma primeira geração (*Pa*-MAP, *Pa*-MAP 1.2, *Pa*-MAP 1.3 e *Pa*-MAP 1.4) e desenhados com base direta nos peptídeos anticongelantes HPLC-6 e -8. Dentre os resultados encontrados para os peptídeos da primeira geração destacou-se o peptídeo *Pa*-MAP, apresentando CIM de 30 μM contra cepas de *E. coli* (Migliolo *et al.*, 2012). A atividade antiviral e antifúngica também foi observada para *Pa*-MAP (90 – 115 μM) contra o vírus da herpes humano 1 e 2 e contra os fungos *Trichophyton mentagrophytes*, *Trichophyton rubrum* e *Candida parapsilosis*. Por fim, a atividade antitumoral frente à células tumorais cólon-retais Caco-2 foram também observadas para *Pa*-MAP (Migliolo *et al.*, 2012). Devido a esses fatores e também almejando-se uma melhora no potencial deste peptídeo contra cepas e biofilmes bacterianos, *Pa*-MAP foi alvo de um redesenho racional de forma a gerar uma segunda geração de peptídeos derivados de *P. americanus* (Tabela 1).

Tabela 1. Sequência de aminoácidos, carga, hidrofobicidade e momento hidrofóbicos para os peptídeos de primeira e segunda geração derivados de *Pleuronectes americanus*.

Peptídeos	Sequência de Aminoácidos	Carga	Hidrofobicidade (%)	Momento hidrofóbico
	Peptídeos de Primeira Geração			
Pa-MAP	HTASDAAAAAALTAANAAAAAAASMA	-1	28,5	0,072
Pa-MAP 1.2	AATAATAAAAAAATAVTAAKAAALTAANA	1	30,0	0,030
Pa-MAP 1.3	KAAAAAALTKAAAAAALTKAAAAAALT	3	31,4	0,015
Pa-MAP 1.4	KAAAAAAKTKAAAAAAKTKAAAAAAKT	6	0,1	0,086
	Peptídeos de Segunda Geração			
Pa-MAP 1.5	LKAAAAAAKLAAKAAKAALKAAAAAAKL	6	23,0	0,254
Pa-MAP 1.6	KTAATLADTLADTAATLAKAAAA	0	27,3	0,355
Pa-MAP 1.7	LKAALTAAKTALTAALTALKAALTAAKT	4	41,1	0,261
Pa-MAP 1.8	LAAALTAKATALTAKLTALAAALTAKAT	3	45,8	0,232
***Pa*-MAP 1.9**	**LAAKLTKAATKLTAALTKLAAALTAAAT**	**4**	**41,1**	**0,395**
Pa-MAP 2	TKAAAAAAKTAAKAAKAATKAAAAAAKT	6	0,2	0,254

Dentre os peptídeos de segunda geração apresentados na Tabela 1 pode-se destacar o peptídeo *Pa*-MAP 1.9. Quando comparado físico-quimicamente com seu peptídeo parental (*Pa*-MAP), *Pa*-MAP 1.9 revelou um aumento de carga (+4) devido a substituição de resíduos de serina e alanina em *Pa*-MAP por resíduos positivamente carregados (Lys^4, Lys^7, Lys^{11}, Lys^{18}) em *Pa*-MAP 1.9. Esta propriedade pode favorecer, por exemplo, sua atuação em membranas de bactérias Gram-negativas por meio de interações eletrostáticas. Ademais, a média relativa do momento hidrofóbico foi também aumentada de 0,072 em *Pa*-MAP para 0,395 em *Pa*-MAP 1.9, respectivamente (Eisenberg *et al.*, 1984), assim como a taxa hidrofóbica (~41% para *Pa*-MAP 1.9 em comparação a ~29% *Pa*-MAP). Quando analisados seus diagramas de hélice, *Pa*-MAP 1.9 revela ainda um arranjo estrutural anfipático, com regiões hidrofóbicas, hidrofílicas e carregadas positivamente bem definidas, ao contrário de *Pa*-MAP (Figura 5).

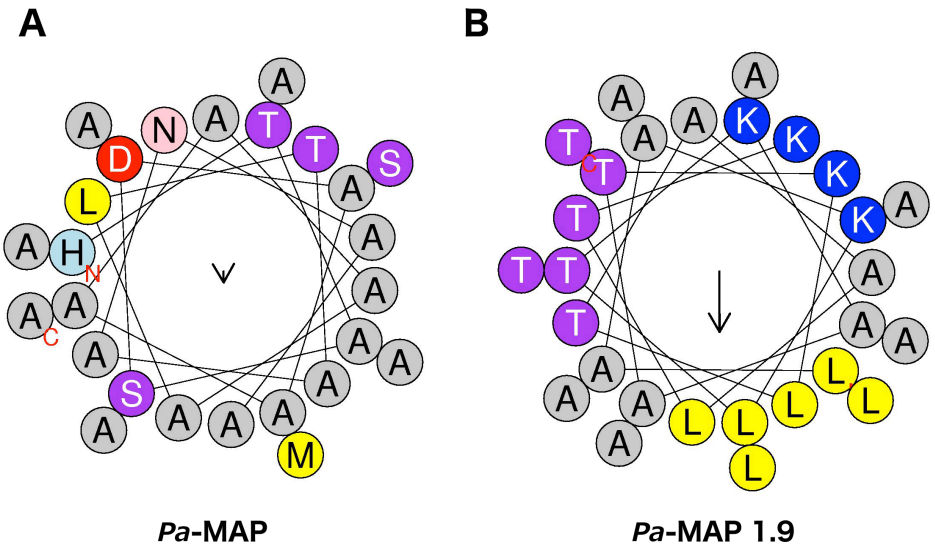

Figura 5. Diagramas de hélice para *Pa*-MAP (A) e *Pa*-MAP 1.9 (B). O vetor de momento hidrofóbico está representado por setas a partir do centro dos diagramas, enquanto que o valor estimado do momento hidrofóbico resultante é proporcional ao tamanho das setas.

Somado a estas características, quando avaliado acerca do potencial antimicrobiano de sua sequência primária segundo três algoritmos de predição do servidor *Collection of Anti-Microbial Peptides* (CAMP) (Waghu *et al.*, 2016), *Pa*-MAP 1.9 se destaca, apresentando probabilidade de ação antimicrobiana maior que 90%, contra apenas 30% de seu parental. Dessa forma, levando-se em consideração seu potencial físico-químico em relação ao seu peptídeo parental, *Pa*-MAP 1.9 foi selecionado neste estudo visando a elucidação de suas atividades biológicas, incluindo ensaios antibacterianos, antibiofilme, citotóxicos e hemolíticos. Ademais, estudos detalhados em relação a sua estrutura tridimensional e mecanismos de ação foram também realizados por meio do uso de ferramentas de biofísica experimental e computacional, objetivando o estabelecimento da relação estrutura-função para este peptídeo candidato a fármaco.

Em paralelo as análises realizadas com *Pa*-MAP 1.9, este estudo buscou ainda a caracterização funcional e estrutural detalhada de um novo PAM desenhado computacionalmente, o qual será apresentado em detalhes no tópico a seguir.

1.7. O peptídeo desenhado computacionalmente EcDBS1R5

Em adição ao desenho guiado por propriedades físico-químicas realizado para o peptídeo polialanina *Pa*-MAP 1.9, o presente estudo buscou também elucidar as atividades

antibacteriana e antibiofilme, assim como a estrutura tridimensional de um PAM, denominado EcDBS1R5, o qual foi desenhado computacionalmente.

O peptídeo EcDBS1R5 foi desenhado a partir do algoritmo Joker, o qual foi desenvolvido em nosso laboratório por Porto *et al.* (2018). Naquele trabalho, os autores inicialmente extraíram padrões de α-hélice a partir de 248 PAMs helicoidais depositados no *Antimicrobial Peptides Database* (APD) (Wang *et al.*, 2009). Como resultado, foi obtido o padrão de α-hélice (KK[ILV]x(3)[AILV]), onde resíduos de aminoácidos entre colchetes indicam que aquela posição pode ser ocupada por um deles, "x" indica a posição que pode ser preenchida por qualquer um dos 20 aminoácidos naturais e (3) indica uma janela de três resíduos proveniente da sequência utilizada como molde para os desenhos automatizados. Este padrão foi posteriormente contrastado contra o banco de dados de proteínas não-redundantes do *National Center for Biotechnology Information* (NCBI) para a identificação de sequências contendo 18 resíduos de aminoácidos (número de resíduos necessários para a formação de três hélices completas ao longo da estrutura dos peptídeos). Esta análise resultou na identificação de seis sequências, dentre elas, um fragmento de uma proteína transportadora de mercúrio expressa por *E. coli* (MerP: MKKLFAALALAAVVAPVW) (Tabela 2) (Porto *et al.*, 2018).

Tabela 2. Sequência de aminoácidos carga, hidrofobicidade e momento hidrofóbico para os peptídeos desenhados por meio do algoritmo Joker e derivados do fragmento de MerP.

Peptídeos	**Sequência de Aminoácidos**	**Carga**	**Hidrofobicidade (%)**	**Momento hidrofóbico**
Fragmento de MerP	–MKKLFAALALAAVVAPVW	2	81,3	0,182
EcDBS1R1	P**KILLRIALKI**AAVVAPVW	3	84,7	0,414
EcDBS1R2	PM**KILFRILAKI**AVVAPVW	3	90,1	0,434
EcDBS1R3	PMK**KLLARLALKI**VVAPVW	4	74,4	0,192
EcDBS1R4	PMKK**KLAARILAKI**VAPVW	5	55,9	0,192
EcDBS1R5	PMKKL**KLALRLAAKI**APVW	**5**	**57,9**	**0,413**
EcDBS1R6	PMKKLF**KLLARIAVKI**PVW	5	71,1	0,536
EcDBS1R7	PMKKLFA**KLALRIVVKI**VW	5	73,7	0,184
EcDBS1R8	PMKKLFAA**KILARVVAKI**W	5	61,6	0,213
EcDBS1R9	PMKKLFAAL**KLAARVAPKI**	5	48,2	0,443

Os resíduos de aminoácidos destacados em negrito correspondem a janela de deslizamento do padrão de α-hélice dentro das sequências geradas pelo algoritmo Joker.

O algoritmo Joker funciona por meio da inserção de padrões em uma sequência modelo (*template*), onde essa inserção ocorre através de janelas de deslizamento. Dessa forma, a sequência (MerP: MKKLFAALALAAVVAPVW) foi utilizada como sequência de entrada, resultando na geração de nove sequências análogas (Tabela 2). Estas foram posteriormente sintetizadas e avaliadas acerca de seu potencial antibacteriano e hemolítico frente a uma cepa bioluminescente de *P. aeruginosa* e eritrócitos humanos, respectivamente (Porto *et al.*, 2018). Como base nessas análises foi observado que o análogo número cinco (EcDBS1R5: PMKKLKLALRLAAKIAPVW) apresentou atividade contra esta cepa de *P. aeruginosa*, com CIM igual a 12,5 $\mu g.mL^{-1}$ (5,8 μM). Ademais, não foram relatadas atividades hemolíticas a 12,5 $\mu g.mL^{-1}$ (93,1 μM) (Porto *et al.*, 2018).

Quando comparado a seu peptídeo parental (fragmento de MerP), EcDBS1R5 apresenta maior carga positiva e momento hidrofóbico, assim como menor hidrofobicidade. Os resíduos de aminoácidos Phe^{6}, Ala^{7}, Ala^{10}, Val^{14} e Val^{15} no peptídeo parental foram substituídos por resíduos de leucina, lisina, arginina e isoleucina em EcDBS1R5, respectivamente. Tais modificações influenciaram diretamente na disposição dos resíduos de aminoácidos de ambos os peptídeos em seus diagramas de hélice (Figura 6). Dessa forma, duas faces definidas com propriedades catiônica e hidrofóbica podem ser observadas em EcDBS1R5, favorecendo anfipaticidade quando comparada a sequência parental.

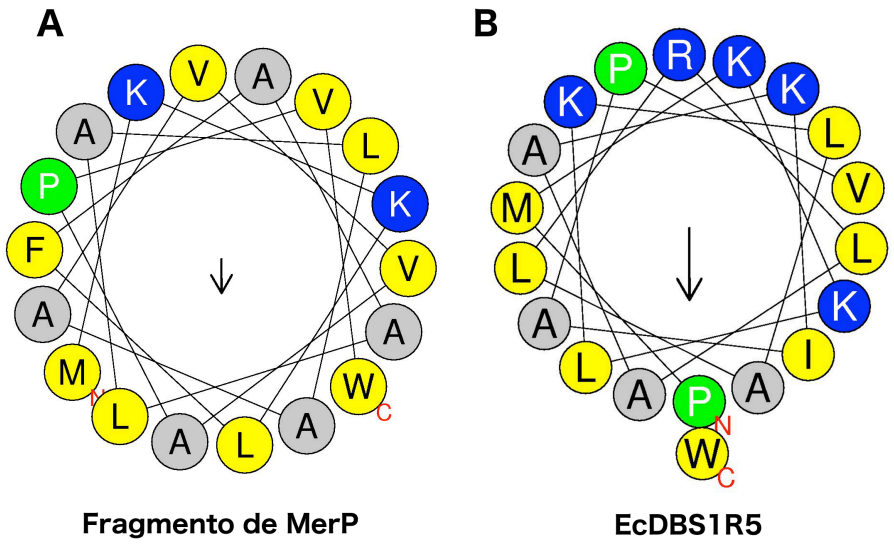

Figura 6. Diagramas de hélice para o fragmento de MerP utilizado como peptídeo parental (A) e EcDBS1R5 (B). O vetor de momento hidrofóbico está representado por setas a partir do centro dos diagramas, enquanto que o valor estimado do momento hidrofóbico resultante é proporcional ao tamanho das setas.

Dessa forma, considerando o potencial antibacteriano previamente estabelecido por Porto *et al.* (2018), bem como o conjunto de propriedades físico-químicas característico de PAMs e observado em EcDBS1R5, este peptídeo foi utilizado neste estudo, em adição ao peptídeo polialanina *Pa*-MAP 1.9, para estudos detalhados em relação ao seu potencial terapêutico.

2. JUSTIFICATIVA

A busca por novos antibióticos tem-se intensificado nas últimas décadas em resposta aos relatos cada vez mais frequentes de patógenos multirresistentes, principalmente aqueles organizados em consórcios, denominados biofilmes. Os efeitos colaterais causados por alguns antibióticos hoje disponíveis no mercado também se mostram um desafio adicional, destacando a necessidade de estudos mais elaborados acerca das propriedades físico-químicas desses medicamentos sobre os patógenos alvos, bem como sobre o ser humano. Neste cenário, aparecem os peptídeos antimicrobianos (PAMs), os quais se mostram presentes em todos os grupos de seres vivos desempenhando papel crucial na proteção contra microrganismos patogênicos, muitas vezes sendo reconhecidos como primeira linha de defesa contra patógenos. PAMs ricos em alanina, por exemplo, são conhecidos pela sua tendência em se organizar em hélice, onde é possível realizar a medição de carga, hidrofobicidade e momento hidrofóbico para estas moléculas. Essas propriedades estão, aparentemente, envolvidas nas interações entre PAMs helicoidais e membranas bacterianas, onde o aumento da hidrofobicidade leva ao aumento das afinidades dos PAMs pelas caudas de fosfolipídios, a intensificação do momento hidrofóbico pode favorecer a conformação em hélice, bem como o aumento da carga pode levar a melhores interações com membranas aniônicas. Interessantemente, estes parâmetros vem sendo amplamente estudados e aplicados também ao desenho computacional automatizado de novos PAMs. Dessa forma, o presente estudo visou caracterizar dois novos PAMs, sendo eles um peptídeo polialanina (*Pa*-MAP1 1.9) e em peptídeo desenhado computacionalmente (EcDSB1R5) acerca de suas propriedades antibacterianas, antibiofilme e anti-infecciosas, bem como possíveis mecanismos de ação e comportamento estrutural em diferentes ambientes miméticos.

3. OBJETIVOS

Analisar funcional e estruturalmente dois peptídeos sintéticos, incluindo um peptídeo polialanina (*Pa*-MAP 1.9) derivado de *Pleuronectes americanus*, e um peptídeo desenhado computacionalmente (EcDBS1R5) derivado de *E. coli*, a partir de ensaios antibacterianos, antibiofilme, hemolítico e citotóxicos *in vitro*, assim como ensaios anti-infecciosos em modelos animais. Ademais, foram também investigados os possíveis mecanismos de ação de *Pa*-MAP 1.9, bem como o comportamento estrutural de ambos os PAMs por meio de ferramentas biofísicas computacionais e experimentais.

3.1. Objetivos específicos

- Sintetizar quimicamente os peptídeos *Pa*-MAP 1.9 e EcDBS1R5 e conferir sua massa molecular por espectrometria de massas;
- Determinar o potencial antibacteriano de *Pa*-MAP 1.9 e EcDBS1R5 perante cepas Gram-negativas e Gram-positivas, susceptíveis e resistentes, bem como avaliar seu potencial antibiofilme frente a *P. aeruginosa*, *E. coli* e *K. pneumoniae*;
- Determinar os efeitos citotóxico de *Pa*-MAP 1.9 e EcDBS1R5 frente a células RAW 264.7, células endoteliais de veia umbilical humana (HUVEC) e adipócitos de camundongos (3T3-L1);
- Avaliar a ação hemolítica de *Pa*-MAP 1.9 e EcDBS1R5 frente a eritrócitos humanos;
- Avaliar o potencial citotóxico de EcDBS1R5 em células cancerígenas, incluindo linhagens celulares de câncer de próstata (PC-3), câncer de mama (MCF-7) e adenocarcinoma de cólon (HT-29);
- Determinar a atividade *in vivo* de EcDBS1R5 em modelo de infecção cutânea causada por *P. aeruginosa*;
- Analisar as alterações morfológicas causadas em cepas de *E. coli* por concentrações crescentes de *Pa*-MAP 1.9 utilizando microscopia de força atômica;

- Investigar o potencial de *Pa*-MAP 1.9 em causar o rompimento de vesículas miméticas constituídas por diferentes proporções de fosfolipídios (POPC; POPG; POPS), lipopolissacarídeos e colesterol;

- Caracterizar a estrutura secundária de *Pa*-MAP 1.9 e EcDBS1R5 por dicroísmo circular (DC) em diferentes ambientes, incluindo água, tampão, 2,2,2-trifluoroetanol (TFE) e SDS.

- Predizer a estrutura tridimensional de *Pa*-MAP 1.9 por meio de modelagem molecular, avaliando as trajetórias do modelo de menor energia livre em condições das similares às de DC, durante 100 ns de dinâmica molecular;

- Realizar a predição das interações atômicas (acoplamento molecular) entre o melhor modelo teórico tridimensional de *Pa*-MAP 1.9 e membranas miméticas constituídas das mesmas proporções de fosfolipídios utilizadas nos experimentos de rompimento de vesículas.

- Analisar os deslocamentos químicos secundários para os hidrogênios alfa (Hα) de EcDBS1R5 por meio RMN em TFE 30%;

- Analisar os deslocamentos químicos dos prótons amídicos de EcDBS1R5 por meio de experimentos de coeficiente de temperatura em TFE 30%;

- Determinar a estrutura tridimensional de EcDBS1R5 em TFE 30%.

www.nature.com/scientificreports

SCIENTIFIC REPORTS

OPEN

A polyalanine peptide derived from polar fish with anti-infectious activities

Received: 14 September 2015
Accepted: 22 January 2016
Published: 26 February 2016

Marlon H. Cardoso[2,3,4], Suzana M. Ribeiro[2,3], Diego O. Nolasco[1,6], César de la Fuente-Núñez[7,9], Mário R. Felício[8], Sónia Gonçalves[8], Carolina O. Matos[5], Luciano M. Liao[5], Nuno C. Santos[8], Robert E. W. Hancock[7], Octávio L. Franco[1,2,3,4] & Ludovico Migliolo[2,3]

Due to the growing concern about antibiotic-resistant microbial infections, increasing support has been given to new drug discovery programs. A promising alternative to counter bacterial infections includes the antimicrobial peptides (AMPs), which have emerged as model molecules for rational design strategies. Here we focused on the study of *Pa*-MAP 1.9, a rationally designed AMP derived from the polar fish *Pleuronectes americanus*. *Pa*-MAP 1.9 was active against Gram-negative planktonic bacteria and biofilms, without being cytotoxic to mammalian cells. By using AFM, leakage assays, CD spectroscopy and *in silico* tools, we found that *Pa*-MAP 1.9 may be acting both on intracellular targets and on the bacterial surface, also being more efficient at interacting with anionic LUVs mimicking Gram-negative bacterial surface, where this peptide adopts α-helical conformations, than cholesterol-enriched LUVs mimicking mammalian cells. Thus, as bacteria present varied physiological features that favor antibiotic-resistance, *Pa*-MAP 1.9 could be a promising candidate in the development of tools against infections caused by pathogenic bacteria.

In recent decades, improvements in the prevention and treatment of infectious diseases caused by pathogenic microorganisms has been of great importance in reducing morbidity and mortality, leading to a better quality of life and longer life expectancy[1]. However, antibiotics have been widely and sometimes indiscriminately used, which has resulted in the emergence of pathogens with multi-drug resistance in a wide range of bacterial species, including *Escherichia coli*, *Staphylococcus aureus, Pseudomonas aeruginosa, Klebsiella pneumoniae* and many other species[2]. Conversely, the rate of discovery of new antibiotics has steadily plummeted. Additionally, the occurrence and treatment of biofilm infections has appeared as one of the biggest challenges in the medical field with no available antibiotics that were developed to treat such infections. Biofilms are characterized as being a structured consortium of microorganisms connected by a complex matrix composed of polysaccharide(s), protein and DNA, that grows on biotic or abiotic surfaces via a multistage process[3]. It has been established that pathogenic bacteria are predominantly organized in biofilms, which are the cause of 65% to 80% of all bacterial infections in humans[3,4]. Biofilm growth represents a unique growth state whereby bacteria have major physiological and organizational differences, in particular leading to 10- to 1000- fold increased (adaptive) resistant to conventional antibiotics[3,4].

[1]Programa de Pós-Graduação em Ciências Genômicas e Biotecnologia, Universidade Católica de Brasília, Brasília-DF, Brazil. [2]Centro de Análises Proteômicas e Bioquímicas, Pós-Graduação em Ciências Genômicas e Biotecnologia, Universidade Católica de Brasília, Brasília-DF, Brazil. [3]S-inova, Programa de Pós-Graduação em Biotecnologia, Universidade Católica Dom Bosco, Campo Grande-MS, Brazil. [4]Programa de Pós-Graduação em Patologia Molecular, Faculdade de Medicina, Universidade de Brasília, Brasília-DF, Brazil. [5]Instituto de Química, Universidade Federal de Goiás, Goiânia-GO, Brazil. [6]Research Laboratory of Electronics, Massachusetts Institute of Technology (MIT), Cambridge, Massachusetts, USA. [7]Centre for Microbial Diseases and Immunity Research, Department of Microbiology and Immunology, University of British Columbia, Vancouver, Canada. [8]Instituto de Medicina Molecular, Faculdade de Medicina, Universidade de Lisboa, Lisbon, Portugal. [9]Synthetic Biology Group, MIT Synthetic Biology Center, Research Laboratory of Electronics, Department of Biological Engineering, Department of Electrical Engineering and Computer Science, Massachusetts Institute of Technology, Cambridge, Massachusetts, United States of America. Broad Institute of MIT and Harvard. Correspondence and requests for materials should be addressed to O.L.F. (email: ocfranco@gmail.com)

In this context, investigating and improving on natural compounds has been of great interest in the search for promising alternatives to conventional medicines. In recent years, cationic amphipathic peptides termed anti-microbial peptides (AMPs) have been widely investigated as a promising alternative for the treatment of infections caused by pathogenic microorganisms[5]. These molecules have been isolated from a wide number of organisms including plants[6], animals[7] and bacteria[8]. These peptides tend to have multiple targets that can include the cytoplasmic membrane permeability barrier, macromolecular processes dependent on the membrane, including cell wall biosynthesis and cell division, and/or other intracellular targets including RNA and protein synthesis[5]. Moreover, recent evidence indicates that AMPs' ability to act on intracellular targets can either occur as a major mechanism of action after having crossed the membrane without causing disruptive processes, or as a secondary and/or additional mechanism to membrane disruption[9].

Currently, some of the largest challenges in working with AMPs involve their cytotoxicity against mammalian cells, as well as their cost of production. Thus, the rational design of AMPs has gained great prominence in the scientific field, aiming to develop AMPs that are more active, less cytotoxic and possible to produce on an industrial scale[10]. Early studies of rational design played an important role in the identification of optimal AMP physicochemical properties, such as appropriate hydrophobicity, charge and amphipathic structural arrangement, which are all directly related with their antimicrobial activities. Template-based designs taking in account charge and amphipathicity have also been used based on modified amino acid residues of well-known AMPs in order to improve their activities[5]. Jiang and co-workers[11] have recently introduced a new concept of template-based design involving the arrangement of lysine and arginine residues in the center of the non-polar region of amphipathic α-helical AMPs in order to enhance peptide's selectivity against both eukaryotic and prokaryotic cell membranes. In addition to these strategies, biophysical studies have been used to evaluate AMP activities and design improved analogues by predicting and characterizing their structures in different environments, as well as performing molecular modelling, dynamics and docking simulations at atomic levels[5].

This work focuses on a novel polyalanine-rich cationic AMP, named *Pa*-MAP 1.9, that was rationally designed based on a synthetic multifunctional peptide (*Pa*-MAP) derived from HPLC-8, a peptide originally isolated from the polar fish *Pleuronectes americanus*[12]. Here, we report the antimicrobial activities of this peptide, mainly against *Enterococcus faecalis*, *S.aureus*, *E. coli* and *K. pneumoniae* planktonic bacteria, as well as *K. pneumoniae* and *E. coli* biofilms. Furthermore, biophysical experiments, using circular dichroism (CD), fluorescence spectroscopy and atomic force microscopy (AFM), in combination with *in silico* studies such as molecular modelling, dynamics and docking, were performed to obtain insights into the structure of *Pa*-MAP 1.9, as well as its mechanism of action.

Results

***Pa*-MAP 1.9 synthesis and mass spectrometry analysis.** *Pa*-MAP 1.9 (NH_2-LAAKLTKAATKLTAALT KLAAALT-COOH) was designed, and synthetized by Fmoc strategy loosely based on the sequence of a previously described multifunctional peptide, *Pa*-MAP (NH_2-HTASDAAAAAALTAANAAAAAAASMA-COOH)[12], in which the net charge and hydrophobic moment were increased, hydrophobic amino acid frequency was decreased (since high hydrophobicity favors toxicity) and alanine residues were distributed along the molecule in order to obtain a linear cationic peptide with predicted helical stretches. MALDI-ToF analysis showed greater than 95% purity and an ion mass of 2668.0 m/z, in agreement with the theoretical calculated molecular mass for this peptide (Fig. S1).

***In vitro* antimicrobial assays.** *Pa*-MAP 1.9 was evaluated for its ability to inhibit the growth of different bacteria grown planktonically and in biofilms. *Pa*-MAP 1.9 was able to inhibit the growth of *Enterococcus faecalis*, *E. coli* and *K. pneumoniae* planktonic cells with minimal inhibitory concentrations (MICs) of 1.5, 6–12 and 24–96 μM, respectively (Table 1). However, no antibacterial activity was observed against *P. aeruginosa* and *S. aureus*, even at the maximum concentration used for this assay (115 μM). Against bacteria in their biofilm growth state, *Pa*-MAP 1.9 was considerably more potent, with (MBICs) of 3.0 and 1.1 μM (Table 1) against *E. coli* and *K. pneumoniae* biofilms respectively. At these same concentrations, flow cell analysis revealed that pre-formed *E. coli* and *K. pneumoniae* biofilms (Fig. 1a,c) were strongly or completely inhibited, with a strong decrease in biofilm volume and height (Fig. 1b,d).

Hemolytic and cytotoxicity assays. *Pa*-MAP 1.9 did not show neither hemolytic activity against human erythrocytes or cytotoxic effects against RAW 264.7 monocyte cell line up to 115 μM, the maximum concentration used in the bioassays (Table 1).

Atomic force microscopy analysis. AFM was used to image the possible AMP-induced damage of the Gram-negative bacterial envelope. At 6 μM (MIC), *Pa*-MAP 1.9 induced slight morphological changes in the form of increased surface roughness in *E. coli* (Fig. 2b), relative to the untreated control (Fig. 2a). Damage was more evident at 300 μM (50-fold the MIC), where substantial bacterial surface disruption was observed (Fig. 2c).

Permeabilization of lipid vesicles. The ability of *Pa*-MAP 1.9 to disrupt large unilamellar vesicles (LUVs) with compositions roughly mimicking bacterial membranes was also analyzed. Vesicles were prepared with encapsulated carboxyfluorescein (CF), and then incubated with *Pa*-MAP 1.9 concentrations up to 1.0 μM. The percentages of leakage were evaluated as previously described[13], by assessing the differences over time in the emission of CF (which fluoresces more strongly upon leakage from the vesicles), with 100% of leakage corresponding to full disruption of lipid vesicles. The data showed that the peptide induced leakage of vesicles containing anionic lipids such as 1-palmitoyl-2-oleoyl-sn-glycero-3-phospho-(1′–sn-glycerol) (POPG), 1-palmitoyl-2-oleoyl-sn-glycero-3-phospho-L-serine (POPS) or lipopolysaccharide (LPS), requiring only 0.25 μM peptide for almost complete permeabilization (Fig. 3a). Moreover, at 0.75 μM of *Pa*-MAP 1.9, full leakage was reached for all other vesicles containing anionic phospholipids (Fig. 3b). In contrast, zwitterionic vesicles

Bacterial strains	MIC for *Pa*-MAP 1.9 (μM)
Enterococcus faecalis (ATCC 19433)	1.5
Escherichia coli (ATCC 8739)	6
Escherichia coli (KPC 001812446)	6
Escherichia coli (KPC 002101123)	12
Klebsiella pneumoniae (ATCC 13883)	24
Klebsiella pneumoniae (KPC 002210477)	24
Klebsiella pneumoniae (KPC 001825971)	96
Pseudomonas aeruginosa (ATCC 27853)	>115
Staphylococcus aureus (ATCC 25923)	>115
Bacterial strains	MBIC (μM)
Escherichia coli (ATCC O157)	3
Klebsiella pneumoniae (KPC 001825971)	1.1
Cell line	Cytotoxic activity (μM)
RAW 264.7 (mouse leukemic monocyte macrophage)	>115
Cell type	Hemolytic activity (μM)
Human erythrocytes	>115

Table 1. Antibacterial, anti-biofilm, cytotoxic and hemolytic activities of *Pa*-MAP 1.9.

of 1-palmitoyl-2-oleoyl-sn-glycero-3-phosphocholine (POPC) or POPC/Cholesterol (Chol) (70:30) clearly demonstrated reduced leakage, even at the maximum concentration used for this experiment (Fig. 3a,b). The results obtained demonstrate the specificity of the AMP for negatively charged membranes, such as those from Gram-negative bacteria and are consistent with the lack of toxicity for mammalian cells, which contain largely neutral or zwitterionic lipids on their external leaflet.

Structural analysis. Circular dichroism spectroscopy studies were performed in water, 2,2,2-trifluoroethanol (TFE) 50% (v:v) and sodium dodecyl sulfate (SDS) 28 mM. When analyzed in water, the peptide showed no stable at pH values ranging from 3 to 10 (Fig. 4a). However, at pH 11 this *Pa*-MAP 1.9 produced a CD spectrum characteristic of an α-helix conformation, with two negative bands at ~205 and ~222 nm, presenting 14% of ellipticity (Fig. 4a). When analyzed in 50% TFE, *Pa*-MAP 1.9 adopted a well-defined α-helix structure at all pH values presenting a positive band at 190 nm and two negative bands at ~205 and ~222 nm (Fig. 4b). Similar results were observer for the CD spectrum in anionic lipid-like environment, where the same positive and negative bands could be observed, indicating helical conformation (Fig. 4c).

To obtain insights into the three-dimensional structure of *Pa*-MAP 1.9, molecular modelling simulations were performed. The lowest free-energy theoretical model for *Pa*-MAP 1.9 revealed a well-defined α-helical conformation (Fig. 5b), and also revealed an amphipathic character (Fig. 5c) when modelled based on the antifreeze peptide (PDB code: 1wfa) isolated from *P. americanus*, which presented 58% identity over part of its sequence with the *Pa*-MAP 1.9 primary sequence (Fig. 5a). When evaluated using PROCHECK[14], the average score for dihedral angles (ϕ-ψ, χ and ω), jointly with the main-chain covalent forces for the best model, was 0.23, which is within the expected range for a reliable structure. Moreover, a Ramachandran plot showed that 100% of the amino acid residues of *Pa*-MAP 1.9 were located in the most favorable regions. Furthermore, three-dimensional structural superposition (3DSS) analysis revealed that the root mean square deviation (RMSD) between the theoretical and experimental models was equal to 0.567 Å. Based on those data, this model was selected for further *in silico* studies.

Like the CD analysis, molecular dynamics simulations of the peptide were implemented in three different environments including pure water, water and TFE mixture 50% (v:v) and water where the peptide was in contact with an SDS micelle. The simulations were performed to better understand the behavior of the three-dimensional theoretical structure of the above-described *Pa*-MAP 1.9 in different environments. After 100 ns of molecular dynamics simulations in water, it was possible to observe high values of RMSD and root mean square fluctuation (RMSF), revealing the instability of *Pa*-MAP 1.9 in this environment. In addition, it was observed a decrease in the radius of gyration (approximately from 1.3 to 0.6 nm), as well as in the solvent-accessible surface area (SASA) (Fig. 6a). These parameters, allied to the three-dimensional structures observed throughout the simulation, revealed that, consistent with the CD spectra, *Pa*-MAP 1.9 seems to lose its α-helical structure in water, also tending to hide its hydrophobic amino acid residues by adopting a coil conformation with a short central α-helix since the 20 ns of simulation (Fig. 7a). It can also be associated with a decrease of approximately 0.8 nm^2 in the SASA (Fig. 6a). On the other hand, simulations performed in water and TFE demonstrated that, in this solvent, *Pa*-MAP 1.9 was able to maintain its initial structure during the 100 ns, presenting only a few structural changes at the N-terminus (Fig. 7b). In comparison with the simulation in water, it was also possible to note decreased RMSD, RMSF, radius of gyration and SASA values, indicating improved structural stability in TFE (Fig. 6b). As expected, simulations in the presence of a micelle containing 128 SDS residues confirmed the preference of *Pa*-MAP 1.9 for amphipathic anionic environments, preserving its α-helical structure. In this simulation, as for 50% TFE, only a slight RMSD variation of 0.3 nm was observed, stabilizing then between 0.4 and 0.6 nm, indicating few deviations in the input and output structures along the 100 ns (Fig. 6c). Moreover, the radius of gyration

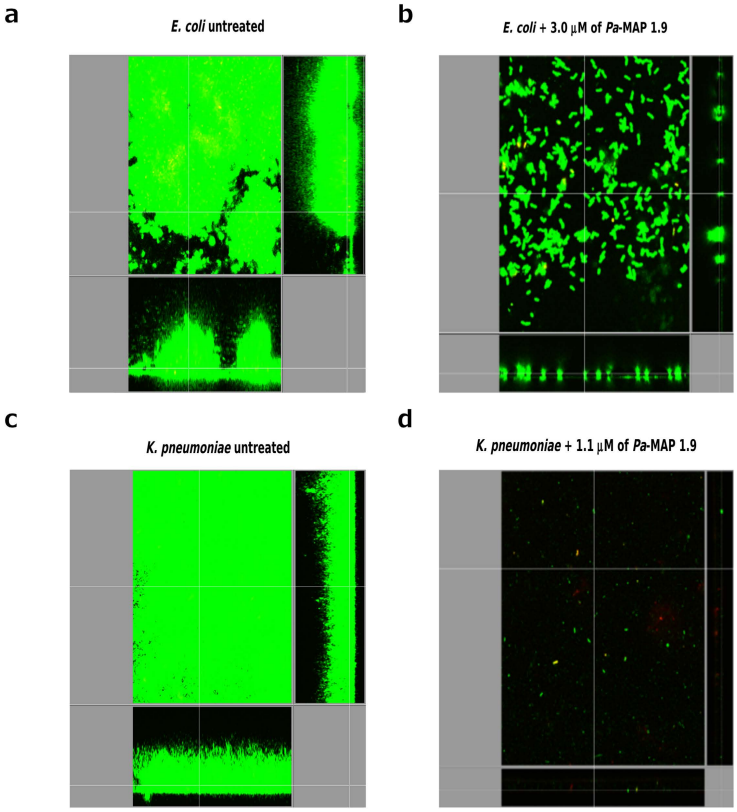

Figure 1. Flow-cell analysis of *E. coli* and *K. pneumoniae* biofilm formation in the absence and presence of *Pa*-MAP 1.9. Pre-formed *E. coli* biofilm before (**a**) and after (**b**) treatment with 3.0 μM of *Pa*-MAP 1.9 (**b**). Pre-formed *K. pneumoniae* biofilm before (**c**) and after (**d**) treatment with 1.1 μM of *Pa*-MAP 1.9.

was also equivalent to that for TFE simulation, remaining around 1.2 nm (Fig. 6c). In addition, SASA seemed to be conserved in these two simulations, varying from 19 to 23 nm during the 100 ns (Fig. 6c). However, contrary to what was obtained in 50% TFE, a more significant fluctuation could be observed at the C-terminus region of *Pa*-MAP 1.9 when in contact with SDS micelles, as demonstrated in Figs 6c and7c.

By using our best theoretical model for *Pa*-MAP 1.9, we also predicted the affinity and atomic interactions of this peptide with mimetic membranes containing the same lipid compositions experimentally tested on the leakage studies. Fifty runs of molecular docking were performed, and all peptide/membrane complexes were ranked by their affinity, in kcal.mol^{-1}. The best affinity values for *Pa*-MAP 1.9 in POPC/POPS (Fig. 8a) and *Pa*-MAP 1.9 in POPC/Chol (Fig. 8b) were −5.4 and −3.7 kcal.mol^{-1}, respectively, corroborating our experimental results, wherein *Pa*-MAP 1.9 seemed to interact better with anionic vesicles and Gram-negative bacteria with anionic lipid compositions. Furthermore, in both complexes, *Pa*-MAP 1.9 maintained a well-defined α-helical conformation during the simulations (Fig. 8a,b). In the complex of *Pa*-MAP 1.9 with POPC/POPS it was possible to predict 10 interactions (Fig. 8c) divided into hydrogen bonds (HB), involving nitrogen (N), oxygen (O/OG1) atoms of Leu1, Thr10, Lys11,18 and Ala15,22 from *Pa*-MAP 1.9, and saline bonds (SB), involving positively charged nitrogen atoms of the side chain (NZ) of Lys4,7,11,18 from *Pa*-MAP 1.9, ranging from 2.8 to 3.6 Å of distance (Table 2). On the other hand, in the complex of *Pa*-MAP 1.9 with POPC/Chol, only 6 HBs could be observed (Fig. 8d), involving O/OG1 atoms of Ala2 and Thr6,10,13,17,28 from *Pa*-MAP 1.9 and oxygen atoms (O3) from cholesterol, with distances between 2.7 and 3.4 (Table 2).

Discussion

Here we describe the functional and structural characterization of *Pa*-MAP 1.9, a rationally-designed cationic AMP based on a multifunctional peptide analogue from *P. americanus*, denominated *Pa*-MAP[12]. In our

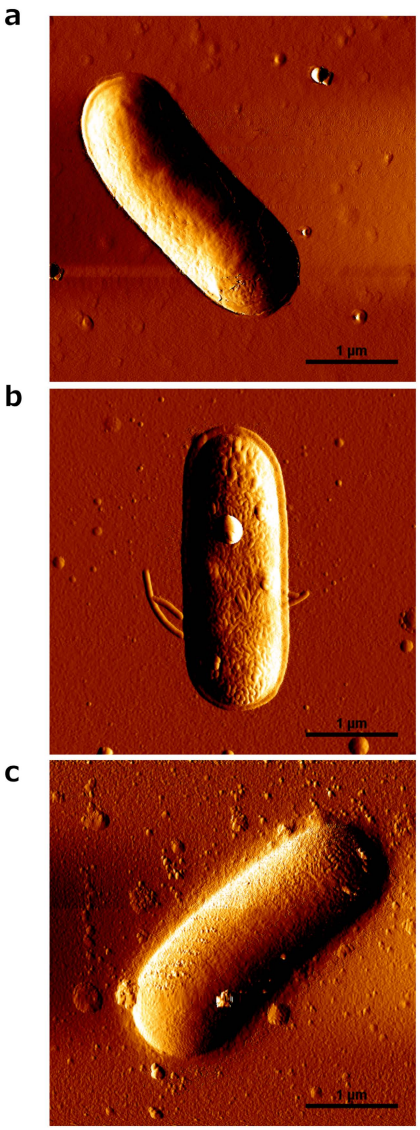

Figure 2. Atomic force microscopy (AFM) images of *E. coli* in the absence and presence of *Pa*-MAP 1.9. Untreated bacteria (control) (**a**), bacteria treated with 6 µM (**b**) and 300 µM (**c**) of *Pa*-MAP 1.9. Total scanning area per image: $4 \times 4\,\mu m^2$; scale bar: 1 µM.

antibacterial assays, *Pa*-MAP 1.9 revealed better activities mainly against Gram-negative bacterial strains (*E. faecalis*, *E. coli* and *K. pneumoniae*), with lower MIC against *E. coli* (6 µM) when compared with its precursor *Pa*-MAP (30 µM)[12]. Similar enhanced activities against Gram-negative strains have also been reported for other AMPs isolated or derived from the winter flounder *P. americanus*, as it is the case of pleurocidin, a cationic α-helical peptide with high activities against *E. coli* and *Pseudomonas aeruginosa*, with MIC values below 1 µM[16]. Moreover, other fish derived AMPs, such as pardaxin (*Purdachirus marmorutus*) and piscidins-1, -2, -3 and -4

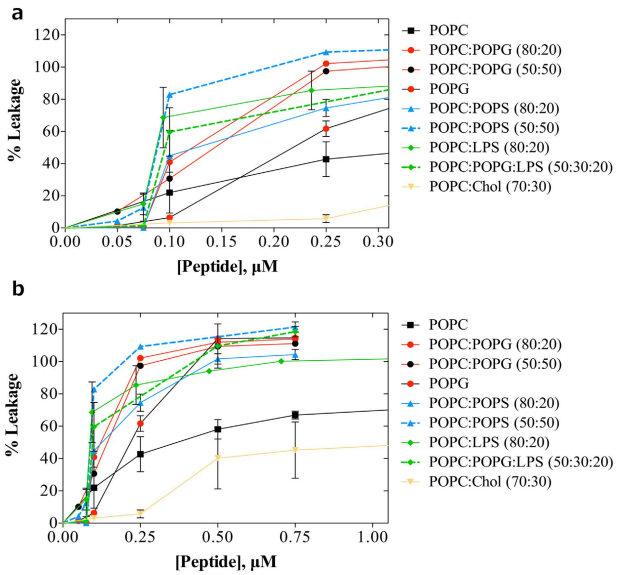

Figure 3. Leakage experiments performed with increasing concentrations of *Pa*-MAP 1.9 against large unilamellar vesicles. Percentage of carboxyfluorescein release (CF) in unilamellar vesicles composed of different proportions of POPC, POPG, POPS, LPS and cholesterol induced by different peptide concentration, ranging from 0.0 to 0.3 μM (**a**) and from 0.0 to 1 μM (**b**).

(*Morone chrysops*; *Morone saxatilis*), were also active against the human pathogens *E. coli*, *Acinetobacter calcoaceticus*, *P. aeruginosa*, *S. typhimurium* and *Shigella flexneri*[18,20].

In addition to direct antibacterial assays, we also studied the antimicrobial ability of *Pa*-MAP 1.9 in preventing biofilm growth, as well as combating pre-formed bacterial biofilms, since different physiological conditions occur in these consortiums when compared to planktonic bacteria, and this leads to increased antibiotic resistance. Previous studies have shown that anti-biofilm activity is independently determined compared to antibacterial activity against planktonic (free-swimming) bacteria. These assays revealed that *Pa*-MAP 1.9 is a promising anti-biofilm peptide with activity at concentrations 90-fold lower than the MIC against one strain of *Klebsiella pneumoniae*. Similar to our results, Tao and colleagues[15] described the anti-biofilm potential of another *P. americanus* derived-peptide (pleurocidin) in combating *Streptococcus mutans* biofilm, causing a reduction in *S. mutans* biomass upon treatment with 11.8 μM of the peptide. In addition, a study performed by Choi and Lee[16] reported that, below 0.7 μM, pleurocidin could inhibit pre-formed *E. coli* and *P. aeruginosa* biofilms, causing biomass reductions of 22.4 and 48.3%, respectively. Interestingly, the concentration of *Pa*-MAP 1.9 required to combat *E. coli* and *K. pneumoniae* biofilms were lower than its MIC values for the two studied strains. Similar findings were previously made for other small synthetic cationic peptides (IDR-1018, and DJK-6), in circumstances where MIC values against *K. pneumoniae* could not be determined ($>64\,\mu g.mL^{-1}$), but relevant anti-biofilm properties were detected at $2–4\,\mu g.mL^{-1}$ (MBIC)[21]. Flow cell experiments showed even better results, with just $2\,\mu g.mL^{-1}$ of IDR-1018 and DJK-6 being necessary to eliminate most pre-existing *K. pneumoniae* biofilms[21]. These findings were consistent with the concept that anti-biofilm peptides act by several mechanisms that include dispersing bacterial biofilms and triggering death of cells within biofilms, but that these activities involve independent mechanisms from those determining AMP activity.

When evaluated with regard to its potential for causing morphological damage to the surface of *E. coli*, *Pa*-MAP 1.9 showed dose-dependent action. Below its MIC, only slight changes were observed, suggesting that *Pa*-MAP 1.9 might insert into the *E. coli* cytoplasmic membrane and translocate to act on intracellular targets. However, substantial cell damage was observed upon 50-fold increasing its concentration suggesting lytic activity at concentrations above the MIC[22]. This behavior was also described for Sub3, an AMP optimized based on bovine bactenecin[23] whereby it was found that Sub3 antimicrobial activity is intrinsically related to membrane binding and its cell-penetrating ability, since at 1 to 10 μM it did not affect the surface of *E. coli* strains[17]. Nevertheless, increasing the concentration of this peptide to 100 μM led to evident morphological damage, including bacterial surface disruption. However, as for *Pa*-MAP 1.9, such a high concentration was not required for the lethal activities of this peptide.

The results obtained in the AFM experiments encouraged us to study the ability of *Pa*-MAP 1.9 to interact with lipid vesicles mimicking different types of biological membranes. *Pa*-MAP 1.9 was effective in disrupting

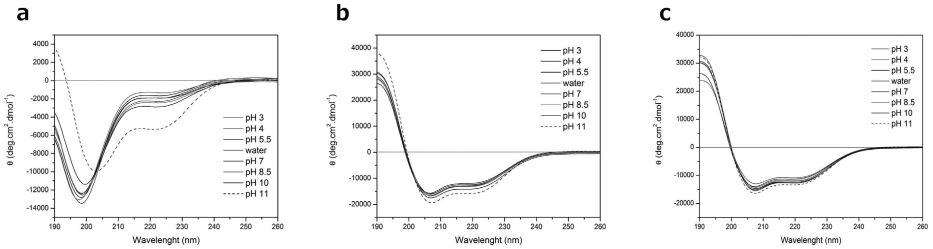

Figure 4. Circular dichroism analysis of *Pa*-MAP 1.9. CD spectra of *Pa*-MAP 1.9 solubilized in water (pH 3–11) (**a**) TFE 50% (v:v; pH 3–11) (**b**) and SDS 28 mM (pH 3–11) (**c**) Higher helical contents (ellipticity) were obtained/calculated at pH 11, highlighted as dashed lines in all conditions.

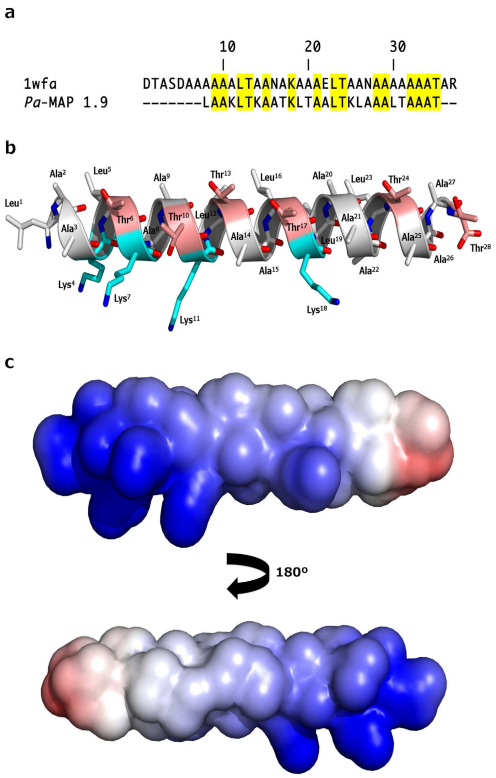

Figure 5. BLASTp analysis, predicted secondary structure and electrostatic potential of *Pa*-MAP 1.9. Alignment between the query (*Pa*-MAP 1.9) and template (PDB: 1wfa) primary sequences, highlighting (yellow) the identical residues (**a**). Lowest free-energy three-dimensional theoretical model for *Pa*-MAP 1.9: in white, non-polar residues; in pink, polar residues; in cyan, basic residues (**b**). Adaptive Poisson-Boltzmann solver (APBS) electrostatic potential of *Pa*-MAP 1.9; potential ranges from −10.9 kT/e (red) to + 10.1 kT/e (blue) (**c**).

vesicles constituted with some proportion of anionic lipids such as POPS, POPG and LPS. However, as anticipated based on our bioassays, much higher concentrations were necessary for the disruption of vesicles composed

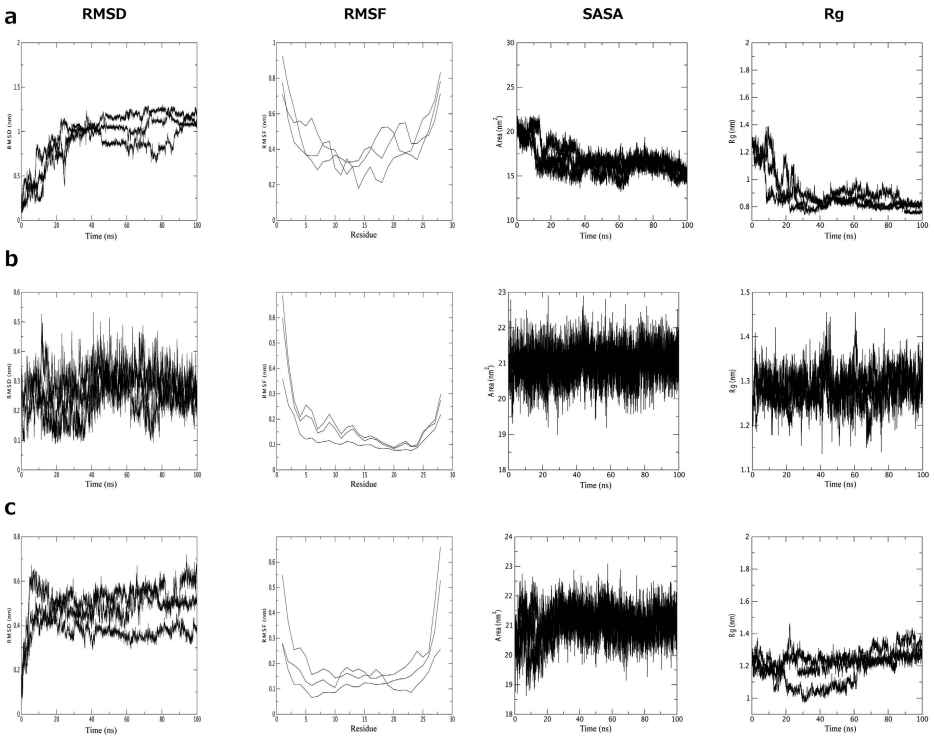

Figure 6. Graphical representation of physicochemical parameters resulted from molecular dynamics simulations. *Pa*-MAP 1.9 molecular dynamics simulations in water (**a**), TFE 50% (v:v) (**b**) and SDS micelle (**c**), yielding the parameters root mean square deviation (RMSD), root mean square fluctuation (RMSF), solvent-surface accessible area (SASA) and radius of gyration (Rg) for each conditions.

solely of zwitterionic or neutral phospholipids (*e.g.*, POPC and cholesterol). Furthermore, cholesterol-containing membranes could not be significantly disrupted even at the highest concentrations tested. Apparently, cholesterol which is present in mammalian cells assists in the stability of these membranes[24]. *Pa*-MAP 1.9 lipid-selective disruption of biomembrane model systems was also consistent with our bioassays, wherein this peptide clearly presented better activities against Gram-negative bacteria, which contains a more anionic surface based on lipid composition. In addition, the observation that *Pa*-MAP 1.9 revealed no cytotoxicity against different mammalian cell lines could have been related in part to its inability to disrupt neutral (zwitterionic) phospholipids and cholesterol-containing membranes. Lee and colleagues[25] observed similar results in studying detergent-like membrane disruption by four magainin analogues, namely MSI-78, MSI-367, MSI-594 and MSI-843. In this context, by using solid-state nuclear magnetic resonance (NMR), the authors concluded that MSI peptides fragmented LUVs by using a detergent-like process. As described here for *Pa*-MAP 1.9, MSI peptides were able to disrupt anionic (POPG; POPS) LUVs at much lower concentrations than zwitterionic (POPC) LUVs. However, when cholesterol was present in the lipid vesicle composition, the disruptive potential of these peptides drastically decreased.

Similarly, in molecular docking simulations, the complex of *Pa*-MAP 1.9 with POPC/POPS revealed improved affinity values and a larger number of atomic interactions of different types (hydrogen and saline bonds), when compared to the *Pa*-MAP 1.9 complex with POPC/Cholesterol (Table 2). In a recent work, the parent peptide *Pa*-MAP was predicted to form hydrophobic interactions with a DPPC membrane with a lower affinity value (-3.1 kcal.mol^{-1}), when compared with the results here[22]. Comparing the primary sequences of *Pa*-MAP and *Pa*-MAP 1.9, it was possible to observe a decrease in the hydrophobic residue content of *Pa*-MAP 1.9 (64%) when compared to *Pa*-MAP (73%), which is due to the substitution of *Pa*-MAP hydrophobic residues by hydrophilic ones in *Pa*-MAP 1.9. Similarly this was reflected in the hydrophobic moment of *Pa*-MAP 1.9, which was higher when compared to *Pa*-MAP, being 0.26 and 0.10 on the Eisenberg scale, respectively[26]. Furthermore, due to the addition of four lysine residues (Lys4, Lys7, Lys11 and Lys18) 1.9 had a net charge of $+4$, which made this peptide much more cationic than its precursor (net charge $= -1$), favouring its interaction with bacterial membranes.

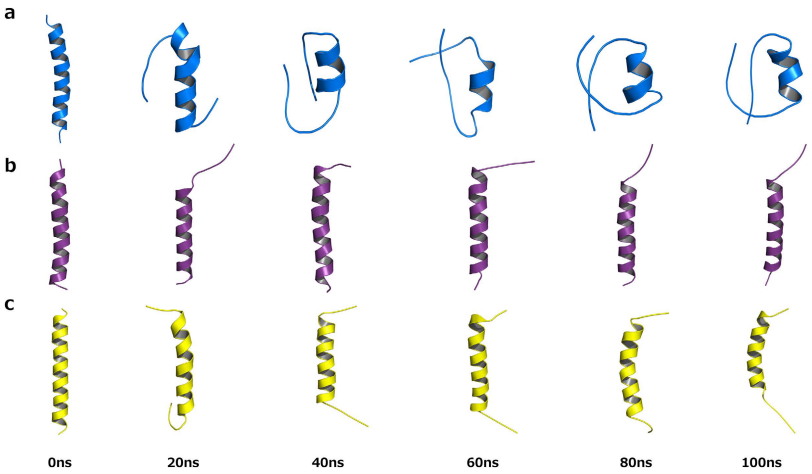

Figure 7. Three-dimensional theoretical structures snapshots of *Pa*-MAP 1.9 during 100 ns of molecular dynamics simulation. Evaluations were performed in water (**a**), TFE 50% (v:v) (**b**) and SDS micelle (**c**). The N-terminal region of the peptide is always at the bottom (top).

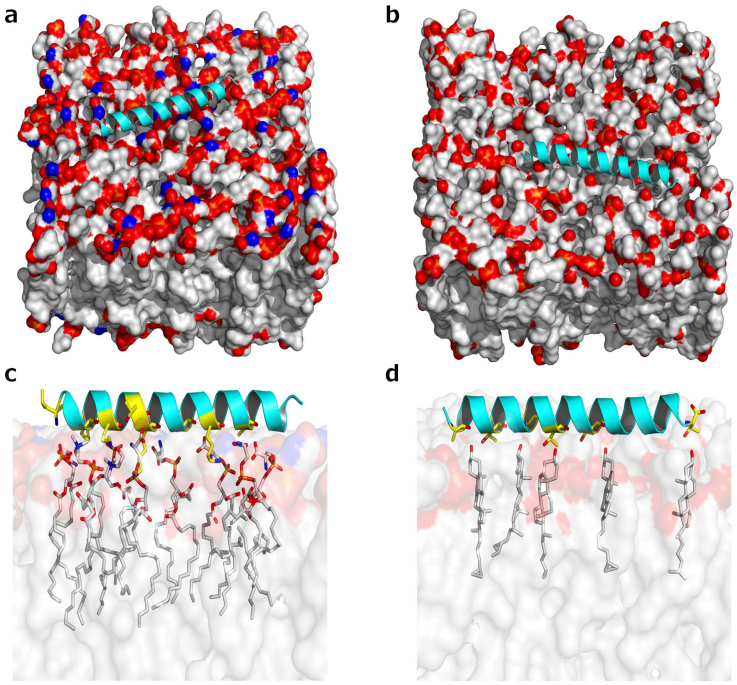

Figure 8. *In silico* interactions between *Pa*-MAP 1.9 and anionic/zwitterionic mimetic membranes. Three-dimensional theoretical representation of the complexes *Pa*-MAP 1.9–POPC/POPS (50:50) (**A**) and *Pa*-MAP 1.9–POPC/Chol (70:30) (**B**), as well as zoom images, revealing the amino acids residues from *Pa*-MAP 1.9 (yellow sticks) possibly involved in interactions with the phospholipids (white sticks) from both POPC/POPS (**C**) and POPC/Chol (**D**) mimetic membranes.

Pa-MAP 1.9			Distances (Å)	POPC/POPS (50:50)			Interactions
Residues	Positions	Atom Names		Lipids	Positions	Atom Names	
Leu	1	N	3.6	POPS	27	O14	HB
Lys	4	NZ	3.5	POPC	10	O14	SB
Lys	7	NZ	3.6	POPC	18	O13	SB
Thr	10	OG1	3.1	POPS	6	O13	HB
Lys	11	NZ	3.6	POPS	6	O13	SB
Lys	11	O	3.3	POPS	3	N	HB
Ala	15	O	3.5	POPS	2	O13	HB
Lys	18	NZ	3.5	POPS	4	O13	SB
Lys	18	O	3.5	POPS	4	O13	HB
Ala	22	O	2.8	POPS	9	O13	HB
Pa-MAP 1.9				POPC/Chol (70:30)			
Ala	2	O	2.7	Chol	7	O3	HB
Thr	6	OG1	3.0	Chol	7	O3	HB
Thr	10	OG1	2.8	Chol	2	O3	HB
Thr	13	OG1	3.4	Chol	9	O3	HB
Thr	17	O	3.2	Chol	15	O3	HB
Thr	28	OG1	2.7	Chol	50	O3	HB

Table 2. *In silico* predicted interactions between *Pa*-MAP 1.9 and anionic/zwitterionic mimetic membranes revealing the types and distances of atomic interactions occurring in these complexes.

In addition, the positioning of the amino acid residues of *Pa*-MAP 1.9 was designed to allow a more efficient distribution of hydrophobic and positively charged faces, favoring the amphipathicity of the molecule, as well as distributing alanine residues more evenly along the entire peptide, increasing the probability of helical structuring. These characteristics of *Pa*-MAP 1.9 would provide a major driving force for α-helix insertion into anionic bilayers, causing their perturbation, as well as entropy loss due to peptide loss of water interactions caused by translocation into the membrane and consequent α-helix structuring, as observed previously for other polyalanine peptides[27].

Structurally, the CD spectra of *Pa*-MAP 1.9 revealed a well-defined α-helix conformation in the presence of SDS or 50% TFE. Similarly, Perrin and colleagues[28] described the CD spectrum of piscidins 1 and 3 which, in the presence of anionic vesicles (POPC/POPG 3:1 and POPE/POPG 1:1), tend to become arranged into α-helical structures. In water, however, Campagna and co-workers[19] reported that piscidins 1 had an unstructured conformation, also observed by NMR spectroscopy. Consistent with this work, when *Pa*-MAP 1.9 was solubilized in water, independently of the pH, a random conformation could be observed. These events could also be three-dimensionally visualized in our molecular dynamics simulations, whereby *Pa*-MAP 1.9 presented a well-defined α-helix conformation when in 50% TFE and in contact with an SDS micelle, but a coil conformation with a small, central α-helix in water. These features are consistent both with other AMPs from polar fishes as with the polyalanine precursor *Pa*-MAP[12]. Such environment-dependent behavior is important not only for the understanding of membrane-based mechanisms of action, but also are crucial for the elucidation of how AMPs reorient, insert into and translocate across membranes to act on intracellular targets.

In summary, *Pa*-MAP 1.9 proved to be a useful candidate for the treatment of Gram negative bacteria infections, especially in their biofilm state. It works through a dose-dependent mechanism of action, without being hemolytic and cytotoxic against mammalian cells. We also demonstrated that *Pa*-MAP 1.9 was able to interact with bacterial mimetic membranes and vesicles, adopting a well-defined α-helical conformation that might favor *Pa*-MAP 1.9 orientation and insertion into lipid bilayers to perform its activities.

Material and Methods

***Pa*-MAP 1.9 synthesis and mass spectrometry analysis.** *Pa*-MAP 1.9 was purchased from Peptide 2.0 Incorporated (USA), which synthesized the peptide at 95% purity (after TFA removal) by the stepwise solid-phase method using the N-9-fluorenylmethyloxycarbonyl (Fmoc) chemistry on a Rink amide resin. *Pa*-MAP 1.9 molecular mass was confirmed by MALDI-ToF MS/MS analysis (Autoflex, Bruker Daltonics, Billerica, MA). The synthetic peptide concentrations for all *in vitro* experiments were determined using the measurement of absorbance at 205, 215 and 225 nm.

***In vitro* antimicrobial assays.** For antimicrobial assays, strains of *E. coli* (ATCC 8739, KPC 001812446 and KPC 002101123), *K. pneumoniae* (KPC 001825971, KPC 002210477 and ATCC 13883), *E. faecalis* (ATCC 19433), *P. aeruginosa* (ATCC 27853) and *S. aureus* (ATCC 25923) were grown in Luria Bertani (LB) broth overnight, at 37°C. MIC measurements were performed in LB medium with 5×10^6 CFU and dilutions of *Pa*-MAP 1.9 from 0.7 to 115 μM. MIC was assessed as the minimal 100% inhibitory concentration of peptide after 12 h of incubation at 37 °C. During this period, the absorbance was measured in a plate reader (Bio-Rad 680 Microplate Reader) at 595 nm every 30 min. Bacteria in LB medium and in several dilution of chloramphenicol were used as negative and positive controls, respectively. All experiments were performed in triplicate.

Anti-biofilm assays. Dilutions (1/100) of overnight cultures of *E. coli* (ATCC O157) and *K. pneumoniae* (KPC 001825971) grown overnight in LB medium were incubated in basal medium 2 (BM2) [62 mM potassium phosphate buffer (pH 7), 7 mM $(NH_4)_2SO_4$, 2 mM $MgSO_4$, 10 μM $FeSO_4$, 0.5% glucose], in 96-well cell culture cluster round bottom microplate in the presence of *Pa*-MAP 1.9 for 24 h at 37 °C. Positive growth control contained only bacteria, and negative control wells contained broth only. Afterwards, planktonic cells were removed and microplate wells were washed twice with deionized water. The attached bacteria remaining were stained with 100 μL of 0.1% (m/v) crystal violet for 20 min. The microplates was rinsed twice with deionized water, air-dried and resolubilized with 110 μL of ethanol 70%. The content of the microplate was transferred to a new microplate, and the MBIC of *Pa*-MAP 1.9 was accessed at 595 nm in a microtiter plate reader (Bio-Tek Instruments Inc., VT).

Flow cell assays. Biofilms were grown for 72 h, at 37 °C in flow chambers with channel dimensions of 1 by 4 by 40 mm, as previously described[29]. For treatment of pre-formed biofilms, bacteria were allowed to develop structured 2-day-old biofilms prior to treatment with *Pa*-MAP 1.9, for the following 24 h. The medium used to allow biofilm growth was (BM2) containing 0.4% (wt/vol) glucose as a carbon source. Silicone tubing (VWR, 0.062 in ID by 0.125 in OD by 0.032 in wall) was autoclaved, and the system was assembled and sterilized by pumping a 0.5% hypochlorite solution through the system at 6 rpm for 30 min using a Watson Marlow 205S multi-channel peristaltic pump. The system was then rinsed at 6 rpm with sterile water and medium for 30 min each. Flow chambers were inoculated by injecting 400 μl of an overnight culture diluted at 1:25 (v/v). After inoculation, chambers were left without flow for 2 h, after which medium was pumped through the system at a constant rate of 0.5 rpm for 48 h. After this time, treatments were diluted in BM2 medium at desired concentration and pumped through the system for 24 h. Biofilm cells were stained using the LIVE/DEAD BacLight Bacterial Viability kit (Molecular Probes, Eugene, OR) prior to microscopy experiments. A ratio of SYTO-9 (green fluorescence, live cells) to propidium iodide (PI) (red fluorescence, dead cells) of 1:5 was used. Microscopy was done using a confocal laser-scanning microscope (Olympus, Fluoview FV1000) and three-dimensional reconstructions were generated using the Imaris software package (Bitplane AG).

Hemolytic assay. The hemolytic activity of *Pa*-MAP 1.9 was assessed by using human erythrocytes approved by the ethics committee of FEPECS (number: 396.061) and registered in Brazil Platform (number: 16131213.0.0000.5553), according with the approved guidelines. The cells were stored at 4 °C. Erythrocytes were washed three times with 50 mM phosphate buffer, pH 7.4. The peptide solution was added to the erythrocyte suspension (1%, by volume), at a final concentration ranging from 0.7 to 115 mM in a final volume of 100 mL. Samples were incubated at room temperature for 60 min. Hemoglobin release was monitored by measuring the supernatant absorbance at 540 nm. Zero hemolysis control (blank) was determined with erythrocytes suspended in the presence of 50 mM phosphate buffer, pH 7.4, and for positive control (100% of erythrocyte lyses); an aqueous solution of 1% (by volume) triton X-100 dissolved in distilled water was used instead of the peptide solution. Hemolytic assays were performed in triplicate.

Cytotoxicity assays. For the cytotoxic assays, confluent RAW 264.7 (mouse leukemic monocyte macrophage) cell line was challenged with 0.7 to 115 μM of *Pa*-MAP 1.9 and incubated at 37 °C in a 5% CO_2 atmospheres for 48 h, according to previously described methodology[12]. Experiments were performed in triplicate and cells imaged using an inverted optical microscope (Leitz) in order to describe morphological alterations. The neutral red dye-uptake method[30] was used to evaluate cell viability. Cells were incubated in the presence of 0.01% (by weight) neutral red solution for 3 h at 37 °C in a 5% CO_2 atmosphere. After, the medium was removed and the cells were fixed with 4% formalin in phosphate-buffered saline, pH 7.2. The dye, incorporated by the viable cells, was eluted by using a mixture of methanol:acetic acid:water (50:1:49,v:v:v), and the dye uptake was determined by measuring the absorbance at 490 nm in an automatic spectrophotometer (ELx800 TM-Bio-TeK Instruments, Inc.). The cytotoxic assays were performed in triplicate.

Bacteria preparation and atomic force microscopy imaging. The effects of *Pa*-MAP 1.9 on *E. coli* (ATCC 25922) were evaluated by AFM imaging as previously described[31,32]. Bacterial cells were incubated with *Pa*-MAP 1.9 at 0, 6 and 300 μM in growth broth, at 37 °C, for 1 h. A 100 μL droplet of each sample was applied onto poly-L-lysine-coated glass slide and left at 25 °C for 30 min. After deposition, the sample was rinsed 10 times with Milli-Q water, and left to air-dry. AFM images were obtained on a JPK Instruments NanoWizard II (Berlin, Germany) mounted on a Carl Zeiss Axiovert 200 inverted microscope (Jena, Germany). Images were performed in intermittent contact mode (air) using ACL silicon cantilevers from AppNano (Huntingdon, UK) with a tip radius of 6 nm, a resonant frequency of approximately 190 kHz and a spring constant of 58 N m^{-1}. All images were obtained with similar AFM parameters (setpoint, scan rate and gain values). The scan rate was set between 0.3 and 0.6 Hz and the setpoint was close to 0.3 V. Height and error signals were collected and images were analyzed with the JPK image processing software v. 5.1.13.

LUV preparation and leakage assays. Large unilamellar vesicles with ~100 nm of diameter were obtained by extrusion of multilamellar vesicles, as described elsewhere[33]. POPC, POPG and POPS were obtained from Avanti Polar Lipids (Alabaster, AL), while LPS (*E. coli* O26:B6) and cholesterol (Chol) were obtained from Sigma (St. Louis, MO). The LUVs studied were zwitterionic (pure POPC and POPC:Chol 70:30) or anionic (POPC:POPG 80:20, POPC:POPG 50:50, pure POPG, POPC:POPS 80:20, POPC:POPS 50:50, POPC:LPS 80:20 and POPC:POPG:LPS 50:30:20). For lipid film formation with LPS, it was dissolved in chloroform:methanol (2:1) and the solution was vortexed and bath sonicated at 40 °C for 15 min. Stock solutions were kept at 4 °C overnight

before measurements. Phosphate buffer saline (20 mM sodium phosphate, 150 mM NaCl) pH 7.4 was used for these measurements.

Peptide-induced lipid vesicle leakage was measured as previously described[13], by fluorescence spectroscopy, on a Varian Cary Eclipse fluorescence spectrophotometer (Mulgrave, AU). In this assay, we monitored the release of 5,(6)-carboxyfluorescein (CF; Sigma, St. Louis, MO), trapped in the LUV. LUVs were prepared as described above, with dried film hydration in phosphate buffered saline (PBS) containing 100 mM CF (pH was adjusted to 7.4 with NaOH). Free CF was removed by passing the suspension through an EconoPac 10 DG column from Bio-Rad (Richmond, CA), where the vesicles are eluted with the void volume[13]. Aliquots of the liposomal stock preparations (diluted to 10 μM) were incubated with different concentrations of the peptide at 25 °C. Fluorescence was recorded continuously for 30 min, with excitation at 492 nm and emission at 517 nm (5 and 10 nm excitation and emission slits, respectively).

Circular dichroism. CD measurements were performed on a JASCO J-815 spectropolarimeter (Easton, MD), equipped with a Peltier-type temperature controller and a thermostable cell holder, also interfaced with a thermostatic bath. Spectra were recorded in 0.1 cm path length quartz cells at a peptide concentration ranging from 0.05 to 0.5 $mg.mL^{-1}$ in 2 mM Na-acetate buffer at pH 3.0, 2 mM Na-acetate buffer at pH 4.0, 2 mM Na-acetate buffer at pH 5.5, deionized water (Milli-Q), 2 mM Tris-HCl buffer at pH 7.0, 2 mM Tris-HCl buffer at pH 8.5, 2 mM glycine-NaOH buffer at pH 10.0 and 2 mM glycine-NaOH buffer at pH 11.0. Four consecutive scans were accumulated and the average spectra stored. *Pa*-MAP 1.9 analysis in the presence of SDS and TFE were performed in the same quartz cell with a 0.1 cm path length at 20 °C. The spectra were recorded between 190 and 260 nm at a scan speed of 50 $nm.min^{-1}$ and four scans were performed per sample. The spectra were recorded in three average environments: distilled water, 28 mM SDS and TFE 50% in water (v:v). The observed ellipticity was converted into the mean residue ellipticity [θ] based on a mean molecular mass per residue of 115 Da. The data were corrected for the baseline contribution of the buffer and the observed ellipticities at 222 nm were recorded. The α-helical content of the peptides was calculated from mean residual ellipticity at 222 nm ($[\theta]_{222}$) using the following equation: $f_H = [\theta]_{222}/[-40{,}000(1 - 2.5/n)]$, where f_H and n represent the α-helical content and the number of peptide bonds, respectively[34]. All spectra were acquired at 37 °C.

Molecular Modelling. Initially, BLASTp[35] was performed in order to find the best primary sequence template for molecular modelling. After that, 200 theoretical three-dimensional models were constructed by using Modeller v. 9.12[36], based on an antifreeze peptide primary sequence (PDB code: 1WFA) isolated from *P. americanus*. The lowest free-energy theoretical model for *Pa*-MAP 1.9 was then selected and used for validation procedures. Firstly, PROCHECK[14] evaluated peptide's geometry, stereochemistry and energy distribution, also calculating its average score for dihedral angles, jointly with covalent forces. Moreover, 3DSS[37] was also used for (RMSD) calculation by superimposing Cα-traces and backbones of both theoretical and template tridimensional structures.

Molecular Dynamics. The molecular dynamics simulations for the *Pa*-MAP1.9 were carried out in three different steps. The first one was performed in water; the second one in water and TFE 50%/50% (volume/volume) and, the third one was carried out in water with an anionic environment (SDS micelle). All simulations were performed by using the computational package GROMACS v.4[38] with the GROMOS96 43A1 force field implemented. As initial structure for dynamics simulations the best tridimensional theoretical model of *Pa*-MAP 1.9 was used, which was immersed in 7,897 water molecules in a cube box with sides measuring 6.22 nm. In order to neutralize the system's charge, chloride ions were also added (four ions in this case). TFE 50% simulation was carried out with 1,892 and 2,023 water molecules, as well as 459 and 354 TFE molecules in a cube box with sides measuring 4.78 nm. The final step (SDS) was carried out in a dodecahedral box with a minimum distance of 0.7 nm between the non-water molecules and the box's frontiers. In this case, *Pa*-MAP 1.9, a SDS micelle with 128 phospholipid residues, 13,021 water molecules and chlorine ions constituted the system. Geometry of water and water/TFE 50% molecules was constrained using the SETTLE algorithm[39]. Moreover, the LINCS algorithm was used to link all the atom bond length. Particle Mesh Ewald (PME) was also used for electrostatic corrections, with a radius cut-off of 1.4 nm in order to minimize the computational simulation time. The same radius cut off was also used for van der Waals interactions. The list of neighbors of each atom was updated every 10 simulation steps of 2 fs each. A conjugate gradient (2 ns) and the steepest descent algorithms (2 ns) were implemented for energy minimization. After that, the system underwent a normalization of pressure and temperature, using the integrator stochastic dynamics (SD), 2 ns each. The system with minimized energy and balanced temperature and pressure was carried out using a step of position restraint, using the integrator Molecular Dynamics (MD), for 2 ns. The simulations were carried out at 27 °C *in silico*, aiming to understand the structural conformation of the peptide more nearly to that observed *in vitro* bioassays. The total time of *Pa*-MAP 1.9 simulation was 100 ns, in triplicate.

Molecular Docking. For molecular docking studies, the program AUTODOCK 4.2[40] was used in order to predict the possible modes of interaction between *Pa*-MAP 1.9 and anionic as well as zwitterionic mimetic membranes, based on what was done in the leakage experiments. For this, the CHARMM-GUI[41] server was used for membrane construction, constituted of POPC/POPS (50:50) (anionic environment) and POPC/cholesterol (70:30) (zwitterionic environment), with $75 \times 75 \times 45$ $Å^3$ of dimension. Moreover, by using AutoDock Tools, all the hydrogen atoms were added and a grid box of $60 \times 60 \times 20$ points with spacing of 1.0 Å was centered on the membrane surfaces. Furthermore, AutoDock Tools were also used for peptide manipulation, where the maximum freedom to side chains was unlocked. The molecular docking simulations were programed for fifty random runs, with the generated structures being ranked based on their affinity values in $kcal.mol^{-1}$. After all

simulations, PyMOL was used to predict peptide-membrane interactions, respecting the distance of 3.6 Å for all atoms involved.

References

1. Alanis, A. J. Resistance to antibiotics: Are we in the post-antibiotic era? *Arch. Med. Res.* **36,** 697–705 (2005).
2. Giamarellou, H. & Poulakou, G. Multidrug-Resistant Gram-Negative Infections What are the Treatment Options? *Drugs* **69,** 1879–1901 (2009).
3. de la Fuente-Núñez, C., Reffuveille, F., Fernandez, L. & Hancock, R. E. W. Bacterial biofilm development as a multicellular adaptation: antibiotic resistance and new therapeutic strategies. *Curr. Opin. Microbiol.* **16,** 580–589 (2013).
4. Van Acker, H., Van Dijck, P. & Coenye, T. Molecular mechanisms of antimicrobial tolerance and resistance in bacterial and fungal biofilms. *Trends Microbiol.* **22,** 326–333 (2014).
5. Fjell, C. D., Hiss, J. A., Hancock, R. E. & Schneider, G. Designing antimicrobial peptides: form follows function. *Nat. Rev. Drug. Discov.* **11,** 37–51 (2012).
6. Candido, E. D. *et al.* The use of versatile plant antimicrobial peptides in agribusiness and human health. *Peptides* **55,** 65–78 (2014).
7. de Oliveira, N. G., Cardoso, M. H. E. S. & Franco, O. L. Snake venoms: attractive antimicrobial proteinaceous compounds for therapeutic purposes. *Cell. Mol. Life Sci.* **70,** 4645–4658 (2013).
8. Yang, S. C., Lin, C. H., Sung, C. T. & Fang, J. Y. Antibacterial activities of bacteriocins: application in foods and pharmaceuticals. *Frontiers Microbiol.* **5,** 1–10 (2014).
9. Hale, J. D. & Hancock, R. E. Alternative mechanisms of action of cationic antimicrobial peptides on bacteria. *Expert Rev. Anti-infe.* **5,** 951–959 (2007).
10. Anderson, A. C. The process of structure-based drug design. *Chem. Biol.* **10,** 787–797 (2003).
11. Jiang, Z., Vasil, A. I., Gera, L., Vasil, M. L. & Hodges, R. S. Rational design of alpha-helical antimicrobial peptides to target Gram-negative pathogens, *Acinetobacter baumannii* and *Pseudomonas aeruginosa*: utilization of charge, 'specificity determinants,' total hydrophobicity, hydrophobe type and location as design parameters to improve the therapeutic ratio. *Chem. Biol. Drug Des.* **77,** 225–240 (2011).
12. Migliolo, L. *et al.* Structural and functional characterization of a multifunctional alanine-rich peptide analogue from *Pleuronectes americanus*. *PLoS One* **7,** e47047 (2012).
13. Domingues, M. M., Castanho, M. A. & Santos, N. C. rBPI(21) promotes lipopolysaccharide aggregation and exerts its antimicrobial effects by (hemi)fusion of PG-containing membranes. *PLoS One* **4,** e8385 (2009).
14. Laskowski, R. A., Macarthur, M. W., Moss, D. S. & Thornton, J. M. Procheck - a Program to Check the Stereochemical Quality of Protein Structures. *J. Appl. Crystallogr.* **26,** 283–291 (1993).
15. Tao, R. *et al.* Antimicrobial and antibiofilm activity of pleurocidin against cariogenic microorganisms. *Peptides* **32,** 1748–1754 (2011).
16. Choi, H. & Lee, D. G. Antimicrobial peptide pleurocidin synergizes with antibiotics through hydroxyl radical formation and membrane damage, and exerts antibiofilm activity. *Bba-Gen Subjects* **1820,** 1831–1838 (2012).
17. Torcato, I. M. *et al.* The Antimicrobial Activity of Sub3 is Dependent on Membrane Binding and Cell-Penetrating Ability. *Chembiochem* **14,** 2013–2022 (2013).
18. Noga, E. J. *et al.* Piscidin 4, a novel member of the piscidin family of antimicrobial peptides. *Comp. Biochem. Phys. B.* **152,** 299–305 (2009).
19. Campagna, S., Saint, N., Molle, G. & Aumelas, A. Structure and mechanism of action of the antimicrobial peptide piscidin. *Biochemistry* **46,** 1771–1778 (2007).
20. Oren, Z. & Shai, Y. A class of highly potent antibacterial peptides derived from pardaxin, a pore-forming peptide isolated from Moses sole fish *Pardachirus marmoratus*. *Eur. J. Biochem.* **237,** 303–310 (1996).
21. Ribeiro, S. M. *et al.* Anti-biofilm peptides increase the susceptibility of carbapenemase-producing *Klebsiella pneumoniae* clinical isolates to beta-lactam antibiotics. *Antimicrob. Agents Chemother.* **32,** 3906–3912 (2015).
22. Nascimento, J. M. *et al.* Elucidation of mechanisms of interaction of a multifunctional peptide Pa-MAP with lipid membranes. *Bba-Biomembranes* **1838,** 2899–2909 (2014).
23. Hilpert, K., Volkmer-Engert, R., Walter, T. & Hancock, R. E. High-throughput generation of small antibacterial peptides with improved activity. *Nat. Biotechnol.* **23,** 1008–1012 (2005).
24. Nguyen, L. T., Haney, E. F. & Vogel, H. J. The expanding scope of antimicrobial peptide structures and their modes of action. *Trends Biotechnol.* **29,** 464–472 (2011).
25. Lee, D. K., Bhunia, A., Kotler, S. A. & Ramamoorthy, A. Detergent-Type Membrane Fragmentation by MSI-78, MSI-367, MSI-594, and MSI-843 Antimicrobial Peptides and Inhibition by Cholesterol: A Solid-State Nuclear Magnetic Resonance Study. *Biochemistry* **54,** 1897–1907 (2015).
26. Eisenberg, D., Weiss, R. M. & Terwilliger, T. C. The hydrophobic moment detects periodicity in protein hydrophobicity. *Proc. Natl. Acad. Sci.* **81,** 140–144 (1984).
27. Ben-Tal, N., Ben-Shaul, A., Nicholls, A. & Honig, B. Free-energy determinants of alpha-helix insertion into lipid bilayers. *Biophys. J.* **70,** 1803–1812 (1996).
28. Perrin, B. S., Jr. *et al.* High-resolution structures and orientations of antimicrobial peptides piscidin 1 and piscidin 3 in fluid bilayers reveal tilting, kinking, and bilayer immersion. *J. Am. Chem. Soc.* **136,** 3491–3504 (2014).
29. de la Fuente-Núñez, C., Reffuveille, F., Haney, E. F., Straus, S. K. & Hancock, R. E. Broad-spectrum anti-biofilm peptide that targets a cellular stress response. *PLoS Pathog.* **10,** e1004152 (2014).
30. Borenfreund, E. & Puerner, J. A. Toxicity determined *in vitro* by morphological alterations and neutral red absorption. *Toxicol. Lett.* **24,** 119–124 (1985).
31. Alves, C. S. *et al.* Escherichia coli cell surface perturbation and disruption induced by antimicrobial peptides BP100 and pepR. *J. Biol. Chem.* **285,** 27536–27544 (2010).
32. Domingues, M. M. *et al.* Antimicrobial protein rBPI21-induced surface changes on Gram-negative and Gram-positive bacteria. *Nanomedicine: NBM* **10,** 543–551 (2015).
33. Mayer, L. D., Hope, M. J. & Cullis, P. R. Vesicles of variable sizes produced by a rapid extrusion procedure. *Biochim. Biophys. Acta.* **858,** 161–168 (1986).
34. Morrisett, J. D., David, J. S., Pownall, H. J. & Gotto, A. M. Jr. Interaction of an apolipoprotein (apoLP-alanine) with phosphatidylcholine. *Biochemistry* **12,** 1290–1299 (1973).
35. Altschul, S. F. *et al.* Gapped BLAST and PSI-BLAST: a new generation of protein database search programs. *Nucleic Acids Res.* **25,** 3389–3402 (1997).
36. Sali, A. & Blundell, T. L. Comparative protein modelling by satisfaction of spatial restraints. *J. Mol. Biol.* **234,** 779–815 (1993).
37. Sumathi, K., Ananthalakshmi, P., Roshan, M. N. A. M. & Sekar, K. 3dss: 3d Structural Superposition. *Nucleic Acids Res.* **34,** W128–W132 (2006).
38. Lindahl, E., Hess, B. & Van Der Spoel, D. GROMACS 3.0: a package for molecular simulation and trajectory analysis. *J. Mol. Model.* **7,** 306–317 (2001).

39. Miyamoto, S. & Kollman, P. A. Settle - an Analytical Version of the Shake and Rattle Algorithm for Rigid Water Models. *J. Comput. Chem.* **13,** 952–962 (1992).
40. Trott, O. & Olson, A. J. Software News and Update AutoDock Vina: Improving the Speed and Accuracy of Docking with a New Scoring Function, Efficient Optimization, and Multithreading. *J. Computat. Chem.* **31,** 455–461 (2010).
41. Jo, S., Lim, J. B., Klauda, J. B. & Im, W. CHARMM-GUI Membrane Builder for Mixed Bilayers and Its Application to Yeast Membranes. *Biophys. J.* **97,** 50–58 (2009).

Acknowledgements
Research reported in this publication was supported by the National Institute of Allergy and Infectious Diseases of the National Institutes of Health under Award Number R21AI098701, and by a grant from the Canadian Institutes. The content is solely the responsibility of the authors and does not necessarily represent the official views of the National Institutes of Health. R.E.W.H. holds a Canada Research Chair in Health and Genomics. C.D.L.F.-N. received a scholarship from the Fundación "la Caixa" and Fundación Canadá (Spain), and currently holds a postdoctoral scholarship from Fundación Ramón Areces (Spain). This work was also supported by Fundação para a Ciência e a Tecnologia–Ministério da Educação e Ciência (FCT-MEC, Portugal), including the fellowship SPRH/BD/100517/2014 to M.R.F., and by Marie Skłodowska-Curie Research and Innovation Staff Exchange (MSCA-RISE, European Union) project INPACT (call H2020-MSCA-RISE-2014, grant agreement 644167). M.H.C., L.M. and O.L.F. acknowledge funding from CNPq, CAPES, FUNDECT and FAPDF.

Author Contributions
M.H.C., L.M.L., N.C.S., R.E.W.H., L.M. and O.L.F. conceived and designed the experiments; M.H.C., S.M.R., D.O.N., C.D.L.F.-N., M.R.F., S.G. and C.O.M. performed the experiments and simulations; M.H.C., S.M.R., C.D.L.F.-N., M.R.F., S.G. and C.O.M. analyzed the data; M.H.C., R.E.W.H., M.R.F., N.C.S. andd O.L.F. wrote and organized the paper. All the authors have reviewed the manuscript.

Additional Information
Supplementary information accompanies this paper at http://www.nature.com/srep

Competing financial interests: The authors declare no competing financial interests.

How to cite this article: Cardoso, M. H. *et al.* A polyalanine peptide derived from polar fish with anti-infectious activities. *Sci. Rep.* **6**, 21385; doi: 10.1038/srep21385 (2016).

SCIENTIFIC REPORTS

OPEN

Corrigendum: A polyalanine peptide derived from polar fish with anti-infectious activities

Marlon H. Cardoso, Suzana M. Ribeiro, Diego O. Nolasco, César de la Fuente-Núñez, Mário R. Felício, Sónia Gonçalves, Carolina O. Matos, Luciano M. Liao, Nuno C. Santos, Robert E. W. Hancock, Octávio L. Franco & Ludovico Migliolo

Scientific Reports **6**:21385; doi: 10.1038/srep21385; published online 26 February 2016; updated 20 July 2016

In this Article, there is a typographical error in the Results section.

"*Pa*-MAP 1.9 (NH2-LAAKLTKAATKLTAALTKLAAALT-COOH) was designed …"

should read:

"*Pa*-MAP 1.9 (NH2-LAAKLTKAATKLTAALTKLAAALTAAAT-COOH) was designed …"

5. ARTIGO CIENTÍFICO PUBLICADO NA AMERICAN CHEMICAL SOCIETY (ACS) INFECTIOUS DISEASES

ACS Infectious Diseases

Article

Cite This: *ACS Infect. Dis.* 2018, 4, 1727−1736

pubs.acs.org/journal/aidcbc

A Computationally Designed Peptide Derived from *Escherichia coli* as a Potential Drug Template for Antibacterial and Antibiofilm Therapies

Marlon H. Cardoso,[†,‡,§,∥] Elizabete S. Cândido,[‡,§] Lai Y. Chan,[∥] Marcelo Der Torossian Torres,[⊥,#,▽] Karen G. N. Oshiro,[†,§] Samilla B. Rezende,[§] William F. Porto,[‡,§,⊗] Timothy K. Lu,[⊥,#] Cesar de la Fuente-Nunez,[⊥,#] David J. Craik,[∥] and Octávio L. Franco*[,†,‡,§]

[†]Programa de Pós-Graduação em Patologia Molecular, Faculdade de Medicina, Universidade de Brasília, Campus Darcy Ribeiro, Asa Norte, Brasília, DF 70910900, Brazil

[‡]Centro de Análises Proteômicas e Bioquímicas, Pós-Graduação em Ciências Genômicas e Biotecnologia, Universidade Católica de Brasília, SGAN 916 Módulo B, Asa Norte, Brasília, DF 70790160, Brazil

[§]S-inova Biotech, Programa de Pós-Graduação em Biotecnologia, Universidade Católica Dom Bosco Avenida Tamandaré 6000, Campo Grande, MS 79117900, Brazil

[∥]Institute for Molecular Bioscience, The University of Queensland, 306 Carmody Road, Brisbane, QLD 4072, Australia

[⊥]Synthetic Biology Group, MIT Synthetic Biology Center; The Center for Microbiome Informatics and Therapeutics; Research Laboratory of Electronics, Department of Biological Engineering, and Department of Electrical Engineering and Computer Science, Massachusetts Institute of Technology, Cambridge, Massachusetts 02139, United States

[#]Broad Institute of MIT and Harvard, Cambridge, Massachusetts 02139, United States

[▽]Centro de Ciências Naturais e Humanas, Universidade Federal do ABC, Santo André, SP 09210170, Brazil

[⊗]Porto Reports, Brasília, DF 70790160, Brazil

Supporting Information

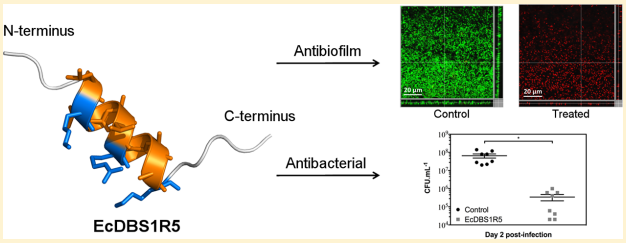

ABSTRACT: Computer-aided screening of antimicrobial peptides (AMPs) is a promising approach for discovering novel therapies against multidrug-resistant bacterial infections. Here, we functionally and structurally characterized an *Escherichia coli*-derived AMP (EcDBS1R5) previously designed through pattern identification [α-helical set (KK[ILV]$_{(3)}$[AILV])], followed by sequence optimization. EcDBS1R5 inhibited the growth of Gram-negative and Gram-positive, susceptible and resistant bacterial strains at low doses (2−32 μM), with no cytotoxicity observed against non-cancerous and cancerous cell lines in the concentration range analyzed (<100 μM). Furthermore, EcDBS1R5 (16 μM) acted on *Pseudomonas aeruginosa* pre-formed biofilms by compromising the viability of biofilm-constituting cells. The *in vivo* antibacterial potential of EcDBS1R5 was confirmed as the peptide reduced bacterial counts by two-logs 2 days post-infection using a skin scarification mouse model. Structurally, circular dichroism analysis revealed that EcDBS1R5 is unstructured in hydrophilic environments, but has strong helicity in 2,2,2-trifluoroethanol (TFE)/water mixtures (v/v) and sodium dodecyl sulfate (SDS) micelles. The TFE-induced nuclear magnetic resonance structure of EcDBS1R5 was determined and showed an amphipathic helical segment with flexible termini. Moreover, we observed that the amide protons for residues Met2-Ala8, Arg10, Ala13-Ala16, and Trp19 in EcDBS1R5 are protected from the solvent, as their temperature coefficients values are more positive than −4.6 ppb·K^{-1}. In summary, this study reports a novel dual-antibacterial/antibiofilm α-helical peptide with therapeutic potential *in vitro* and *in vivo* against clinically relevant bacterial strains.

KEYWORDS: *antimicrobial peptides, bacterial resistance, bacterial biofilm, skin infection, biophysics*

Multidrug bacterial resistance is among the most significant health threats of the 21st century.[1] Approximately 15 million deaths were associated with bacterial infections in 2010, and

Received: August 24, 2018
Published: October 22, 2018

DOI: 10.1021/acsinfecdis.8b00219
ACS Infect. Dis. 2018, 4, 1727−1736

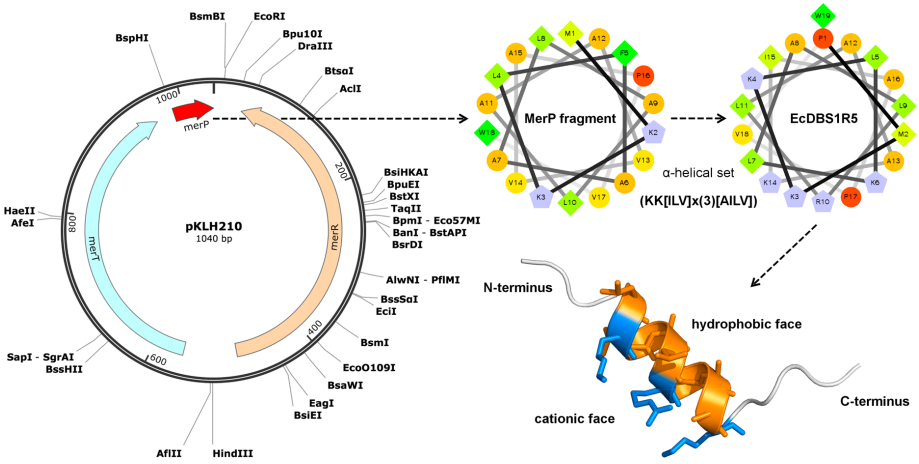

Figure 1. EcDBS1R5 design and solution NMR structure. Schematic representation of the *E. coli* plasmid (pKLH210) encoding the mercury ion transport protein fragment MerP (in red), which was used as template sequence for the computational design of EcDBS1R5 based on the α-helical set (KK[ILV]$x_{(3)}$[AILV]). The TFE-induced NMR structure of EcDBS1R5 is also shown, revealing a central α-helix arrangement with flexible termini.

the mortality indexes are rising.[2] Recently, the World Health Organization (WHO) described a global priority list of antibiotic-resistant bacteria, in which carbapenem-resistant *Acinetobacter baumannii* and *Pseudomonas aeruginosa*, carbapenem- and cephalosporin-resistant Enterobactereaceae strains are classified as critical priorities, whereas methicillin-resistant *Staphylococcus aureus* (MRSA) strains, as critical/high priority.[3] Bacterial infections caused by these strains may persist inside the host for long periods of time due to immunosuppression, immune evasion by the pathogen and/or ineffective killing by antibiotics.[1] The situation may become worse when persistent bacteria organize in multicellular consortiums known as biofilms,[4] which currently represent >60% of all human infections. In an attempt to counter this health crisis, several efforts are underway to develop novel antibiotic compounds based on natural and/or synthetic molecules.

Antimicrobial peptides (AMPs) represent promising alternatives to no-longer-effective antibiotics. These antimicrobials are well known for their broad-spectrum activity and diverse structures.[5] The search for natural AMPs started back in the 1920s[6] and has continued to the present day with a core focus on peptide purification and peptidomic approaches. Indeed, the isolation of AMPs from natural sources has allowed researchers to discover numerous AMP classes.[7−9] Although these discoveries represent an important first step for novel antibiotics formulation, their therapeutic index, stability, and *in vivo* bioavailability may be compromised due to high hemolytic and cytotoxic effects, as well as susceptibility to enzymatic degradation. In an attempt to overcome these obstacles, computer-aided design approaches have appeared as strategies to generate optimized synthetic AMPs.[5,10]

Since the post-genomic era, the number of sequences deposited in public databases has increased significantly, thus providing diverse biological information.[10] As a result of these advances, bioinformatics tools have been developed aiming to screen potential antimicrobial sequences within databases.[10] Recently, Porto et al.[11] reported a new bioinformatics tool, called Joker, to insert patterns into sequences for designing AMPs. In that work, the pattern (KK[ILV]$x_{(3)}$[AILV]) was retrieved from 248 α-helical AMPs deposited in the Antimicrobial Peptide Database (APD).[11,12] This method allowed the identification of template sequences from the National Center for Biotechnology Information (NCBI) non-redundant (NR) protein database that were further optimized by Joker in order to enhance antimicrobial effectiveness. Among the template sequences identified, a fragment of a mercury transporter protein from *Escherichia coli* (MerP, MKKLFAALALAA-VVAPVW) was selected, and nine variants were designed by Joker and denominated EcDBS1R1 to R9 (EcDBS: ***E. coli*** **d**ata**b**ase **s**equence). All the variants were tested against an engineered bioluminescent *P. aeruginosa* strain (H1001). The hemolytic property of all variants was also measured against human erythrocytes. Among the variants tested, EcDBS1R5 had a minimal inhibitory concentration (MIC) of 12.5 $\mu g \cdot mL^{-1}$ (5.8 μM), with no hemolytic effect reported at 200 $\mu g \cdot mL^{-1}$ (93.1 μM).[11]

In this context, this current study focused on the functional and structural characterization of this computationally designed AMP (EcDBS1R5: PMKKLKLALRLAAKIAPVW), which was derived from *E. coli* (Figure 1). The biological properties of EcDBS1R5 were investigated, including its antibacterial and antibiofilm activities, followed by detailed structural characterization using circular dichroism (CD) and nuclear magnetic resonance (NMR). So far, a total of 11 entries are listed in the APD[12] when searching for AMPs derived from *E. coli*, all of them belonging to the microcin (bacteriocin) family of AMPs.[13] Thus, here we also provide results that may lead to the generation of a new family of *E. coli*-derived AMPs with extended antimicrobial properties.

RESULTS AND DISCUSSION

EcDBS1R5 Background and Synthesis. The *E. coli* MerP fragment (MKKLFAALALAAVVAPVW) identified by Porto et al.[11] is an 18-amino acid peptide that, despite matching the α-helical pattern (KK[ILV]$x_{(3)}$[AILV]) described above, has physicochemical properties that may discourage its application as an AMP. This includes low net positive charge vs peptide

DOI: 10.1021/acsinfecdis.8b00219
ACS Infect. Dis. 2018, 4, 1727−1736

Table 1. Physicochemical Properties and Antimicrobial Prediction of EcDBS1R5 and Its Parent Peptide (MerP Fragment)

peptide	sequence	net charge (z)	hydrophobicity (%)	hydrophobic moment[a]	SVM[b]	RF[c]	DA[d]
MerP fragment	–MKKLFAALALAAVVAPVW	2	81.3	0.182	0.058	0.354	0.783
EcDBS1R5	PMKKL**KLALRLAAKI**APVW	5	57.9	0.413	0.356	0.635	0.870

[a]Hydrophobic moment calculated according to the Eisenberg scale.[43] [b]Support vector machine. [c]Random forest. [d]Discriminant analysis. The physicochemical properties were calculated on HeliQuest server.[44] The antimicrobial predictions were carried out using $CAMP_{R3}$.[45] Amino acid replacements in EcDBS1R5 are in bold type.

length, along with a high content of hydrophobic residues that are distributed along the entire helical segment, thus resulting in a low hydrophobic moment and amphipaticity. Thus, EcDBS1R5 was designed focusing on increasing the net positive charge and hydrophobic moment, as well as decreasing the overall hydrophobicity of this peptide. Residues Phe6, Ala7, Ala10, Val14, and Val15 in the MerP fragment were replaced by lysine, leucine, arginine, and isoleucine residues in EcDBS1R5 (Table 1), respectively, using the Joker algorithm.[11] These modifications directly interfered with the helical wheel diagram for EcDBS1R5, resulting in a defined distribution of cationic and hydrophobic residues along the sequence, thus favoring amphipaticity (Figure 1). Thus, to evaluate the biological potential and structural arrangement of EcDBS1R5, this peptides was chemically synthesized by solid-phase (Fmoc) at >95% purity, which was confirmed by UHPLC and MALDI-TOF (monoisotopic mass = 2147.3 Da) (Figure S1).

EcDBS1R5 Inhibits Planktonic Bacterial Growth and Compromises the Viability of Biofilm Cells. Only a few *E. coli*-derived AMPs have been reported to date, mostly including microcin family members. Microcin peptides belong to the bacteriocin class of AMPs and have been divided into two subgroups (1 and 2) according to their size (<5 kDa for subgroup 1 and 5−20 kDa for subgroup 2).[14] Antibacterial properties have been reported mainly for microcin subgroup 1 members.[13] Although promising inhibitory activities have been reported for these peptides (e.g., MICs ranging from 2.5 to 5 $\mu g \cdot mL^{-1}$ for microcin 25 against *E. coli*);[13] they have not yet been tested on antibiofilm assays. In the present study, we evaluated the antibacterial (free-floating bacteria) and antibiofilm properties of EcDBS1R5. Among the 12 bacterial strains tested, EcDBS1R5 shows promising activity against both a *E. coli* KpC+ resistant (MIC = 2 μM) free-floating strain and a clinical isolate of *A. baumannii* (MIC = 4 μM), which have been listed by the WHO in their high/critical priority list of pathogens.[3] *P. aeruginosa*, *K. pneumoniae*, and MRSA strains were included in this study as they are also part of the WHO list. Susceptible *K. pneumoniae* and *P. aeruginosa* PA14 were inhibited (MIC) at 8 μM, whereas *P. aeruginosa* PAO1 and MRSA strains were inhibited at 16 and 32 μM, respectively (Table 2). On the other hand, EcDBS1R5 was not active against a clinical isolate of *E. cloacae* and *K. pneumoniae* KpC+ at the highest concentration tested in the MIC assay (32 μM). The minimal bactericidal concentrations (MBCs) of EcDB1R5 are summarized in Table 2, revealing that, at 32 μM, this peptide not only inhibited the growth, but also killed the bacterial strains tested.

In addition to its broad-spectrum activity against planktonic (free-floating) bacteria, EcDBS1R5 was also characterized as an antibiofilm agent. Other AMPs have been described as dual-antibacterial/antibiofilm peptides (e.g., *Pa*-MAP 1.9 derived from a polar fish,[15] and clavanin A derived from tunicate hemocytes).[16] Moreover, AMPs lacking effectiveness toward planktonic bacteria have shown, in some cases, to be extremely active against biofilms and vice versa,[15,17] revealing how complex

Table 2. Antibacterial, Cytotoxic, and Hemolytic Activities for EcDBS1R5

	MIC[a] (μM)	MBC[b] (μM)
Bacterial Strains		
A. baumannii (clinical isolate 003326263)	4	16
E. cloacae (clinical isolate 1383251)	>32	>32
E. coli (ATCC 25922)	8	8
E. coli (KpC+ 001812446)	2	2
E. coli BL21	2	2
K. pneumoniae (ATCC 13883)	8	32
K. pneumoniae (KpC+ 001825971)	>32	>32
MRSA (clinical isolate 713623)	32	32
P. aeruginosa PA14	8	8
P. aeruginosa PAO1	16	16
S. aureus (ATCC 25923)	8	32
S. aureus (ATCC 12600)	16	16
Cell Line (Cytotoxicity Assays, IC_{50}[c])		
mouse adipocyte, 3T3-L1	nd	
human umbilical vein endothelial cells, HUVEC	nd	
human prostate cancer, PC-3	nd	
human breast cancer, MCF-7	nd	
human colon adenocarcinoma, HT-29	nd	
Cell Type (Hemolytic Assays)		
red blood cells	nd	

[a]MIC: minimal inhibitory concentration. [b]MBC: minimal bactericidal concentration. [c]IC_{50}: half maximal inhibitory concentration; nd: not determined at the highest concentration tested (100 μM). Three replicates for each condition were performed.

and distinct the modes of action of AMPs are on different bacterial modes of growth.

For the biofilm study, a *P. aeruginosa* strain was selected, as this bacterium is one of the main microorganisms involved in nosocomial infections. Moreover, the formation of biofilms represents a bottleneck in the treatment of *P. aeruginosa* infections.[18] The MIC of EcDBS1R5 against *P. aeruginosa* PAO1 (16 μM) was used to treat two-day-old biofilms. EcDBS1R5 caused the dispersion of *P. aeruginosa* biofilms by decreasing both the volume and height of the biofilms compared to the untreated control (Figure 2b−d). Moreover, EcDBS1R5 also compromised the viability of biofilm cells (Figure 2d). Similarly, Bessa et al.[18] recently reported that an ocellatin peptide (ocellatin-PT3) derived from frog skin has the ability to decrease the viability of *P. aeruginosa* cells within biofilms, also inducing slight biofilm disaggregation without completely eradicating the biofilms. In addition to the single action of AMPs toward biofilms, the synergy potential of this class of antimicrobials have been evaluated and expected to revert installed resistance to a particular antibiotic.[18] Ocellatin-PT3, for instance, have shown synergistic activities with ciprofloxacin and ceftazidime against *P. aeruginosa* biofilms.[18] Moreover, a

DOI: 10.1021/acsinfecdis.8b00219
ACS Infect. Dis. 2018, 4, 1727−1736

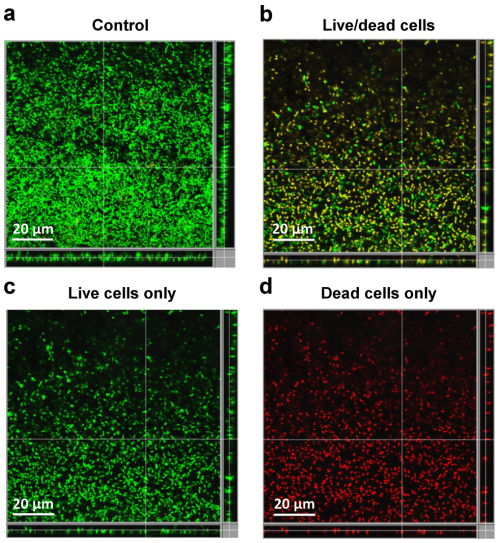

Figure 2. Antibiofilm activity of EcDBS15. Flow-cell analysis of two-day-old *P. aeruginosa* biofilms untreated (a) and treated (b, live/dead cells; c, live cells only; and d, dead cells only) with EcDBS1R5 at 16 μM. Scale bar = 20 μm.

study by Balaban et al.[19] has shown that a synthetic, 7-amino acid peptide (RNAIII-inhibiting peptide) was capable of inhibiting *Staphylococcus epidermidis* biofilm formation, also being able to act synergistically with antibiotics, which may represent an advantage for the treatment of biofilm-associated infection.[19] In this context, although EcDBS1R5 was not capable of completely eradicating *P. aeruginosa* biofilms, future studies are encouraged to evaluate the synergistic potential of this peptide with antibiotics on bacterial biofilms.

EcDBS1R5 Is Not Toxic Toward Mammalian Cells. The hemolytic and cytotoxicity properties of naturally occurring and rationally designed AMPs usually represent a bottleneck in the treatment of bacterial infections using these molecules.[5] In this context, before conducting *in vivo* studies, the hemolytic activity of EcDBS1R5 was investigated using human erythrocytes, and the cytotoxic potential of the peptide was evaluated on both non-cancerous (mouse adipocytes, 3T3-L1; and human umbilical vein endothelial cells, HUVEC) and cancerous cell lines (human prostate cancer, PC-3; human breast cancer, MCF-7; and human colon adenocarcinoma, HT-29). At the highest concentration tested in these assays (100 μM), EcDBS1R5 was not hemolytic nor cytotoxic against any of the cell lines tested (Table 2), suggesting its selectivity for bacterial cells, thus encouraging antibacterial studies in animals.

EcDBS1R5 Reduces *P. aeruginosa* Counts by Two-Logs 2 Days Post-infection. Epidemiology and risk factors associated with *P. aeruginosa* infections have been extensively reviewed, highlighting the deleterious role of this bacterium in hospital environments.[20] We therefore investigated the *in vivo* antibacterial potential of EcDBS1R5 in skin infections caused by *P. aeruginosa* in mice. First, we determined the lowest concentration at which EcDBS1R5 killed *P. aeruginosa* PA14, revealing a minimal bactericidal concentration (MBC) of 8 μM (Figure 3a). From this point on, an 8-fold higher MBC, non-toxic concentration (64 μM) was used to treat one-day-old skin

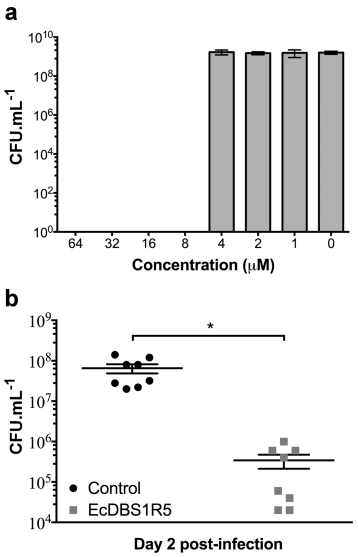

Figure 3. Killing assays and *in vivo* antibacterial properties of EcDBS1R5 against *P. aeruginosa* PA14. (a) EcDBS1R5 bactericidal activity against *P. aeruginosa* PA14 with concentrations ranging from 0 to 64 μM. (b) *In vivo* activity of EcDBS1R5 at 64 μM using the scarification skin infection mouse model. The *in vivo* antibacterial potential was evaluated 2 days post-infection. Statistical significance was assessed using one-way ANOVA, followed by Dunnett's multiple comparison tests (*$p > 0.001$, ns: not significant).

infections in mice, using a scarification skin infection mouse model. EcDBS1R5 (64 μM) exhibited *in vivo* antibacterial activity, as it led to two-log reduction in *P. aeruginosa* bacterial counts at 2 days post-infection (Figure 3b).[21] The efficacy of EcDBS1R5 at day two was significant and comparable to that of other AMPs. For example, a previous study[22] reported that two arginine-rich AMPs (RR and RRIKA) were able to reduce MRSA bacterial counts in skin infections by approximately 10^2 CFU·mL^{-1}. Interestingly, in that study the animals were treated twice a day for a total of 3 days.[22] In our study, we observed a similar effect with a single dose of EcDBS1R5. In addition, our findings can also be compared to colistin and A3-APO (a proline-rich host defense peptide incorporated into poly(vinyl alcohol) nanofibers), which have been previously evaluated in *A. baumannii*-infected skin wounds in mice.[23] Even though EcDBS1R5 comprises a linear, disulfide free AMP, its *in vivo* antibacterial potential is comparable to that of highly stable cyclic peptides, including cycloviolacin 2 (cyO2) and kalata B2 (kB2), which have been reported as anti-staphylococcal agents in a subcutaneous infection model at concentration from 0.75 to 3.0 mg·kg^{-1}.[24]

EcDBS1R5 Undergoes a Coil-to-Helix Transition (Environment-Dependent). The structure−activity relationships of AMPs have been thoroughly investigated, and a range of scaffolds have been reported and linked to diverse modes of action.[5] Thus, understanding the structures of novel AMPs is considered not only a crucial first step for mechanism of action

DOI: 10.1021/acsinfecdis.8b00219
ACS Infect. Dis. 2018, 4, 1727−1736

elucidation, but also a guide for future structure-based design of AMPs.[25] Here, in addition to characterizing the biological properties of EcDBS1R5, we carried out a detailed analysis of its three-dimensional structure. Initially, CD spectroscopy was used to characterize the secondary structure of EcDBS1R5 in water, buffer, 2,2,2-trifluoroethanol (TFE), and sodium dodecyl sulfate (SDS). As expected for linear peptides, random coil conformations were recorded in water (Figure 4). Interestingly,

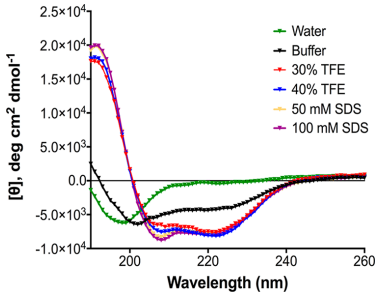

Figure 4. Secondary structure characterization of EcDBS1R5. CD spectra of EcDBS1R5 at 25 °C in different biomimetic conditions, including ultrapure water, 10 mM KH_2PO_4 (pH 7.4), 30% and 40% TFE, as well as 50 and 100 mM SDS.

however, in a high-salt content environment (10 mM KH_2PO_4 in water, pH 7.4), a transition from coil to helical conformation was noted (Figure 4). By increasing the TFE and SDS concentrations, a maximal helical content was achieved (Figure 4), which indicated that both conditions were suitable for the NMR studies.

TFE has been used as a co-solvent in AMP structure determination due to its ability to displace water molecules around the peptide, thus favoring intrapeptide hydrogen bond formation.[26] Moreover, the TFE-induced method for determining AMPs structures has been used in several studies, including clavanin,[16] phylloseptins,[27] and mollusc-derived peptides.[28] Here, NMR spectroscopy experiments were carried out to evaluate the EcDBS1R5 secondary structure transition from random coil (water) to α-helix (TFE-induced), as well as to determine the three-dimensional structure of EcDBS1R5. Corroborating the CD experiments, the αH secondary shifts of EcDBS1R5 in water are characteristic of unstructured (random coil) peptides (Figure 5a), whereas the αH secondary shifts in the presence of 30% TFE-d_3 indicate an α-helical structure from residues Lys3 to Lys14 (Figure 5a).

Based on data in 30% TFE-d_3 solvent, a total of 200 structures were calculated from 92 distance restraints, including 73 intraresidue, 7 sequential, and 12 hydrogen bond restraints (Table 3). The 10 lowest energy structures calculated for EcDBS1R5 had an α-helix from residues Lys4 to Lys14 (Lys3 to Lys14 in the αH secondary shifts), which may be attributed to unfolding from residues 1 to 3 during the refinement steps in water using CNS.[29] Moreover, we observed that the amide protons for residues Met2-Ala8, Arg10, Ala13-Ala16, and Trp19 are protected from the solvent as their temperature coefficients values are more positive than -4.6 ppb·K^{-1} (Figure 5b), thus indicating intrapeptide hydrogen-bonding interactions.

Among the 200 calculated structures for EcDSB1R5, the 10 lowest energy structures are deposited in the PDB under accession 6CT4, and structural statistics are summarized in

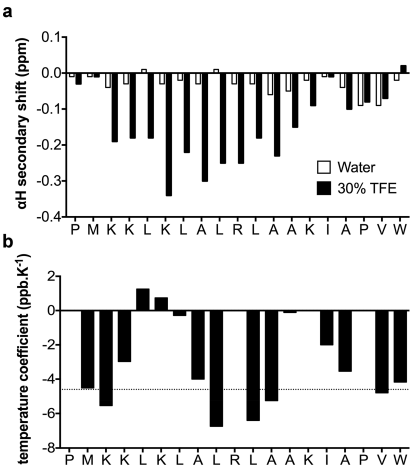

Figure 5. EcDBS1R5 αH secondary chemical shifts and temperature coefficient analysis. (a) EcDBS1R5 αH secondary chemical shifts were determined from ^{1}H NMR spectra recorded at 298 K in 90% H_2O (v/v) and 10% D_2O (v/v), as well as in 60% (v/v) H_2O, 30% (v/v) TFE-d_3, and 10% (v/v) D_2O. The αH secondary shifts of EcDBS1R5 were calculated by subtracting the random coil ^{1}H NMR chemical shifts previously reported by Wishart et al.[38] from the experimental αH chemical shifts. (b) Amide proton chemical shifts in temperature coefficient experiments were obtained from 285 to 310 K in 70% (v/v) D_2O and 30% (v/v) TFE-d_3. Temperature coefficient values more positive than -4.6 ppb·K^{-1} (dashed line) were interpreted as the presence of a hydrogen bond.

Table 3. Briefly, >90% of the residues are in the most favorable regions in the Ramachandran plot with a low overall MolProbity scores (<1.80) (Table 3). Moreover, the root-mean-square deviation (RMSD) calculated for the helical segment of EcDBS1R5 (residues 4−14) was <0.4 Å for backbone atoms and <1.70 Å for heavy atoms (Table 3), indicating the precision of the structures. As observed in Figure 6a, the superimposition of the 10 lowest energy structures clearly indicates the stability of the helical segment (residues 4−14), along with flexible N- and C-terminal regions. In addition, the cartoon representation for the lowest energy structure shows that EcDBS1R5 adopts a coil−helix−coil arrangement in the presence of TFE (Figure 6b), with an amphipathic helical segment (Figure 6c). Amphipaticity is often considered to play an important role in AMPs electrostatic and hydrophobic interactions with microbial surfaces, triggering both membrane-mediated and intracellular mechanisms of action.[30] There are four residues (i.e., Lys3, Lys6, Lys14, and Arg10) constituting the cationic face of the helical segment in EcDBS1R5, and that could be expected to participate in initial peptide/bacterial surface interactions, as previously described.[15] In addition, amphipaticity combined with structural flexibility in AMPs has shown to be an important factor for functional diversity against bacteria.[31] A recent report by Wu et al.[32] showed a similar structural arrangement for a peptide derived from *Phyllomedusa camba* that displayed dual-antimicrobial/antibiofilm activities.[32] Similar findings have also been reported for polyalanine AMPs with strong antibiofilm properties.[15] Altogether, these data reinforce that the modulation of amphipaticity and flexibility in parent sequences may lead to improved AMPs with broad-spectrum activities and low cytotoxicity.[31,33]

DOI: 10.1021/acsinfecdis.8b00219
ACS Infect. Dis. 2018, 4, 1727−1736

Table 3. Structural Statistics for the 10 Lowest Energy Structures of EcDBS1R5

Energies (kcal·mol^{-1})	
overall	−501.66 ± 10.98
bonds	5.18 ± 0.52
angles	19.65 ± 2.62
improper	6.05 ± 1.07
van der Waals	−49.65 ± 5.08
NOE	0.01 ± 0.01
cDih	0.13 ± 0.13
dihedral	83.90 ± 1.26
electrostatic	−566.94 ± 12.61
Distance Restraints	
intraresidue ($i - j = 0$)	73
sequential ($\|i - j\| = 1$)	7
medium range ($1 < \|i - j\| < 5$)	0
long range ($\|i - j\| \geq 5$)	0
hydrogen bonds	12
total	92
Dihedral Angle Restraints	
ϕ	16
χ^1	13
total	29
Violations from Experimental Restraints	
total NOE violations exceeding 0.2 Å	0
total dihedral violations exceeding 2.0°	0
RMSD from Mean Structure (Å)	
backbone atoms	2.11 ± 0.73
heavy atoms	3.64 ± 1.00
RMSD from Mean Structure (Å) − Helical Segment (4−14)	
backbone atoms	0.36 ± 0.13
heavy atoms	1.62 ± 0.37
Stereochemical Quality	
Ramachandran favored (%)	90.59 ± 3.92
Ramachandran outliers (%)	0.58 ± 1.96
favorable side chain rotamers (%)	95.99 ± 3.51
unfavorable side chain rotamers (%)	0.66 ± 0.0
overall MolProbity score	1.72 ± 0.33

In summary, this study provides a detailed characterization of a novel computationally designed AMP with dual-antibacterial/antibiofilm activities that was nontoxic toward mammalian cells. The peptide exhibited antibacterial activity *in vivo*, thus providing a promising template for the treatment of bacterial infections. Moreover, an amphipathic, α-helical arrangement with flexible terminals was here described for EcDBS1R5 in the presence of TFE, supporting previous findings regarding environment-depend helical AMPs. Overall, we have demonstrated the potential use of EcDBS1R5 as a promising starting point for the generation of a new class of *E. coli*-derived peptides with extended antimicrobial activities.

EXPERIMENTAL SECTION

Peptide Synthesis, Purity Confirmation, and Mass Spectrometry. EcDBS1R5 was purchased from Peptide 2.0 Incorporated (USA). This peptide was synthesized using

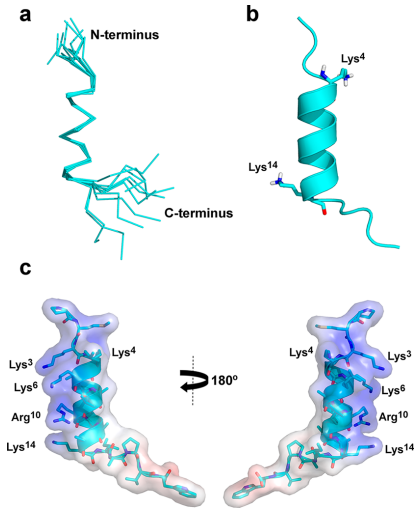

Figure 6. TFE-induced NMR structure of EcDBS1R5. (a) Superimposition of the 10 lowest energy structures of EcDBS1R5 in the presence of 30% TFE-d_3 (v/v). (b) The lowest energy structure of EcDBS1R5, revealing a coil−helix−coil arrangement. (c) Adaptive Poisson−Boltzmann solver (APBS) electrostatic potential of EcDBS1R5 with potential ranging from −5 kT/e (red) to +5 kT/e (blue). Cationic residues are labeled.

N-9-fluorenylmethyloxycarbonyl (Fmoc) solid-phase chemistry on a Rink-amide resin, with >95% purity. Purity was confirmed on a Nexera UHPLC (LC-30AD, Shimadzu) with a volumetric flow rate of 0.4 mL·min^{-1} on a 0.8 mL·min^{-1} Agilent column using a 4% gradient of 0−60% solvent B (90% MeCN in 0.045% aq TFA). The mass of EcDBS1R5 was confirmed by MALDI-TOF analysis (Ultraflex III, Bruker Daltonics) in reflector mode, using the Peptide Calibration Standard II for mass spectrometry (up to 4000 Da mass range) as an external calibration.

Minimal Inhibitory Concentration (MIC) and Minimal Bactericidal Concentration (MBC) Assays. Antimicrobial assays were performed against *E. coli* (ATCC 25922, BL21, and KpC+ 001812446), *K. pneumoniae* (ATCC 13883 and KpC+ 001825971), *S. aureus* (ATCC 25923 and 12600), MRSA (clinical isolate 713623), *P. aeruginosa* (PA14 and PAO1), *A. baumannii* (clinical isolate 003326263), and *E. cloacae* (clinical isolate 1383251) strains. All bacteria were cultivated in Mueller−Hinton agar plates (MHA) and incubated at 37 °C for 18 h. After growth, three isolated colonies were selected and incubated in 5 mL of MH broth (MHB) at 37 °C, overnight, at 200 rpm. Bacterial growth was monitored in a spectrophotometer at 600 nm. MIC assays were performed using the broth microdilution method in 96-well microplates,[34] in triplicates. EcDBS1R5 was initially diluted in ultrapure water, and then a stock of 64 μM was prepared in MHB. EcDBS1R5 was incubated with bacterial suspensions at 5 × 10^5 CFU·mL^{-1} per well, in concentrations ranging from 1 to 32 μM (serial dilutions from 64 μM). Bacterial suspensions (5 × 10^5 CFU·mL^{-1}) in broth were used as negative control. In addition, the antibiotics ampicillin, cefaclor, chloramphenicol, ciprofloxacin, and imipinem were tested against the resistant strains and clinical isolates used in this study to confirm their antibiotic-resistance profile

DOI: 10.1021/acsinfecdis.8b00219
ACS Infect. Dis. 2018, 4, 1727−1736

(Table S1). The microplates were incubated at 37 °C for 24 h. The MICs were defined as the lowest concentration of EcDBS1R5, at which no growth was observed at 600 nm, using a microplate reader. Three independent experiments were performed. The MBCs were obtained by plating 10 μL from the microplate wells containing bacteria treated with EcDBS1R5 in MH agar plates. The plates were incubated at 37 °C for 24 h. MBC was determined as the lowest concentration at which no bacterial growth (colonies) were observed. The experiments were performed in triplicate.

Biofilm Cultivation in Flow Chambers and Confocal Microscopy. Biofilms of *P. aeruginosa* PAO1 were grown for 48 h in the absence or presence of peptide EcDBS1R5 (16 μM) at 37 °C in flow chambers with channel dimensions of 1 × 4 × 40 mm. BM2 minimal medium [62 mM potassium phosphate buffer, pH 7.0, 7 mM $(NH_4)_2SO_4$, 2 mM $MgSO_4$, 10 M $FeSO_4$] containing 0.4% (wt/vol) glucose was used as the carbon source. Silicone tubing (inner diameter, 0.062 in.; outer diameter, 0.125 in.; wall thickness, 0.032 in.) was used, and the system was assembled and sterilized by pumping a 10% hypochlorite solution through the system for 5 min, using a multichannel peristaltic pump. The system was rinsed with sterile water and medium for 5 min each. Flow chambers were inoculated by injecting 400 μL of an overnight culture diluted to an optical density at 600 nm of approximately 0.5. After inoculation, the chambers were left without flow for 4 h, after which medium was pumped through the system at a constant rate of 2.6 mL·h^{-1}. For treatment of preformed biofilms, bacteria were allowed to develop structured 2-day-old biofilms prior to peptide treatment for the following 12 h. Biofilm cells were stained using a LIVE/DEAD BacLight bacterial viability kit prior to the microscopy experiments. A ratio of Syto-9 (green fluorescence, live cells) to propidium iodide (PI; red fluorescence, dead cells) of 1:1 was used. Microscopy was done using a confocal laser-scanning microscope (Zeiss LSM 700 Laser Scanning Confocal), and three-dimensional reconstructions were generated using the Imaris software package (Bitplane, AG). Two replicates for each condition were performed.

Hemolytic Assay. The hemolytic assay was performed using human erythrocytes isolated from healthy volunteers. Fresh venous blood was collected and stored in tubes containing sterile phosphate buffered saline (PBS). Blood samples were centrifuged at 4000 rpm for 1 min, after which serum was discarded, and blood cells were washed three times with 1 mL of sterile PBS. After the last wash, stocks containing 0.25% erythrocytes in PBS were prepared. EcDBS1R5 was prepared through serial dilutions, with final concentrations ranging from 0.781 to 100 μM per well. The assay was carried out on a 96-well microplate at 37 °C, for 1 h. Erythrocytes in sterile PBS was used as negative control, whereas the AMP melittin (concentrations ranging from 0.15 to 20 μM) and 1% (v/v) Triton X-100 were used as positive controls. Sample absorbance was measured at 415 nm using a microplate reader (BioTek PowerWave XS). Experiments were performed in triplicates.

Cell Culture and Cell Cytotoxicity Assays on Non-cancerous and Cancerous Cells. Non-cancerous cells, including HUVEC and 3T3-L1, were cultivated using EGM-2 BulletKit supplemented with SingleQuots (supplements: growth factors, cytokines, antibiotics; Lonza) and 10% BCS (bovine calf serum)/DMEM. Cancerous cells, including MCF-7 and HT-29, were cultivated in 10% (v/v) FBS/DMEM with 1% (v/v) penicillin−streptomycin (5000 U·mL^{-1}; Life Technologies), whereas PC-3 cells were cultivated in 10% (v/v) FBS/DMEM media with 1% (v/v) penicillin−streptomycin (5000 U·mL^{-1}; Life Technologies). Cell were cultured at 37 °C in 5% CO_2.

Cytotoxicity assays were performed according to Chan et al.[35] Briefly, passages 2−10 were used for all cell lines mentioned above. Final concentrations of 5 × 10^3 cells per well (100 μL) were used for the non-cancerous cells, whereas 2.5 × 10^3 cells per well (100 μL) were used for the cancerous cell lines. Cells were allowed to attach for 24 h after plating and treated with fresh media prior the addition of EcDBS1R5 (final concentrations ranging from 0.781 to 100 μM per well). Moreover, 0.1% (v/v) Triton X-100 was used as positive control. To evaluate cells' viability, 3-(4,5-dimethylthiazolyl-2)-2,5-diphenyltetrazolium bromide (MTT) (5 mg·mL^{-1} in PBS) was added after 2 h incubation. Subsequently, cells were incubated for an additional 4 h. The supernatants were removed, and 100 μL of DMSO was added. Experiments were performed in triplicates. Absorbances were measured at 600 nm using a microplate reader (BioTek PowerWave XS).

Bacterial Killing Assay and Skin Scarification Infection Mouse Model. The killing experiment was carried out using 1:100 dilutions of overnight cultures of *P. aeruginosa* PA14 (prior to *in vivo* studies) in the absence or presence of increasing concentrations of EcDBS1R5 (0−64 μM). After 24 h of treatment, 10-fold serial dilutions were performed; *P. aeruginosa* PA14 was plated on *Pseudomonas* Isolation Agar and allowed to grow overnight at 37 °C, after which colony-forming unit (CFU) counts were recorded. Three independent experiments were performed.

For the *in vivo* experiments, *P. aeruginosa* PA14 was grown in tryptic soy broth (TSB) medium to an optical density at 600 nm (OD_{600}) of 1.0. Subsequently, cells were washed twice with sterile PBS, pH 7.4, at 13 000 rpm for 1 min, and resuspended to a final concentration of 5 × 10^7 CFU·20 μL^{-1}. To generate skin infection, female CD-1 mice (6 weeks old) were anesthetized with isoflurane and had their backs shaved. A superficial linear skin abrasion was made with a needle to damage the stratum corneum and upper-layer of the epidermis. Five minutes after wounding, an aliquot of 20 μL containing 5 × 10^7 CFU of bacteria in PBS was inoculated over each defined area containing the scratch. One day after the infection, EcDBS1R5 was administered to the infected area at a final concentration of 64 μM. Animals were euthanized, and the area of scarified skin (1 cm^2) was excised 2 and 4 days post-infection, homogenized using a bead beater for 20 min (25 Hz), and serially diluted for CFU quantification. Two independent experiments were performed with four mice per group in each condition. Animals were maintained in accordance with the Guide for the Care and Use of Laboratory Animals in an AAALAC-accredited facility. All the procedures were approved by the MIT's Institutional Animal Care and Use Committee (IACUC), protocol number 1016-064-19. Statistical significance was assessed using a one-way ANOVA, followed by Dunnett's multiple comparison tests.

Circular Dichroism (CD) Spectroscopy. CD measurements were carried out on a JASCO (J-810) spectropolarimeter, coupled to a Peltier Jasco temperature controller system. CD spectra were obtained at 25 °C using 0.1 cm path length quartz cells and recorded from 185 to 260 nm at a scan speed of 50 nm·min^{-1}. The resolution was 0.1 nm with a 1 s response time and five scan accumulations for each sample. The secondary structure of EcDBS1R5 (50 μM) was characterized in ultrapure water (Milli-Q), 10 mM KH_2PO_4 (pH 7.4), TFE/water (30% and 40%, v/v) and SDS micelles (50 and 100 mM).

DOI: 10.1021/acsinfecdis.8b00219
ACS Infect. Dis. 2018, 4, 1727−1736

The CD signals obtained for the solvents alone were subtracted from all spectra containing peptide solutions. All spectra were smoothed using the Jasco Fast Fourier algorithm and baseline corrected.

Nuclear Magnetic Resonance (NMR) Spectroscopy and Structure Calculations. NMR spectroscopy was performed first using 90% H_2O (v/v) and 10% D_2O (v/v), in which 1 mM of EcDBS1R5 was dissolved. Subsequently, 30% TFE-d_3 (v/v) was used to evaluate secondary structure formation. For that, EcDBS1R5 was dissolved in 60% (v/v) H_2O, 30% (v/v) TFE-d_3 and 10% (v/v) D_2O (Cambridge Isotope Laboratories) at a concentration of 1 mM (pH 4.3). 4,4-Dimethyl-4-silapentane-1-sulfonic acid (DSS) was used as a chemical shift reference for spectral calibration. NMR analysis in the presence of SDS micelles was not possible due to the poor quality of the spectra. One-dimensional ^{1}H spectra and two-dimensional spectra, including TOCSY, NOESY, ^{13}C-HSQC and ^{15}N-HSQC, were recorded at 298 K on a Bruker Avance 600 MHz spectrometer. Temperature coefficient experiments were carried out in 70% (v/v) D_2O and 30% (v/v) TFE-d_3 (pH 4.3). Spectra were recorded from 285 to 310 K, at intervals of 5 K. Coefficients more positive than -4.6 ppb·K^{-1} were interpreted as the presence of a hydrogen bond, as previously described.[36] Spectra were processed using TopSpin 2.1 (Bruker) and assigned using CCPNMR v.2.4.[37] Secondary chemical shifts were calculated according to the random coil values reported by Wishart et al.[38] EcDBS1R5 TFE-induced three-dimensional structure was calculated on the basis of distance and angle restraints. Empirical prediction of phi (ϕ) and psi (ψ) backbone torsion angles was performed from the Hα, Cα, Cβ, HN, and N chemical shifts, using TALOS.[39] CYANA[40] was used to generate a list of interproton distances from the chemical shifts and NOE intensities, as well as to calculate an ensemble of 100 initial structures from which the 20 lowest energy structures were selected for further calculations. Subsequently, the protocols from the RECOORD database[41] were used to calculate 200 final structures and perform structural refinement in water using CNS.[29] A total of 10 final structures with lowest energy were selected with no NOE and dihedral violations greater than 0.2 Å and 2.0°, respectively. These structures were then selected for MolProbity validation.[42] Figures were generated using PyMOL v. 1.8.

PDB ID Code. Structural coordinates have been deposited in the Protein Data Bank (PDB code: 6CT4). Authors will release the atomic coordinates and experimental data upon article publication.

■ ASSOCIATED CONTENT

Supporting Information

The Supporting Information is available free of charge on the ACS Publications website at DOI: 10.1021/acsinfecdis.8b00219.

Table S1, listing additional MIC and MBC assays for different antibiotics against the resistant strains and clinical isolates used in the present study, and Figure S1, showing UHPLC/MALDI-TOF analyses of EcDBS1R5 (PDF)

■ AUTHOR INFORMATION

Corresponding Author

*E-mail: ocfranco@gmail.com. Phone: +55 61 34487167 or +55 61 34487220.

ORCID

Timothy K. Lu: 0000-0002-3918-8923
David J. Craik: 0000-0003-0007-6796
Octávio L. Franco: 0000-0001-9546-0525

Author Contributions

M.H.C. and E.S.C. contributed equally. M.H.C., L.Y.C., C.F.N., D.J.C., and O.L.F. designed the research. M.H.C., E.S.C., K.G.N.O., S.B.R., M.D.T.T., S.M.R., and C.F.N. performed the antimicrobial assays. M.D.T.T. and C.F.N. performed the flow-cell analysis and *in vivo* assays. W.F.P. performed the computationally guided design of EcDSB1R5. M.H.C., E.S.C., and L.Y.C. performed the hemolytic and cytotoxicity assays. M.H.C., E.S.C., and L.Y.C. performed and analyzed the CD experiments. M.H.C. and L.Y.C. performed and analyzed the NMR experiments and structure calculations. M.H.C., D.J.C., and O.L.F. wrote the paper with input from all authors. L.Y.C., T.K.L., C.F.N., D.J.C., and O.L.F. supervised the research.

Notes

The authors declare no competing financial interest.

■ ACKNOWLEDGMENTS

This work was supported by grants from Fundação de Apoio à Pesquisa do Distrito Federal (FAPDF), Coordenação de Aperfeiçoamento de Pessoal de Nível Superior (CAPES) (to M.H.C., 88881.134423/2016-01), Conselho Nacional de Desenvolvimento e Tecnológico (CNPq) (to M.H.C., 141518/2015-4) and Fundação de Apoio ao Desenvolvimento do Ensino, Ciência e Tecnologia do Estado de Mato Grosso do Sul (FUNDECT), Brazil, Ramon Areces Foundation (to C.F.N.), DTRA (DTRA HDTRA1-15-1-0050 to T.K.L.), and Fundação de Amparo à Pesquisa do Estado de São Paulo (MDTT nos. 2014/04507-5 and 2016/24413-0). D.J.C. is an ARC Australian Laureate Fellow (FL150100146). L.Y.C. was supported by the Advance Queensland Women's Academic Fund (WAF-6884942288). We thank Robin Kramer for her assistance with the skin scarification mouse model.

■ REFERENCES

(1) Fisher, R. A., Gollan, B., and Helaine, S. (2017) Persistent bacterial infections and persister cells. *Nat. Rev. Microbiol. 15*, 453−464.

(2) Nicolaou, K. C., and Rigol, S. (2018) A brief history of antibiotics and select advances in their synthesis. *J. Antibiot. 71*, 153−184.

(3) World Health Organization (2017) Global priority list of antibiotic-resistant bacteria to guide research, discovery, and development of new antibiotics, https://www.who.int/medicines/publications/global-priority-list-antibiotic-resistant-bacteria/en/.

(4) Hall-Stoodley, L., Costerton, J. W., and Stoodley, P. (2004) Bacterial biofilms: from the natural environment to infectious diseases. *Nat. Rev. Microbiol. 2*, 95−108.

(5) Fjell, C. D., Hiss, J. A., Hancock, R. E., and Schneider, G. (2012) Designing antimicrobial peptides: form follows function. *Nat. Rev. Drug Discovery 11*, 37−51.

(6) Rogers, L. A. (1928) The inhibiting effect of *Streptococcus lactis* on *Lactobacillus bulgaricus*. *J. Bacteriol. 16*, 321−325.

(7) Gao, W., Xing, L., Qu, P., Tan, T., Yang, N., Li, D., Chen, H., and Feng, X. (2015) Identification of a novel cathelicidin antimicrobial peptide from ducks and determination of its functional activity and antibacterial mechanism. *Sci. Rep. 5*, 17260.

(8) Pinto, M. F., Fensterseifer, I. C., Migliolo, L., Sousa, D. A., de Capdville, G., Arboleda-Valencia, J. W., Colgrave, M. L., Craik, D. J., Magalhaes, B. S., Dias, S. C., and Franco, O. L. (2012) Identification and structural characterization of novel cyclotide with activity against an insect pest of sugar cane. *J. Biol. Chem. 287*, 134−147.

(9) Yamamoto, Y., Togawa, Y., Shimosaka, M., and Okazaki, M. (2003) Purification and characterization of a novel bacteriocin produced by *Enterococcus faecalis* strain RJ-11. *Appl. Environ. Microbiol. 69*, 5746−5753.
(10) Porto, W. F., Pires, A. S., and Franco, O. L. (2017) Computational tools for exploring sequence databases as a resource for antimicrobial peptides. *Biotechnol. Adv. 35*, 337−349.
(11) Porto, W. F., Fensterseifer, I. C. M., Ribeiro, S. M., and Franco, O. L. (2018) Joker: An algorithm to insert patterns into sequences for designing antimicrobial peptides antimicrobial peptides. *Biochim. Biophys. Acta, Gen. Subj. 1862*, 2043.
(12) Wang, G., Li, X., and Wang, Z. (2016) APD3: the antimicrobial peptide database as a tool for research and education. *Nucleic Acids Res. 44*, D1087−1093.
(13) Salomon, R. A., and Farias, R. N. (1992) Microcin 25, a novel antimicrobial peptide produced by *Escherichia coli*. *J. Bacteriol. 174*, 7428−7435.
(14) Hassan, M., Kjos, M., Nes, I. F., Diep, D. B., and Lotfipour, F. (2012) Natural antimicrobial peptides from bacteria: characteristics and potential applications to fight against antibiotic resistance. *J. Appl. Microbiol. 113*, 723−736.
(15) Cardoso, M. H., Ribeiro, S. M., Nolasco, D. O., de laFuente-Nunez, C., Felicio, M. R., Goncalves, S., Matos, C. O., Liao, L. M., Santos, N. C., Hancock, R. E., Franco, O. L., and Migliolo, L. (2016) A polyalanine peptide derived from polar fish with anti-infectious activities. *Sci. Rep. 6*, 21385.
(16) Silva, O. N., Alves, E. S., de la Fuente-Nunez, C., Ribeiro, S. M., Mandal, S. M., Gaspar, D., Veiga, A. S., Castanho, M. A., Andrade, C. A., Nascimento, J. M., Fensterseifer, I. C., Porto, W. F., Correa, J. R., Hancock, R. E., Korpole, S., Oliveira, A. L., Liao, L. M., and Franco, O. L. (2016) Structural studies of a lipid-binding peptide from tunicate hemocytes with anti-biofilm activity. *Sci. Rep. 6*, 27128.
(17) Ribeiro, S. M., de la Fuente-Nunez, C., Baquir, B., Faria-Junior, C., Franco, O. L., and Hancock, R. E. (2015) Antibiofilm peptides increase the susceptibility of carbapenemase-producing *Klebsiella pneumoniae* clinical isolates to beta-lactam antibiotics. *Antimicrob. Agents Chemother. 59*, 3906−3912.
(18) Bessa, L. J., Eaton, P., Dematei, A., Placido, A., Vale, N., Gomes, P., Delerue-Matos, C., Sa Leite, J. R., and Gameiro, P. (2018) Synergistic and antibiofilm properties of ocellatin peptides against multidrug-resistant *Pseudomonas aeruginosa*. *Future Microbiol. 13*, 151−163.
(19) Balaban, N., Giacometti, A., Cirioni, O., Gov, Y., Ghiselli, R., Mocchegiani, F., Viticchi, C., Del Prete, M. S., Saba, V., Scalise, G., and Dell'Acqua, G. (2003) Use of the quorum-sensing inhibitor RNAIII-inhibiting peptide to prevent biofilm formation *in vivo* by drug-resistant *Staphylococcus epidermidis*. *J. Infect. Dis. 187*, 625−630.
(20) Palavutitotai, N., Jitmuang, A., Tongsai, S., Kiratisin, P., and Angkasekwinai, N. (2018) Epidemiology and risk factors of extensively drug-resistant *Pseudomonas aeruginosa* infections. *PLoS One 13*, e0193431.
(21) Piras, A. M., Maisetta, G., Sandreschi, S., Gazzarri, M., Bartoli, C., Grassi, L., Esin, S., Chiellini, F., and Batoni, G. (2015) Chitosan nanoparticles loaded with the antimicrobial peptide temporin B exert a long-term antibacterial activity *in vitro* against clinical isolates of *Staphylococcus epidermidis*. *Front. Microbiol. 6*, 372.
(22) Mohamed, M. F., and Seleem, M. N. (2014) Efficacy of short novel antimicrobial and anti-inflammatory peptides in a mouse model of methicillin-resistant *Staphylococcus aureus* (MRSA) skin infection. *Drug Des., Dev. Ther. 8*, 1979−1983.
(23) Sebe, I., Ostorhazi, E., Fekete, A., Kovacs, K. N., Zelko, R., Kovalszky, I., Li, W., Wade, J. D., Szabo, D., and Otvos, L., Jr. (2016) Polyvinyl alcohol nanofiber formulation of the designer antimicrobial peptide APO sterilizes *Acinetobacter baumannii*-infected skin wounds in mice. *Amino Acids 48*, 203−211.
(24) Fensterseifer, I. C., Silva, O. N., Malik, U., Ravipati, A. S., Novaes, N. R., Miranda, P. R., Rodrigues, E. A., Moreno, S. E., Craik, D. J., and Franco, O. L. (2015) Effects of cyclotides against cutaneous infections caused by *Staphylococcus aureus*. *Peptides 63*, 38−42.
(25) Mishra, B., Reiling, S., Zarena, D., and Wang, G. (2017) Host defense antimicrobial peptides as antibiotics: design and application strategies. *Curr. Opin. Chem. Biol. 38*, 87−96.
(26) Roccatano, D., Colombo, G., Fioroni, M., and Mark, A. E. (2002) Mechanism by which 2,2,2-trifluoroethanol/water mixtures stabilize secondary-structure formation in peptides: a molecular dynamics study. *Proc. Natl. Acad. Sci. U. S. A. 99*, 12179−12184.
(27) Resende, J. M., Moraes, C. M., Prates, M. V., Cesar, A., Almeida, F. C., Mundim, N. C., Valente, A. P., Bemquerer, M. P., Pilo-Veloso, D., and Bechinger, B. (2008) Solution NMR structures of the antimicrobial peptides phylloseptin-1, -2, and -3 and biological activity: the role of charges and Hydrogen Bonding interactions in stabilizing helix conformations. *Peptides 29*, 1633−1644.
(28) Lopez-Abarrategui, C., McBeth, C., Mandal, S. M., Sun, Z. J., Heffron, G., Alba-Menendez, A., Migliolo, L., Reyes-Acosta, O., Garcia-Villarino, M., Nolasco, D. O., Falcao, R., Cherobim, M. D., Dias, S. C., Brandt, W., Wessjohann, L., Starnbach, M., Franco, O. L., and Otero-Gonzalez, A. J. (2015) Cm-p5: an antifungal hydrophilic peptide derived from the coastal mollusk *Cenchritis muricatus* (Gastropoda: Littorinidae). *FASEB J. 29*, 3315−3325.
(29) Brunger, A. T., Adams, P. D., Clore, G. M., DeLano, W. L., Gros, P., Grosse-Kunstleve, R. W., Jiang, J. S., Kuszewski, J., Nilges, M., Pannu, N. S., Read, R. J., Rice, L. M., Simonson, T., and Warren, G. L. (1998) Crystallography & NMR system: A new software suite for macromolecular structure determination. *Acta Crystallogr., Sect. D: Biol. Crystallogr. 54*, 905−921.
(30) Gagnon, M. C., Strandberg, E., Grau-Campistany, A., Wadhwani, P., Reichert, J., Burck, J., Rabanal, F., Auger, M., Paquin, J. F., and Ulrich, A. S. (2017) Influence of the length and charge on the activity of alpha-helical amphipathic antimicrobial peptides. *Biochemistry 56*, 1680−1695.
(31) Roncevic, T., Vukicevic, D., Ilic, N., Krce, L., Gajski, G., Tonkic, M., Goic-Barisic, I., Zoranic, L., Sonavane, Y., Benincasa, M., Juretic, D., Maravic, A., and Tossi, A. (2018) Antibacterial activity affected by the conformational flexibility in glycine-lysine based alpha-helical antimicrobial peptides. *J. Med. Chem. 61*, 2924−2936.
(32) Wu, X., Pan, J., Wu, Y., Xi, X., Ma, C., Wang, L., Zhou, M., and Chen, T. (2017) PSN-PC: A novel antimicrobial and anti-biofilm peptide from the skin secretion of *Phyllomedusa-camba* with cytotoxicity on human lung cancer cell. *Molecules 22*, 1896.
(33) Peschel, A., and Sahl, H. G. (2006) The co-evolution of host cationic antimicrobial peptides and microbial resistance. *Nat. Rev. Microbiol. 4*, 529−536.
(34) Wiegand, I., Hilpert, K., and Hancock, R. E. (2008) Agar and broth dilution methods to determine the minimal inhibitory concentration (MIC) of antimicrobial substances. *Nat. Protoc. 3*, 163−175.
(35) Chan, L. Y., Craik, D. J., and Daly, N. L. (2016) Dual-targeting anti-angiogenic cyclic peptides as potential drug leads for cancer therapy. *Sci. Rep. 6*, 35347.
(36) Cierpicki, T., and Otlewski, J. (2001) Amide proton temperature coefficients as hydrogen bond indicators in proteins. *J. Biomol. NMR 21*, 249−261.
(37) Vranken, W. F., Boucher, W., Stevens, T. J., Fogh, R. H., Pajon, A., Llinas, M., Ulrich, E. L., Markley, J. L., Ionides, J., and Laue, E. D. (2005) The CCPN data model for NMR spectroscopy: development of a software pipeline. *Proteins: Struct., Funct., Genet. 59*, 687−696.
(38) Wishart, D. S., Bigam, C. G., Holm, A., Hodges, R. S., and Sykes, B. D. (1995) 1H, 13C and 15N random coil NMR chemical shifts of the common amino acids. Investigations of nearest-neighbor effects. *J. Biomol. NMR 5*, 67−81.
(39) Shen, Y., Delaglio, F., Cornilescu, G., and Bax, A. (2009) TALOS +: a hybrid method for predicting protein backbone torsion angles from NMR chemical shifts. *J. Biomol. NMR 44*, 213−223.
(40) Guntert, P. (2004) Automated NMR structure calculation with CYANA. *Methods Mol. Biol. 278*, 353−378.
(41) Nederveen, A. J., Doreleijers, J. F., Vranken, W., Miller, Z., Spronk, C. A., Nabuurs, S. B., Guntert, P., Livny, M., Markley, J. L., Nilges, M., Ulrich, E. L., Kaptein, R., and Bonvin, A. M. (2005)

DOI: 10.1021/acsinfecdis.8b00219
ACS Infect. Dis. 2018, 4, 1727−1736

RECOORD: a recalculated coordinate database of 500+ proteins from the PDB using restraints from the BioMagResBank. *Proteins: Struct., Funct., Genet. 59*, 662−672.
(42) Chen, V. B., Arendall, W. B., 3rd, Headd, J. J., Keedy, D. A., Immormino, R. M., Kapral, G. J., Murray, L. W., Richardson, J. S., and Richardson, D. C. (2010) MolProbity: all-atom structure validation for macromolecular crystallography. *Acta Crystallogr., Sect. D: Biol. Crystallogr. 66*, 12−21.
(43) Eisenberg, D., Weiss, R. M., Terwilliger, T. C., and Wilcox, W. (1982) Hydrohpobic moments and protein structure. *Faraday Symp. Chem. Soc. 17*, 109−120.
(44) Gautier, R., Douguet, D., Antonny, B., and Drin, G. (2008) HELIQUEST: a web server to screen sequences with specific alpha-helical properties. *Bioinformatics 24*, 2101−2102.
(45) Waghu, F. H., Barai, R. S., Gurung, P., and Idicula-Thomas, S. (2016) CAMPR3: a database on sequences, structures and signatures of antimicrobial peptides. *Nucleic Acids Res. 44*, D1094−D1097.

DOI: 10.1021/acsinfecdis.8b00219
ACS Infect. Dis. 2018, 4, 1727−1736

MATERIAL SUPLEMENTAR

A computationally designed peptide derived from *Escherichia coli* as a potential drug template for antibacterial and antibiofilm therapies

Marlon H. Cardoso[a,b,c,d†], Elizabete S. Cândido[b,c†], Lai Y. Chan[d], Marcelo Der Torossian Torres[e,f,g], Karen G. N. Oshiro[a,c], Samilla B. Rezende[c], William F. Porto[b,c,h], Timothy K. Lu[e,f], César de la Fuente-Núñez[e,f], David J. Craik[d] and Octávio L. Franco[a,b,c*]

[a]Programa de Pós-Graduação em Patologia Molecular, Faculdade de Medicina, Universidade de Brasília, Campus Darcy Ribeiro, Asa Norte, Brasília – DF, 70910900, Brazil;

[b]Centro de Análises Proteômicas e Bioquímicas, Pós-Graduação em Ciências Genômicas e Biotecnologia, Universidade Católica de Brasília, SGAN 916 Módulo B, Asa Norte, Brasília – DF, 70790160, Brazil;

[c]S-inova Biotech, Programa de Pós-Graduação em Biotecnologia, Universidade Católica Dom Bosco Avenida Tamandaré 6000, Campo Grande – MS, 79117900, Brazil;

[d]Institute for Molecular Bioscience, The University of Queensland, 306 Carmody Road, Brisbane – QLD, 4072, Australia;

[e]Synthetic Biology Group, MIT Synthetic Biology Center; The Center for Microbiome Informatics and Therapeutics; Research Laboratory of Electronics, Department of Biological Engineering, and Department of Electrical Engineering and Computer Science, Massachusetts Institute of Technology, Cambridge – MA, 02139, United States of America;

[f]Broad Institute of MIT and Harvard, Cambridge – MA, 02139, United States of America;

[g]Centro de Ciências Naturais e Humanas, Universidade Federal do ABC, Santo André – SP, 09210170, Brazil;

[h]Porto Reports, Brasília – DF, 70790160, Brazil.

[†]These authors contributed equally.

[*]To whom correspondence should be addressed.

Pages S2 and S3

Table S1

Figure S1

Table S1. Minimal inhibitory concentration (MIC) and minimal bactericidal concentration (MBC) for ampicillin, cefaclor, chloramphenicol, ciprofloxacin and imipinem against the resistant strains and clinical isolates used in the present study.

	MIC (MBC) μg.mL^{-1}				
Bacterial strains	Ampicillin	Cefaclor	Chloramphenicol	Ciprofloxacin	Imipinem
A. baumannii (clinical isolate 003326263)	nd (nd)[a]	nd (nd)	2 (4)	nd (nd)	nd (nd)
E. cloacae (clinical isolate 1383251)	nd (nd)	nd (nd)	2 (16)	2 (2)	nd (nd)
E. coli (KpC+ 001812446)	nd (nd)	16 (32)	8 (64)	2 (2)	nd (nd)
K. pneumoniae (KpC+ 001825971)	nd (nd)	nd (nd)	8 (16)	2 (2)	nd (nd)
MRSA (clinical isolate 713623)	nd (nd)	nd (nd)	2 (16)	16 (32)	nd (nd)

nd: not determined at the highest concentration tested (64 μg.mL^{-1}). Three replicates for each condition were performed.

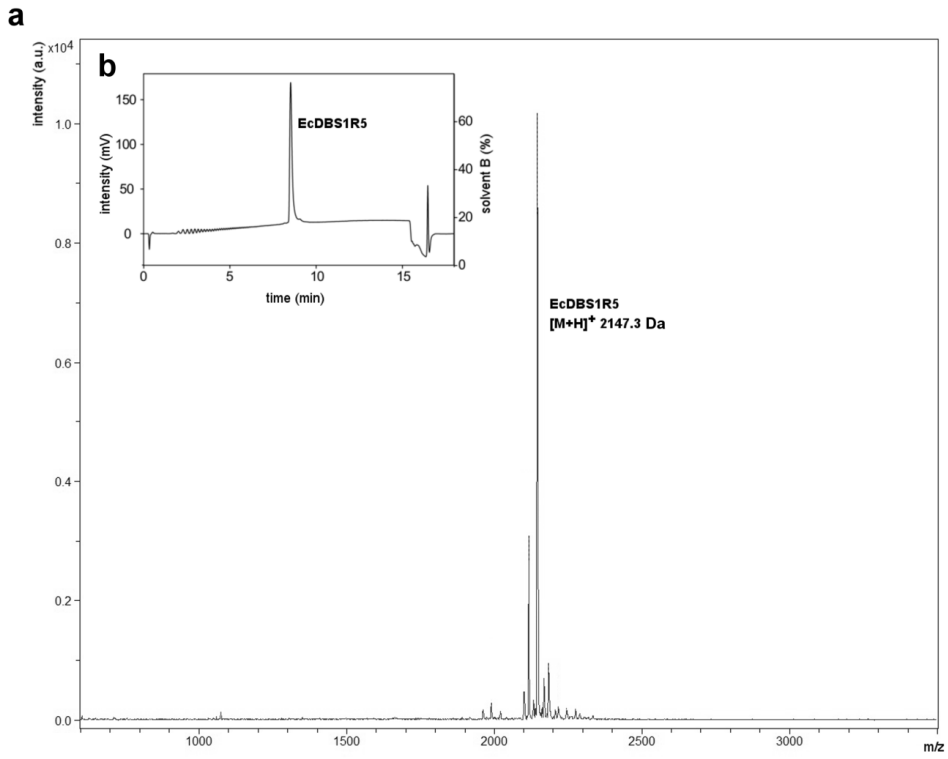

Figure S1. UHPLC and MALDI-TOF analyzes of EcDBS1R5. The molecular mass of EcDBS1R5 was confirmed by MALDI-TOF, revealing a monoisotopic mass of 2147.3 Da (a). The purity (>95%) of EcDBS1R5 after F-moc synthesis was confirmed by UHPLC (b) with a volumetric flow rate of 0.4 $mL.min^{-1}$ on a 0.8 $mL.min^{-1}$ Agilent column using a 4% gradient of 0-60% solvent B (90% MeCN in 0.045% aq. TFA).

6. DISCUSSÃO GERAL

Os agentes antimicrobianos têm sido desenvolvidos ao longo dos anos como carro-chefe na medicina moderna. Durante a metade do século 20, mais precisamente a partir de 1940, a "Era de Ouro" do descobrimento e aplicação dos antibióticos foi estabelecida (Arias e Murray, 2015). De fato, esta classe de antimicrobianos revolucionou a medicina e, de muitas formas, impactou na saúde pública (Li e Webster, 2018). Contudo, em meados de 1970, essa realidade foi drasticamente abalada devido a ampla descoberta de antibióticos associada ao uso desenfreado desses medicamentos levando, assim, a rápida seleção de cepas bacterianas multirresistentes (Arias e Murray, 2015). Tais eventos de resistência se estendem até os dias atuais, estando entre as maiores ameaças a saúde humana. Ademais, desde a década de 80, a descoberta e desenvolvimento de antibióticos vem diminuindo rapidamente. Estimativas mostram, por exemplo, que 16, 14, 10 e 7 novos antibióticos foram aprovados entre 1983-1987, 1988-1992, 1993-1997 e 1998-2002, respectivamente. Enquanto que apenas 5 e 2 novos antibióticos foram aprovados entre 2003-2007 e 2008-2012, respectivamente (Boucher *et al.*, 2013; Li e Webster, 2018). Neste contexto, cada vez mais estudos têm focado no desenvolvimento de novos compostos capazes de combater infecções de difícil tratamento protagonizadas por bactérias resistentes aos antibióticos convencionais.

Os PAMs vêm ganhando grande destaque na última década devido a suas múltiplas atividades biológicas no contexto da resistência bacteriana. Ao longo dos anos, estudos têm demonstrado que as atividades dessa classe de peptídeos consistem em um mapa complexo envolvendo relações estrutura-função (Fjell *et al.*, 2012). Essa correlação tem sido amplamente explorada e utilizada como base para inúmeros estudos de optimização de PAMs por meio de estratégias de desenho e redesenho racional, automatizados ou não, visando o desenvolvimento de PAMs ativos contra diversas bactérias. Neste contexto, o trabalho aqui desenvolvido teve como foco principal o estabelecimento da relação estrutura-função para dois PAMs, denominados *Pa*-MAP 1.9 e EcDBS1R5, os quais foram desenhados por meio de estratégias de desenho guiado por propriedades físico-químicas, assim como metodologias computacionais automatizadas, respectivamente.

Como descrito anteriormente o peptídeo *Pa*-MAP 1.9 foi desenhado com base no peptídeo polialanina *Pa*-MAP, derivado de *P. americanus*. Esse desenho, o qual foi baseado na modificação das propriedades físico-químicas do peptídeo parental, resultou em um aumento de carga, hidrofobicidade e momento hidrofóbico em *Pa*-MAP 1.9. Em termos de

atividade biológica, isso se traduziu em propriedades antibacterianas superiores no peptídeo redesenhado. Por exemplo, *Pa*-MAP 1.9 apresentou CIM cinco vezes mais baixa (CIM = 6 μM) frente a *E. coli* ATCC 8739, quando comparado a *Pa*-MAP (CIM = 30 μM). Somado a isso, *Pa*-MAP 1.9 foi ainda efetivo na inibição do crescimento de cepas de *E. coli* e *K. pneumoniae* resistentes a antibióticos carbapenêmicos. Por outro lado, ambos *Pa*-MAP e *Pa*-MAP 1.9 não se mostraram ativos contra cepas de *S. aureus*. Interessantemente, contudo, a melhor atividade de *Pa*-MAP 1.9 foi obtida contra a *Enterococcus faecalis*, uma bactéria Gram-positiva comensal do sistema digestivo de mamíferos. Mesmo fazendo parte da microbiota intestinal em humanos, cepas de *E. faecalis* são também associadas a infecções nosocomais, incluindo infecções no trato urinário, meningite, endocardites e sepse (Whiteside *et al.*, 2018). Dessa forma, o desenvolvimento de novos agentes antimicrobianos, como *Pa*-MAP 1.9, no combate a este microrganismo se mostra de grande importância a nível clínico.

Em adição ao trabalho desenvolvido com o peptídeo parental *Pa*-MAP, Migliolo *et al.* (2016) descreveram a função e estrutura de *Pa*-MAP 2, um peptídeo de segunda geração também desenhado com base em *Pa*-MAP. Quando avaliado acerca do seu potencial em inibir *E. coli* ATCC 8739, *Pa*-MAP 2 apresentou atividades ainda mais promissoras (CIM = 3.2 μM) quando comparado a *Pa*-MAP e *Pa*-MAP 1.9 (Migliolo *et al.*, 2016). Assim como para *Pa*-MAP e *Pa*-MAP 1.9, *Pa*-MAP 2 não apresentou potencial de inibição frente a cepas de *S. aureus*.

Em adição aos dados obtidos para *Pa*-MAP 1.9, este estudo também determinou o potencial antibacteriano de EcDBS1R5 contra cepas bacterianas susceptíveis e resistentes, Gram-positivas e Gram-negativas. Como resultado, foram observadas CIMs entre 2 – 32 μM frente a 10 das 12 cepas testadas. Assim como para *Pa*-MAP 1.9, as melhores atividades foram obtidas contra cepas de *E. coli*. No caso do peptídeo EcDBS1R5, mais especificamente, destacou-se a atividade contra *E. coli* resistente a antibióticos carbapenêmicos, com CIM igual a 2 μM (6 μM para *Pa*-MAP 1.9). Contudo, este peptídeo não demonstrou atividade contra *Enterobacter cloacae* e uma cepa de *K. pneumoniae* resistente (KpC+ 001825971). Interessantemente, *Pa*-MAP 1.9 também não se mostrou eficaz na inibição do crescimento dessa cepa de *K. pneumoniae* resistente (CIM = 96 μM).

Estudos mostram que a taxa de mortalidade em pacientes acometidos por infecções sanguíneas causadas por cepas de *K. pneumoniae* produtoras de carbapenemase (KpC) é de 50% (Pagano *et al.*, 2014). O tratamento de infecções protagonizadas por essas cepas se

mostra como um grande desafio na clínica, uma vez que as cepas KpC positivas (KpC+) são resistentes ao antibióticos β-lactâmicos, os quais são, em sua maioria, utilizados como último recurso (Mckenna, 2013). Estudos mostram ainda que cepas de *K. pneumoniae* KpC+ podem formar biofilmes altamente resistentes (Naparstek *et al.*, 2014). Ribeiro *et al.* (2015) demonstraram que biofilmes formados por diferentes cepas KpC+ puderam ser inibidos e parcialmente erradicados por peptídeos sintéticos, denominados DJK-5, DJK-6 e IDR-1018, em concentrações inferiores a suas CIMs frente a cepas planctônicas. Tais resultados, assim como outros já disponíveis na literatura, indicam que os mecanismos pelos quais PAMs atuam em cepas planctônicas e biofilmes é diferenciado, uma vez que uma atividade independe da outra. No presente trabalho, o mesmo foi observado para *Pa*-MAP 1.9. Como descrito acima, a CIM de *Pa*-MAP 1.9 frente a *K. pneumoniae* (KpC+ 001825971) em seu estágio planctônico foi igual a 96 μM. Quando avaliado acerca de seu potencial em inibir a formação de biofilmes (concentração inibitória mínima para biofilmes: CIMB) dessa mesma cepa foi observada CIMB igual a 1,1 μM. Posteriormente, esta concentração (1,1 μM) foi utilizada para tratar biofilmes pré-formados de *K. pneumoniae* (KpC+ 001825971), onde foi observado o alto efeito erradicatório de *Pa*-MAP 1.9. Resultados de erradicação promissores foram também obtidos frente a biofilmes pré-formados de *E. coli* a 3 μM (Cardoso *et al.*, 2016). Com base nesses resultados, *Pa*-MAP 1.9 se encaixa atualmente como o peptídeo polialanina mais efetivo, se não o único, contra biofilmes e depositado no BaAMPs (Di Luca *et al.*, 2015).

Somado a relevância de bactérias KpC+ formadoras de biofilmes, cepas resistentes de *P. aeruginosa* estão também comumente associadas a infecções recalcitrantes no contexto hospitalar. Ademais, a patogenicidade de várias infecções por *P. aeruginosa* está diretamente interligada a sua capacidade de formação de biofilmes cuja estrutura oferece proteção a resposta imune do hospedeiro e tratamentos antibacterianos (Maurice *et al.*, 2018). No presente estudo, a potencial antibiofilme do peptídeo EcDBS1R5 frente a *P. aeruginosa* PAO1 foi investigado. Para isso, a CIM de EcDBS1R5 contra esta cepa (CIM = 16 μM) foi utilizada para tratar biofilmes pré-formados. Diferentemente de *Pa*-MAP 1.9, o peptídeo EcDBS1R5 não foi capaz de erradicar completamente os biofilmes de *P. aeruginosa* PAO1 (Cardoso*, et al.*, 2018). Contudo, foi observada uma redução no volume e altura dos biofilmes tratados, bem como o comprometimento da viabilidade de células bacterianas que constituíam os biofilmes. Considerando que a comunicação células-células nos biofilmes representa um dos principais fatores envolvidos na coordenação estrutural e química desses consórcios

bacterianos, a inviabilização de cepas pelo tratamento com EcDBS1R5 pode ser considerada um passo inicial para a desorganização desses biofilmes. Tal hipótese vem sendo levantada por trabalhos com outros PAMs antibiofilme, os quais podem ser utilizados em combinação com outros agentes antimicrobianos visando a eliminação total de biofilmes resistentes (Balaban *et al.*, 2003; Bessa *et al.*, 2018).

De forma a explorar o potencial terapêutico de PAMs inúmeros trabalhos avaliam as atividades hemolítica e citotóxica desses peptídeos frente a células de mamíferos. De fato, os primeiros PAMs naturais estudados demonstravam grande toxicidade em células saudáveis, como é o caso das melitinas, cecropinas e magaininas (Tachi *et al.*, 2002). Dentre os parâmetros físico-químicos mais estudados, a hidrofobicidade em PAMs se mostra de crucial importância para as propriedades hemolíticas desses peptídeos, sendo um dos fatores que encorajam otimização de PAMs de origem natural. Assim, estudos têm demonstrado que hidrofobicidades entre 40% e 60% representa uma escala adequada para atividade antibacteriana, associada ausência de toxicidade em células humanas (Strempel *et al.*, 2015). Neste trabalho, ambos os PAMs estudados, *Pa*-MAP 1.9 e EcDBS1R5, apresentam hidrofobicidades dentro desse intervalo (41,1% e 57,9%, respectivamente). As propriedades hemolíticas para esses peptídeos foram investigadas nas concentrações mais altas testadas nos ensaios antimicrobianos, sendo elas 115 μM e 100 μM para *Pa*-MAP 1.9 e EcDBS1R5, respectivamente. Nessas condições, atividades hemolíticas não foram observadas. Ademais, diferentes linhagens celulares foram utilizadas em ensaios de viabilidade celular, demonstrando que tanto *Pa*-MAP 1.9 quanto EcDBS1R5 não são citotóxicos frente a células de mamíferos, encorajando estudos posteriores em modelos de infecção em animais.

Dentre as multifuncionalidades mais comumente relatadas para os PAMs podemos citar suas atividades anticâncer. A superfície de linhagens celulares cancerígenas apresenta, em sua maioria, maior carga negativa (assim como bactérias Gram-negativas) quando comparado a células saudáveis (Gaspar *et al.*, 2013). Essa caraterística favorece o efeito citotóxico seletivo de alguns PAMs por células cancerígenas e, consequentemente, propriedades anticâncer. As membranas de células saudáveis são assimétricas em sua distribuição de fosfolipídios, sendo o fosfolipídio carregado negativamente fosfatidilserina (PS) restrito a monocamada interna da membrana plasmática dessas células (Alves *et al.*, 2016). Como consequência, a monocamada externa (contato com o ambiente extracelular) apresenta carga neutra. Em células cancerígenas, contudo, essa assimetria é perdida e

fosfolipídios PS ficam expostos na superfície celular (Alves *et al.*, 2016), favorecendo o ancoramento de PAMs catiônicos por meio de interações eletrostáticas. Henriques *et al.* (2017), por exemplo, relataram o potencial antibacteriano e anticâncer de uma série de PAMs cíclicos redesenhados com base no PAM gomesina. Naquele trabalho, os autores observaram um aumento de atividade antibacteriana de 10 vezes quando comparado ao peptídeo parental. Ademais, os PAMs desenvolvidos mostraram citotoxicidade seletiva por células de melanoma e leucemia, sendo essa atividade relacionada a perturbação e rompimento de membranas dessas linhagens celulares (Troeira Henriques *et al.*, 2017). No presente estudo, a propriedade anticâncer de EcDBS1R5 foi investigada frente a três linhagens cancerígenas, incluindo câncer de próstata (PC-3), câncer de mama (MCF-7) e adenocarcinoma de colón (HT-29). Interessantemente, contudo, mesmo na concentração mais alta avaliada (100 μM) não foi observado o comprometimento da viabilidade celular nas linhagens testadas. Esses dados podem sugerir que a carga negativa característica de superfícies de bactérias Gram-negativas e células cancerígenas pode não ser o principal fator por trás do mecanismo de atuação de EcDBS1R5. Contudo, estudos mais aprofundados acerca da afinidade de ligação desse peptídeo a superfícies bacterianas, assim como sua possível atuação em alvos intracelulares, são necessários para esclarecer a atividade antibacteriana seletiva de EcDBS1R5.

Em adição as atividades biológicas descritas acima, o potencial anti-infeccioso para o peptídeo EcDBS1R5 foi determinado em modelo de infecção cutânea, enquanto que as atividades *in vivo* para *Pa*-MAP 1.9 ainda estão sob investigação. Para os estudos *in vivo* com o peptídeo EcDBS1R5, assim como para os experimentos antibiofilme, foi utilizada uma cepa de *P. aeruginosa* (PA14). Infecções causadas por *P. aeruginosa*, incluindo infecções cutâneas, pulmonares e urinárias, continuam a ser um grande desafio na clínica, uma vez que a oferta de medicamentos eficazes é escassa (Palavutitotai *et al.*, 2018). Neste estudo, a atividade anti-infecciosa de EcDBS1R5 foi confirmada, uma vez que este peptídeo, a 64 μM, foi capaz de reduzir em 100 vezes a contagem bacteriana nos sítios de infecção causada por *P. aeruginosa*. Atividades similares usando este mesmo modelo de infecção por *P. aeruginosa* foram recentemente relatadas por Torres *et al.* (2018), onde uma série de peptídeos desenhados com base no peptídeo polibia-CP, a 64 μM, reduziram de 100 a 1000 vezes a contagem bacteriana nos sítios de infecção. Interessantemente, mesmo sendo um peptídeo linear e sem modificações que favoreçam sua estabilidade em modelos animais, a atividade de EcDBS1R5 em modelos de infecção cutânea pode ser ainda comparada aquelas já observadas para PAMs ultra-estáveis, conhecidos como ciclotídeos (Fensterseifer *et al.*, 2015).

Os mecanismos pelos quais os PAMs exercem suas atividades antibacterianas vem sendo amplamente investigados. Dentre os mecanismos mais bem aceitos podemos citar aqueles relacionados a perturbação de membranas bacterianas, assim como mecanismos intracelulares, incluindo interações com o DNA bacteriano, inativação de enzimas e ribossomos (Fjell *et al.*, 2012). No estudo realizado com *Pa*-MAP 1.9 estratégias de microscopia de força atômica e permeabilização/rompimento de vesículas miméticas foram realizados de forma a avaliar possíveis danos morfológicos em uma cepa de *E. coli*, bem como melhor compreender a atividade seletiva desse peptídeo frente a cepas bacterianas, respectivamente. Inicialmente, uma cepa de *E. coli* foi tratada com 6 μM de *Pa*-MAP 1.9 mostrando que, em sua CIM contra *E. coli*, este peptídeo inviabiliza essa bactéria sem causar danos significativos a superfície celular. Aumentando essa concentração em 50 vezes (300 μM), contudo, foi observada a formação de rugosidades na superfície de *E. coli*. Resultados similares foram descritos por Troeira *et al.* (2013), onde um PAM optimizado e denominado Sub3 não afetou a superfície de *E. coli* em suas CIMs (1 a 10 μM), enquanto que uma concentração 10 vezes superior (100 μM) claramente induziu danos morfológicos.

Em adição aos estudos de microscopia realizados com *Pa*-MAP 1.9, Nascimento *et al.* (2014) e Migliolo *et al.* (2016) também investigaram os efeitos dos peptídeos *Pa*-MAP (parental) e *Pa*-MAP 2 (análogo de mesma geração) em bicamadas de dipalmitoilfosfatidilcolina (DPPC) e cepas de *E. coli*, respectivamente. Interessantemente, ao contrário do observado para *Pa*-MAP 1.9, seu peptídeo parental (*Pa*-MAP) causou perturbações na bicamada mimética testada por meio de mecanismos de carpete e detergente (Nascimento *et al.*, 2014). Ademais, o peptídeo *Pa*-MAP 2 também demonstrou mecanismos de membrana mais pronunciados que *Pa*-MAP 1.9. Quando incubado com uma cepa de *E. coli* em sua CIM (3,2 μM), *Pa*-MAP 2 induziu a formação de rugosidades na superfície celular, enquanto que a 32 μM este peptídeo demonstrou grande ação de superfície, causando o rompimento total das membranas bacterianas (Migliolo *et al.*, 2016). Dessa forma, estes dados sugerem que, mesmo pertencendo a classe dos peptídeos polialaninas, diferentes mecanismos de ação foram obtidos para *Pa*-MAP, *Pa*-MAP 1.9 e *Pa*-MAP 2 por meio do desenho baseado nas propriedades físico-químicas destes análogos. Ademais, considerando que em altas concentrações (300 μM) o peptídeo *Pa*-MAP 1.9 induziu somente a formação de rugosidades em *E. coli*, sugere-se ainda que, em sua CIM (6 μM), este peptídeo atravesse a

membrana bacteriana e atue em alvos intracelulares, como característico de outros peptídeos polialaninas já descritos (Bechinger, 2001).

Diversos trabalhos vem demostrando que a habilidade de PAMs em se ligar a membranas lipídicas representa um fator crucial para a seletividade desses peptídeos por células bacterianas (Troeira Henriques *et al.*, 2017). Dessa forma, estudos com vesículas/bicamadas miméticas são comumente empregados de forma a avaliar a ligação de PAMs nessas construções lipídicas, sendo essa ligação diretamente dependente da constituição e proporção de fosfolipídios. Assim, somado aos estudos de microscopia de força atômica, o peptídeo *Pa*-MAP 1.9 foi também avaliado acerca da sua capacidade de se ligar e romper vesículas mimetizando superfícies de células bacterianas e eucariotas (mamíferos). Como resultado foi observado que *Pa*-MAP 1.9 é altamente eficaz em interagir e romper vesículas contendo fosfolipídios carregados negativamente, como POPG e POPS. Ademais, a presença de lipopolissacarídeos (LPS) em algumas vesículas favoreceu a interação peptídeo/vesícula. Por outro lado, vesículas contendo fosfolipídios neutros, como POPC associado a presença de colesterol, claramente foram menos afetadas pela presença do peptídeo mesmo nas concentrações mais altas testadas. Essas seletividades por vesículas miméticas de caráter aniônico é ainda consistente com os dados antibacterianos para este peptídeo, o qual se mostra ativo contra uma maior número de cepas Gram-negativas (superfície aniônica). Ademais, a falta de atividade hemolítica e citotóxica frente a células de mamíferos saudáveis pode estar relacionada, em parte, pela inabilidade deste peptídeo em interagir e romper vesículas neutras ricas em colesterol. Os dados de permeabilização de vesículas obtidos para *Pa*-MAP 1.9 são ainda bastante similares aqueles adquiridos para seu análogo de mesma geração, *Pa*-MAP 2. Esses dados indicam que o potencial de se ligar seletivamente a superfícies aniônicas pode, possivelmente, ser um fator crucial tanto para o rompimento de membranas bacterianas por *Pa*-MAP 2 (Migliolo *et al.*, 2016), quanto para a translocação através destas para atuação em alvos intracelulares, como proposto para *Pa*-MAP 1.9 nos dados de microscopia.

Os estudos estruturais para PAMs são de grande importância para uma melhor compreensão dos mecanismos de ação dessa classe de peptídeos (relação estrutura-função) (Cardoso *et al.*, 2018). Uma das principais características dos PAMs consiste em sua habilidade de se ligar a superfícies bacterianas (como citado acima), sendo essas superfícies constituídas de diversos fosfolipídios, carboidratos e proteínas (Su *et al.*, 2013). Dentre as

metodologias mais utilizadas para estudos estruturais de PAMs em ambientes miméticos podemos citar as técnicas de DC, RMN e dinâmica molecular. Técnicas de RMN podem ainda ser divididas em RMN em solução e RMN de fase-sólida. Atualmente, o maior número de PAMs depositados no PDB foram estudados por RMN em solução, principalmente por meio da utilização de co-solventes e micelas miméticas constituídas de SDS e DPC. O solvente orgânico mais comumente utilizado para determinar a estrutura de PAMs consiste em misturas de água com TFE em diferentes proporções (Haney *et al.*, 2009). O TFE é conhecido por ser um co-solvente que favorece a estabilidade de estruturas secundárias em peptídeos, incluindo a formação de α-hélice, folhas-β e *hairpins* (Roccatano et al., 2002). Além disso, estudos estruturais rebuscados utilizando técnicas de RMN, cristalografia e dinâmica molecular mostram que o TFE desloca moléculas de água ao redor de peptídeos, favorecendo a formação de ligações de hidrogênio intrapeptídicas (Fioroni *et al.*, 2002). Assim, inúmeros estudos têm resolvido a estrutura de PAMs por meio de RMN em solução usando TFE como co-solvente, como é o caso da magainina-2 (Marion *et al.*, 1988), filoseptinas (Resende *et al.*, 2008), clavanina (Silva *et al.*, 2016), assim como PAMs derivados de moluscos (Lopez-Abarrategui *et al.*, 2015).

Visando a otimização da determinação ou predição da estrutura tridimensional de PAMs em solução, experimentos de DC são comumente aplicados de forma caracterizar a estrutura secundária desses peptídeos sob diferentes condições. No presente trabalho os arranjos estruturais de *Pa*-MAP 1.9 e EcDBS1R5 foram inicialmente investigados por DC em água ultrapura, tampão e TFE. Ademais, espectros de DC foram também obtidos para *Pa*-MAP 1.9 em contato com micelas de SDS. Como esperado para PAMs lineares e sem ligações dissulfeto, ambos os peptídeos avaliados mostraram conformações randômicas (*random coil*) em água e tampão. Por outro lado, quando avaliados em TFE e SDS (este sendo exclusivo para *Pa*-MAP 1.9) estruturas em α-hélice foram observadas. Considerando que TFE e SDS são utilizados como condições hidrofóbicas e aniônicas, respectivamente, mimetizando superfícies bacterianas, conclui-se que essas estruturas em hélice podem estar relacionadas com os mecanismos de ação para estes peptídeos, como já bem descrito para outros PAMs (Cardoso, Oshiro*, et al.*, 2018).

Uma vez obtidos os espectros de DC, estudos mais aprofundados de RMN e dinâmica/acoplamento molecular foram realizados para EcDBS1R5 e *Pa*-MAP 1.9, respectivamente. A estrutura tridimensional para o peptídeo EcDBS1R5 foi resolvida por

RMN em 30% TFE/água (v:v) e depositada no PDB sob o código 6CT4. Os deslocamentos químicos secundários para αH foram assinalados, demonstrando que o segmento helicoidal de EcDBS1R5 vai do resíduo 3 (lisina) a 14 (lisina). Esses resultados, adicionados dos experimentos de coeficiente de temperaturas, indicam ainda que as regiões N- e C-terminal deste peptídeo são altamente flexíveis, sugerindo uma arranjo *coil*-hélice-*coil*. Utilizando os deslocamentos químicos secundários para ^{1}H,^{13}C e ^{15}N em conjunto com as ligações de hidrogênio extraídas a partir dos dados de coeficiente de temperatura, foi possível calcular 200 estruturas tridimensionais, das quais 10 foram selecionadas devido a suas menores energias livres. Dessa forma, a estrutura tridimensional para EcDBS1R5 foi caracterizada por regiões terminais flexíveis com um segmento helicoidal central.

O segmento helicoidal de EcDBS1R5 apresenta características anfipáticas, contendo quatro resíduos carregados positivamente em lado oposto a resíduos hidrofóbicos. A anfipaticidade em PAMs é considerada um dos principais fatores para interações eletrostáticas e hidrofóbicas com superfícies bacterianas, levando a mecanismos de ação em membrana ou intracelular. Ademais, a anfipaticidade, quando em associação com flexibilidade em PAMs, tem se mostrado de grande importância para o amplo espectro de atividades desses peptídeos (Roncevic *et al.*, 2018). Neste contexto, trabalhos vem mostrando a influência da flexibilidade de PAMs nas suas atividades contra bactérias em seu estágio planctônico e biofilmes (Wu *et al.*, 2017).

Somado às técnicas de RMN as metodologias computacionais têm ganhado grande destaque ao longo dos anos, se tornando cada vez mais relevantes em estudos estruturais de peptídeos e proteínas. Uma das técnicas mais utilizada na biologia computacional consiste na descrição de sistemas moleculares a nível atômico. Em relação as técnicas experimentais de RMN, cristalografia e DC, a modelagem molecular e dinâmica molecular entregam ao usuário uma metodologia rápida e confiável na predição de estruturas de proteínas, assim como no desenho e redesenho de proteínas e peptídeos com maior estabilidade estrutural e seletividade (Cardoso*, et al.*, 2018). No presente estudo, a estrutura tridimensional de *Pa*-MAP 1.9 foi inicialmente investigada por modelagem molecular, seguido de simulações de dinâmica molecular em condições similares aquelas usadas nos experimentos de DC, incluindo água, TFE e SDS. Corroborando os dados de DC, as dinâmicas moleculares durante 100 ns mostram que a estrutura em α-hélice para *Pa*-MAP 1.9 é ambiente-dependente (TFE e SDS). Esses dados podem ainda ser comparados aqueles obtidos para o peptídeo perante *Pa*-MAP e

Pa-MAP 2, onde conteúdos de hélice só foram observados em TFE e SDS (Migliolo *et al.*, 2012; Migliolo *et al.*, 2016). Ademais, estudos de dinâmica molecular vem também sendo empregados em estudos estruturais de outros PAMs. Como exemplo, podemos citar o trabalho realizado por Mehrnejad *et al.* (2007) que, a partir da estrutura de RMN para magainina, realizou diversas comparações estruturais por dinâmica molecular em diferentes ambientes. Somado a isso, estudos têm proposto a utilização de técnicas de dinâmica molecular em complexos PAM/membranas previamente estudados por RMN de fase-sólida (Perrin *et al.*, 2014), levando a uma elucidação mais acurada acerca da afinidade e interações atômicas nesses complexos moleculares.

A associação de metodologias de acoplamento molecular e dinâmica molecular representa, atualmente, uma ferramenta atrativa para o estudo de interações moleculares entre PAMs e membranas biológicas, DNA bacteriano, proteínas alvo, dentre outros. Nessa linha de pensamento, o estudo realizado com o peptídeo *Pa*-MAP 1.9 incluiu estudos de acoplamento molecular com membranas modelo constituídas das mesmas proporções de fosfolipídios utilizados nos experimentos de permeabilização e rompimento de vesículas miméticas. De forma a otimizar o processo computacional, as membranas foram modeladas somente com base nas vesículas que foram mais e menos permeadas/rompidas por *Pa*-MAP 1.9, incluindo POPC/POPS (50:50) e POPC/colesterol (70:30), respectivamente. Como resultado, foi observado que *Pa*-MAP 1.9 apresentar maior afinidade pela membrana aniônica, bem como um maior número de interações atômicas estabelecidas por meio de ligações de hidrogênio e interações eletrostáticas. Esses resultados foram ainda similares aos obtidos por Migliolo *et al.* (Migliolo *et al.*, 2016) para o peptídeo *Pa*-MAP 2 em contado com bicamadas lipídicas aniônicas constituídas de DPPG/dipalmitoil-3-fosfatidil-etanolamina (DPPE) (9:1). Interessantemente, em um estudo similar realizado com o peptídeo parental (*Pa*-MAP) (Nascimento *et al.*, 2014), foram observadas afinidades de interação inferiores comparadas as afinidades obtidas para *Pa*-MAP 1.9 e *Pa*-MAP 2 em contato com membranas modelos explicando, em parte, o maior potencial antibacteriano desses análogos em relação ao seu peptídeo parental.

7. CONCLUSÕES

Em suma, neste trabalho dois novos PAMs foram caracterizados acerca de suas propriedades antibacteriana, antibiofilme e anti-infecciosa. Ademais, estudos estruturais foram detalhadamente desenvolvidos de forma a melhor compreender como o arranjo estrutural desses PAMs pode estar influenciado em suas atividades de amplo espectro. O peptídeo *Pa*-MAP 1.9 revelou uma estrutura helicoidal ambiente-dependente e possível mecanismos de ação intracelular quando administrado em sua CIM. Foi observada também uma seletividade de ligação em membranas modelo de caráter aniônico, mimetizando superfícies bacterianas. Ademais, *Pa*-MAP 1.9 atualmente representa o peptídeo polialanina depositado em bancos de dados com maior potencial de inibição da formação e erradicação de biofilmes de *K. pneumoniae* KpC+, sugerindo sua aplicação como agente antibiofilme. Em paralelo, o peptídeo EcDBS1R5 foi também caracterizado como um peptídeo helicoidal, contudo com regiões terminais flexíveis. De fato, a flexibilidade estrutural em PAMs tem sido considerada nos últimos anos como um importante fator para as múltiplas ações desses peptídeos, uma vez que diferentes estágios de transição estrutural poderiam levar a interações com diferentes alvos em bactérias. Essa hipótese foi explorada neste estudo devido a multifuncionalidade de EcDBS1R5 frente a cepas bacterianas planctônicas, biofilmes e infecções cutâneas. Assim, tanto *Pa*-MAP 1.9 quanto EcDBS1R5 representam moléculas modelo promissoras para o desenvolvimento de novos agentes antibacterianos.

8. PERSPECTIVAS

Considerando o atual e alarmante cenário acercas das infecções bacterianas, associadas ou não a biofilmes, é de suma importância o desenvolvimento de novos compostos eficazes e com baixo potencial de seleção de cepas resistentes. Como apresentado e discutido ao longo deste trabalho, dois novos PAMs foram detalhadamente caracterizados como moléculas modelo e de interesse clínico. Contudo, algumas perguntas ainda precisam ser respondidas em relação a esses candidatos a fármaco. Apesar do promissor potencial antibacteriano e, principalmente, antibiofilme do peptídeo *Pa*-MAP 1.9, mais experimento são necessários para a confirmação do seu potencial terapêutico, incluindo a utilização desse PAM no tratamento de infecções bacterianas em modelos animais. Ademais, este trabalho sugere que, em sua CIM, este peptídeo polialanina seja capaz de atravessar membranas biológicas para exercer sua atividade antibacteriana. Por outro lado, ainda não foram

comprovados os possíveis alvos intracelulares deste peptídeo, encorajando estudos futuros neste sentido. Em relação ao peptídeo EcDBS1R5, atividades *in vitro* e *in vivo* demonstraram o potencial terapêutico desse PAM. Além disso, foram utilizadas análises de biofísica experimental para compreender não somente seu arranjo estrutural, mas também as leis que governam a flexibilidade nesse peptídeo. Assim como para *Pa*-MAP 1.9, contudo, mais estudos são necessários visando a elucidação dos mecanismos de ação de EcDBS1R5. Nesse âmbito, as metodologias aplicadas a *Pa*-MAP 1.9, incluindo microscopia de força atômica, permeabilização e rompimento de vesículas miméticas e acoplamento/dinâmica molecular com membranas modelo, poderiam ser estendidas a EcDBS1R5. Por meio dessas abordagens é esperado que os PAMs aqui apresentados, assim como toda a informação biológica atrelada a eles, encoraje seu uso como moléculas modelo para o desenvolvimento guiado de PAMs cada vez mais efetivos e seguros e que possam, futuramente, ser submetidos a testes pré-clínicos.

9. ANEXOS

Artigo 1

Biochimie 112 (2015) 172–186

Contents lists available at ScienceDirect

Biochimie

journal homepage: www.elsevier.com/locate/biochi

Research paper

Effects of proteinase inhibitor from Adenanthera pavonina seeds on short- and long term larval development of Aedes aegypti

Daniele Yumi Sasaki [a], Ana Cristina Jacobowski [a], Antônio Pancrácio de Souza [b], Marlon Henrique Cardoso [d], Octávio Luiz Franco [c, d], Maria Lígia Rodrigues Macedo [a, *]

[a] Laboratório de Purificação de Proteínas e suas Funções Biológicas, Centro de Ciências Biológicas e Saúde, Universidade Federal do Mato Grosso do Sul, Campo Grande, MS, Brazil
[b] Departamento de Morfofisiologia, Centro de Ciências Biológicas e Saúde, Universidade Federal do Mato Grosso do Sul, Campo Grande, MS, Brazil
[c] S-Inova, Programa de Pós-graduação em Ciências Genômicas e Biotecnologia, Universidade Católica de Brasília, Brasília, DF, Brazil
[d] Centro de Análises Proteômicas e Bioquímicas, Pós-graduação em Ciências Genômicas e Biotecnologia, Universidade Católica de Brasília, Brasília, DF, Brazil

ARTICLE INFO

Article history:
Received 25 September 2014
Accepted 9 March 2015
Available online 18 March 2015

Keywords:
Aedes aegypti
Digestive enzyme
Kunitz-type inhibitor
Molecular docking
Molecular modeling

ABSTRACT

Currently, one of the major global public health concerns is related to the transmission of dengue/yellow fever virus by the vector *Aedes aegypti*. The most abundant digestive enzymes in *Ae. aegypti* midgut larvae are trypsin and chymotrypsin. Since protease inhibitors have the capacity to bind to and inhibit the action of insect digestive proteinases, we investigated the short- and long-term effects of *Adenanthera pavonina* seed proteinase inhibitor (ApTI) on *Ae. aegypti* larvae, as well as a possible mechanism of adaptation. ApTI had a significant effect on *Ae. aegypti* larvae exposed to a non-lethal concentration of ApTI during short- and long-duration assays, decreasing survival, weight and proteinase activities of midgut extracts of larvae. The zymographic profile of ApTI demonstrated seven bands; three bands apparently have trypsin-like activity. Moreover, the peritrophic membrane was not disrupted. The enzymes of ApTI-fed larvae were found to be sensitive to ApTI and to have a normal feedback mechanism; also, the larval digestive enzymes were not able to degrade the inhibitor. In addition, ApTI delayed larval development time. Histological studies demonstrated a degeneration of the microvilli of the posterior midgut region epithelium cells, hypertrophy of the gastric caeca cells and an augmented ectoperitrophic space in larvae. Moreover, *Ae. aegypti* larvae were incapable of overcoming the negative effects of ApTI, indicating that this inhibitor might be used as a promising agent against *Ae. aegypti*. In addition, molecular modeling and molecular docking studies were also performed in order to construct three-dimensional theoretical models for ApTI, trypsin and chymotrypsin from *Ae. aegypti*, as well as to predict the possible interactions and affinity values for the complexes ApTI/trypsin and ApTI/chymotrypsin. In this context, this study broadens the base of our understanding about the modes of action of proteinase inhibitors in insects, as well as the way insects adapt to them.

1. Introduction

There is major global public health concern regarding the vector of dengue and yellow fever, *Aedes aegypti*. L. (Diptera: Culicidae). This mosquito is responsible for transmitting flaviviruses (DENV1–4), and it is widely distributed in the tropical and subtropical zones [1]. The incidence of dengue fever has increased 30-fold over the last 50 years, and approximately 2.5 billion people live in dengue-endemic countries, with 50–100 million new cases of infection reported annually [2]. Infected mosquitoes can transmit the virus in two ways; by horizontal transmission between mosquito vectors and human hosts, which is the primary mechanism for the maintenance of the virus in urban areas; and by vertical transmission via transovarial route in female Aedes mosquitoes, which also occurs in nature. This mechanism is particularly important from the point of view of dengue transmission to

* Corresponding author. Laboratório de Purificação de Proteínas e suas Funções Biológicas, Centro de Ciências Biológicas e da Saúde/UFMS Cidade Universitária S/N, Caixa Postal 549 79070-900 Campo Grande, MS, Brazil. Tel.: +55 (67) 3345 7743, +55 (67) 3345 7612.
E-mail address: bioplant@terra.com.br (M.L.R. Macedo).

http://dx.doi.org/10.1016/j.biochi.2015.03.011
0300-9084/

Artigo 2

Biochimica et Biophysica Acta 1858 (2016) 1061–1069

Contents lists available at ScienceDirect

Biochimica et Biophysica Acta

journal homepage: www.elsevier.com/locate/bbamem

Synthetic antibiofilm peptides☆

César de la Fuente-Núñez [a,1], Marlon Henrique Cardoso [b,c], Elizabete de Souza Cândido [c,d], Octavio Luiz Franco [b,c,d], Robert E.W. Hancock [a,*]

[a] Centre for Microbial Diseases and Immunity Research, Department of Microbiology and Immunology, University of British Columbia, Vancouver, Canada
[b] Departamento de Patologia Molecular, Universidade de Brasília, Brasília, DF, Brazil
[c] Centro de Análises Proteômicas e Bioquímicas, Universidade Católica de Brasília, Brasília, DF, Brazil
[d] S-Inova Biotech, Programa de Pós Graduação em Biotecnologia, Universidade Católica Dom Bosco, Campo Grande, MS, Brazil

ARTICLE INFO

Article history:
Received 2 October 2015
Received in revised form 3 December 2015
Accepted 9 December 2015
Available online 23 December 2015

Keywords:
Biofilms
Synthetic peptides
Persistent infections
Synergy
Antibiotic resistance
Biomaterials

ABSTRACT

Bacteria predominantly exist as multicellular aggregates known as biofilms that are associated with at least two thirds of all infections and exhibit increased adaptive resistance to conventional antibiotic therapies. Therefore, biofilms are major contributors to the global health problem of antibiotic resistance, and novel approaches to counter them are urgently needed. Small molecules of the innate immune system called host defense peptides (HDPs) have emerged as promising templates for the design of potent, broad-spectrum antibiofilm agents. Here, we review recent developments in the new field of synthetic antibiofilm peptides, including mechanistic insights, synergistic interactions with available antibiotics, and their potential as novel antimicrobials against persistent infections caused by biofilms. This article is part of a Special Issue entitled: Antimicrobial peptides edited by Karl Lohner and Kai Hilpert.

1. Introduction

It has now been well established that bacteria are found not only as planktonic, free-swimming cells, but can also engage in a developmental cycle that allows them to form sessile, surface-associated multicellular communities called biofilms [1–4]. Biofilms are the predominant lifestyle of bacteria as they account for at least two thirds of all infections in humans and are found in many different natural environments. Indeed, biofilms are known to form in diverse environmental niches, including hydrothermal hot springs and deep-sea vents, freshwater rivers and rocks. Biofilms are formed when planktonic bacteria encounter certain environmental signals that are not yet completely understood. This process entails a complex adaptation that involves numerous regulatory gene networks, which translate the input signals into gene expression changes thus allowing the spatial and temporal organization of individual bacterial cells into biofilm aggregates [1–4].

Biofilm development usually begins with bacteria associating with a surface and forming microcolonies that, over time, turn into mature biofilm colonies. Bacteria within biofilms are encapsulated in a self-produced extracellular matrix made of various components that include polysaccharides, proteins, extracellular DNA, lipids and water [1–4]. One of the most significant characteristics of biofilms is their increased resistance to stress signals, including biocides and antibiotics used in industrial and clinical settings, as well as UV damage, metal toxicity, anaerobic conditions, acid exposure, salinity, pH gradients, desiccation, bacteriophages, amoebae, etc. [1–4]. Biofilms are also estimated to be 10 to 1000-times more resistant to conventional antibiotics than planktonic (free-swimming) bacteria. This has led to the recognition that biofilms are major contributors to chronic infections, which are highly resistant to antimicrobial therapies and are a major concern in hospitals worldwide. Moreover, currently available antibiotics have been shown to extensively damage the host microbiota, thus allowing reinfection by opportunistic pathogens that can form biofilms, and further intensifying the selective pressure towards antibiotic resistance [3].

In this daunting scenario, host defense (antimicrobial) peptides (HDPs) have emerged as a promising alternative to traditional antibiotics for the treatment of persistent infections caused by biofilms [5]. HDPs constitute the major component of the innate immune system of most living organisms, including mammals, insects, bacteria and fungi. In conferring protection to the organism from microbial attack, these molecules exhibit multiple mechanisms of action and, consequently, a low potential to select for resistance in bacteria [6]. In recent

☆ This article is part of a Special Issue entitled: Antimicrobial peptides edited by Karl Lohner and Kai Hilpert.

* Corresponding author at: 232-2259 Lower Mall Research Station, Vancouver, V6T 1Z4, BC, Canada.
E-mail address: bob@hancocklab.com (R.E.W. Hancock).
[1] Present address: Synthetic Biology Group, MIT Synthetic Biology Center, Research Laboratory of Electronics, Department of Biological Engineering, Department of Electrical Engineering and Computer Science, Massachusetts Institute of Technology, Cambridge, Massachusetts, United States of America. Broad Institute of MIT and Harvard University, Cambridge, Massachusetts, United States of America.

http://dx.doi.org/10.1016/j.bbamem.2015.12.015
0005-2736/

www.nature.com/scientificreports

SCIENTIFIC REPORTS

OPEN

Venom gland transcriptome analyses of two freshwater stingrays (Myliobatiformes: Potamotrygonidae) from Brazil

Received: 13 August 2015
Accepted: 03 February 2016
Published: 26 February 2016

Nelson Gomes de Oliveira Júnior[2,4], Gabriel da Rocha Fernandes[1,2], Marlon Henrique Cardoso[2,4,5], Fabrício F. Costa[1], Elizabete de Souza Cândido[1,2], Domingos Garrone Neto[6], Márcia Renata Mortari[3], Elisabeth Ferroni Schwartz[3], Octávio Luiz Franco[1,2,4,5] & Sérgio Amorim de Alencar[1,2]

Stingrays commonly cause human envenoming related accidents in populations of the sea, near rivers and lakes. Transcriptomic profiles have been used to elucidate components of animal venom, since they are capable of providing molecular information on the biology of the animal and could have biomedical applications. In this study, we elucidated the transcriptomic profile of the venom glands from two different freshwater stingray species that are endemic to the Paraná-Paraguay basin in Brazil, *Potamotrygon amandae* and *Potamotrygon falkneri*. Using RNA-Seq, we identified species-specific transcripts and overlapping proteins in the venom gland of both species. Among the transcripts related with envenoming, high abundance of hyaluronidases was observed in both species. In addition, we built three-dimensional homology models based on several venom transcripts identified. Our study represents a significant improvement in the information about the venoms employed by these two species and their molecular characteristics. Moreover, the information generated by our group helps in a better understanding of the biology of freshwater cartilaginous fishes and offers clues for the development of clinical treatments for stingray envenoming in Brazil and around the world. Finally, our results might have biomedical implications in developing treatments for complex diseases.

The Potamotrygonidae family comprises the only group of Elasmobranchii restricted to freshwater environments, with their occurrence limited to some river systems of South America. This group is represented by four genera, among which *Potamotrygon* comprises the largest number of species with broad geographic distribution[1].

The *Potamotrygon* genus includes benthic freshwater stingrays that are known for their long tail appendage with the presence of one to four serrated bone stings covered by a glandular epithelium whose cells produce venom[2,3] (Fig. 1). Injuries caused by stingrays have always been present in riverine communities of inland waters and in South American coasts. Indeed, envenomation by stingrays is quite common in freshwater and marine fishing communities. Although having high morbidity, such injuries are neglected because they have low lethality and usually occur in remote areas, which favor the use of folk remedies[2]. Moreover, accidents are caused due to a reflex contact between stingrays and humans, yielding an animal tail whiplash and further leading to a sting introduction at the limb during direct contact, causing epithelial lining destruction and subsequent venom release[2,4]. Clinical manifestations occur by triggering painful processes and injuries, even producing ulcers and necrosis of affected tissues[2]. Erythema, edema and bleeding of different degrees around the sting site appear in the first

[1]Programa de Pós-Graduação em Ciências Genômicas e Biotecnologia, Universidade Católica de Brasília, Brasília-DF, Brazil. [2]Centro de Análises Proteômicas e Bioquímicas, Pós-Graduação em Ciências Genômicas e Biotecnologia, Universidade Católica de Brasília, Brasília-DF, Brazil. [3]Departamento de Ciências Fisiológicas, Programa de Pós-Graduação em Biologia Animal, Universidade de Brasília, Brazil. [4]Programa de Pós-Graduação em Patologia Molecular, Universidade de Brasília, Brasília-DF, Brazil. [5]S-Inova Biotech, Pós-graduação em Biotecnologia, Universidade Católica Dom Bosco, Reitoria, Campo Grande, MS – Brazil. [6]UNESP – Universidade Estadual Paulista Júlio de Mesquita Filho, Campus Experimental de Registro, Registro, SP – Brazil. Correspondence and requests for materials should be addressed to O.L.F. (email: ocfranco@gmail.com)

www.nature.com/scientificreports

SCIENTIFIC REPORTS

OPEN

A polyalanine peptide derived from polar fish with anti-infectious activities

Received: 14 September 2015
Accepted: 22 January 2016
Published: 26 February 2016

Marlon H. Cardoso[2,3,4], Suzana M. Ribeiro[2,3], Diego O. Nolasco[1,6], César de la Fuente-Núñez[7,9], Mário R. Felício[8], Sónia Gonçalves[8], Carolina O. Matos[5], Luciano M. Liao[5], Nuno C. Santos[8], Robert E. W. Hancock[7], Octávio L. Franco[1,2,3,4] & Ludovico Migliolo[2,3]

Due to the growing concern about antibiotic-resistant microbial infections, increasing support has been given to new drug discovery programs. A promising alternative to counter bacterial infections includes the antimicrobial peptides (AMPs), which have emerged as model molecules for rational design strategies. Here we focused on the study of *Pa*-MAP 1.9, a rationally designed AMP derived from the polar fish *Pleuronectes americanus*. *Pa*-MAP 1.9 was active against Gram-negative planktonic bacteria and biofilms, without being cytotoxic to mammalian cells. By using AFM, leakage assays, CD spectroscopy and *in silico* tools, we found that *Pa*-MAP 1.9 may be acting both on intracellular targets and on the bacterial surface, also being more efficient at interacting with anionic LUVs mimicking Gram-negative bacterial surface, where this peptide adopts α-helical conformations, than cholesterol-enriched LUVs mimicking mammalian cells. Thus, as bacteria present varied physiological features that favor antibiotic-resistance, *Pa*-MAP 1.9 could be a promising candidate in the development of tools against infections caused by pathogenic bacteria.

In recent decades, improvements in the prevention and treatment of infectious diseases caused by pathogenic microorganisms has been of great importance in reducing morbidity and mortality, leading to a better quality of life and longer life expectancy[1]. However, antibiotics have been widely and sometimes indiscriminately used, which has resulted in the emergence of pathogens with multi-drug resistance in a wide range of bacterial species, including *Escherichia coli*, *Staphylococcus aureus, Pseudomonas aeruginosa, Klebsiella pneumoniae* and many other species[2]. Conversely, the rate of discovery of new antibiotics has steadily plummeted. Additionally, the occurrence and treatment of biofilm infections has appeared as one of the biggest challenges in the medical field with no available antibiotics that were developed to treat such infections. Biofilms are characterized as being a structured consortium of microorganisms connected by a complex matrix composed of polysaccharide(s), protein and DNA, that grows on biotic or abiotic surfaces via a multistage process[3]. It has been established that pathogenic bacteria are predominantly organized in biofilms, which are the cause of 65% to 80% of all bacterial infections in humans[3,4]. Biofilm growth represents a unique growth state whereby bacteria have major physiological and organizational differences, in particular leading to 10- to 1000- fold increased (adaptive) resistant to conventional antibiotics[3,4].

[1]Programa de Pós-Graduação em Ciências Genômicas e Biotecnologia, Universidade Católica de Brasília, Brasília-DF, Brazil. [2]Centro de Análises Proteômicas e Bioquímicas, Pós-Graduação em Ciências Genômicas e Biotecnologia, Universidade Católica de Brasília, Brasília-DF, Brazil. [3]S-inova, Programa de Pós-Graduação em Biotecnologia, Universidade Católica Dom Bosco, Campo Grande-MS, Brazil. [4]Programa de Pós-Graduação em Patologia Molecular, Faculdade de Medicina, Universidade de Brasília, Brasília-DF, Brazil. [5]Instituto de Química, Universidade Federal de Goiás, Goiânia-GO, Brazil. [6]Research Laboratory of Electronics, Massachusetts Institute of Technology (MIT), Cambridge, Massachusetts, USA. [7]Centre for Microbial Diseases and Immunity Research, Department of Microbiology and Immunology, University of British Columbia, Vancouver, Canada. [8]Instituto de Medicina Molecular, Faculdade de Medicina, Universidade de Lisboa, Lisbon, Portugal. [9]Synthetic Biology Group, MIT Synthetic Biology Center, Research Laboratory of Electronics, Department of Biological Engineering, Department of Electrical Engineering and Computer Science, Massachusetts Institute of Technology, Cambridge, Massachusetts, United States of America. Broad Institute of MIT and Harvard. Correspondence and requests for materials should be addressed to O.L.F. (email: ocfranco@gmail.com)

Metallomics

MINIREVIEW

View Article Online
View Journal | View Issue

CrossMark click for updates

Cite this: *Metallomics*, 2016, **8**, 1159

Designing metallodrugs with nuclease and protease activity

Caleb Mawuli Agbale,[ab] Marlon Henrique Cardoso,[bcd] Isaac Kojo Galyuon[a] and Octávio Luiz Franco*[bcd]

Received 9th June 2016,
Accepted 20th September 2016

DOI: 10.1039/c6mt00133e

www.rsc.org/metallomics

The accidental discovery of cisplatin some 50 years ago generated renewed interest in metallopharmaceuticals. Beyond cisplatin, many useful metallodrugs have been synthesized for the diagnosis and treatment of various diseases, but toxicity concerns, and the propensity to induce chemoresistance and secondary cancers make it imperative to search for novel metallodrugs that address these limitations. The Amino Terminal Cu(II) and Ni(II) (ATCUN) binding motif has emerged as a suitable template to design catalytic metallodrugs with nuclease and protease activities. Unlike their classical counterparts, ATCUN-based metallodrugs exhibit low toxicity, employ novel mechanisms to irreversibly inactivate disease-associated genes or proteins providing in principle, a channel to circumvent the rapid emergence of chemoresistance. The ATCUN motif thus presents novel strategies for the treatment of many diseases including cancers, HIV and infections caused by drug-resistant bacteria at the genetic level. This review discusses their design, mechanisms of action and potential for further development to expand their scope of application.

1. Introduction

The clinical application of metal-based compounds predates the modern era. Metals such as silver and copper were known by ancient Greeks and Romans to possess antibiotic properties and, in fact, silver solutions were among the first group of antiseptics to be approved by the U.S. Food and Drug Administration in the 1920s before the discovery of antibiotics.[1] For noble metals like gold, its use in medicine was greatly influenced by beliefs in its exceptional properties and mystique. For instance, the alchemists in ancient Egypt and the Middle Ages believed that elixirs of drinkable gold could 'remove the corruptions of the human body to such a degree that it could prolong life through many ages'.[2] The limited understanding of diseases and chemistry of these metals obviously led to many fatalities; but that notwithstanding, the use of various metals remained a key component of many therapeutic interventions for centuries. Thus, naturally, advances in medical science at the dawn of the 20th century, such as discovery of antibiotics, knowledge about the origin of diseases and advances in aseptic surgical interventions caused a shift towards better treatment options and led to a gradual decline in their extensive use. However, the popularity of metals in medicine received a major boost following the accidental rediscovery of cisplatin, a Pt–metal complex as an antitumor drug by Barnet Rosenberg and coworkers in the 1960s.[3] That singular discovery naturally generated renewed research interest in transition metals, more specifically in rationally designed metallodrugs for clinical application as antibiotics and chemotherapeutic agents.

The field of rationally designed metallodrugs has rapidly expanded since the discovery of cisplatin [*cis*-diammine dichloro Pt(II)] and the exciting chemistry of transition metals makes it even easier to predict further expansions to address contemporary challenges in biomedicine. This is because transition metals offer a platform for the design of compounds with complex architectures, chemical diversity and novel mechanisms of action, which had hitherto not been possible with organic chemistry.[4–9] The evolutionary path of metallodrugs has benefited greatly from advances in systems biology approaches. Therefore, it is expected that further advances in these areas should fuel more research interest in metallodrugs.

The current arsenal of metallodrugs, mostly anticancer agents such as cisplatin derivatives and antibiotics, are basically coordination complexes of transition metals designed specifically to inactivate therapeutically important targets through various mechanisms, including through generation of reactive oxygen species (ROS), enzyme inhibition, and intercalation of DNA or the formation of DNA adducts.[10–18] Although significant clinical

[a] *School of Biological Sciences, College of Agriculture and Natural Sciences, University of Cape Coast, Cape Coast, Ghana*
[b] *S-Inova Biotech, Programa de Pós-Graduação em Biotecnologia, Universidade Católica Dom Bosco, 79117-900 Campo Grande, MS, Brazil. E-mail: ocfranco@gmail.com*
[c] *Centro de Análises Proteômicas e Bioquímicas, Programa de Pós-Graduação em Ciências Genômicas e Biotecnologia, Universidade Católica de Brasília, 70719-100 Brasília, DF, Brazil*
[d] *Programa de Pós-Graduação em Patologia Molecular, Faculdade de Medicina, Universidade de Brasília, 70910-900 Brasília, DF, Brazil*

Artigo 6

Future MICROBIOLOGY

REVIEW

For reprint orders, please contact: reprints@futuremedicine.com

Understanding, preventing and eradicating *Klebsiella pneumoniae* biofilms

Suzana Meira Ribeiro[1,2], Marlon Henrique Cardoso[1,2,3], Elizabete de Souza Cândido[1,2] & Octávio Luiz Franco*[,1,2,3]

The ability of pathogenic bacteria to aggregate and form biofilm represents a great problem for public health, since they present extracellular components that encase these microorganisms, making them more resistant to antibiotics and host immune attack. This may become worse when antibiotic-resistant bacterial strains form biofilms. However, antibiofilm screens with different compounds may reveal potential therapies to prevent/treat biofilm infections. Here, we focused on *Klebsiella pneumoniae*, an opportunistic bacterium that causes different types of infections, including in the bloodstream, meninges, lungs, urinary system and at surgical sites. We also highlight aspects involved in the formation and maintenance of *K. pneumoniae* biofilms, as well as resistance and the emergence of new trends to combat this health challenge.

First draft submitted: 22 September 2015; Accepted for publication: 21 January 2016; Published online: 11 April 2016

KEYWORDS
- antibiofilm agents
- bacterial resistance
- biofilm • infections
- *Klebsiella pneumonia*

Klebsiella pneumoniae is an opportunistic pathogen associated with numerous cases of infection across the world. Together with a few other bacteria, *K. pneumoniae* has been recognized in the group of 'ESKAPE' pathogens (*Enterococcus faecium, Staphylococcus aureus, K. pneumoniae, Acinetobacter baumannii, Pseudomonas aeruginosa* and *Enterobacter* species), because they often 'escape' from the action of several antibiotics [1]. Currently, most bacterial infections (60–80%) are linked to microbial biofilm formation, a lifestyle in the bacterial community that presents inherent resistance to antibiotics and to host immune defense [2,3]. Biofilms are a bacterial aggregate enclosed in a matrix of polysaccharide(s), extracellular DNA and proteins. They can form through bacterial attachment to solid surfaces or through bacterial aggregation on liquid culture [4]. After biofilms become mature, the cells that constitute them disperse to colonize new environments [5]. In the case of *K. pneumoniae*, there is particular concern regarding biofilm formation by bacteria resistant to carbapenems (an antibiotic resistance type at cell level), known as a last resort antibiotic. Currently, there are limited antibiotic options for the treatment of infections caused by carbapenem-resistant Gram-negative bacteria [6]. Carbapenem resistance can arise by means of different enzymes, but those conferred by the enzymes *K. pneumoniae* carbapenemase (KPC) and New Delhi metallo-β-lactamase (NDM), first detected in *K. pneumoniae*, have been considered particularly as urgent threats. Besides conferring resistance to multiple β-lactams antibiotics, the genes that produce these enzymes can easily spread between different bacterial species by horizontal transfer [7]. This characteristic can be an issue in biofilms. Due to the proximity between cells in this lifestyle,

[1]Centro de Análises Proteômicas e Bioquímicas, Programa de Pós-Graduação em Ciências Genômicas e Biotecnologia, Universidade Católica de Brasília, Brasília-DF, Brazil
[2]S-Inova, Pós-Graduação em Biotecnologia, Universidade Católica Dom Bosco, Campo Grande- MS, Brazil
[3]Programa de Pós-Graduação em Patologia Molecular, Faculdade de Medicina, Universidade de Brasília, Brasília-DF, Brazil
*Author for correspondence: Tel.: +55 61 34487167/+55 61 34487220, Fax: +55 61 33474797; ocfranco@gmail.com

Future Medicine part of fsg

Artigo 7

Biochimica et Biophysica Acta 1858 (2016) 1488–1498

Contents lists available at ScienceDirect

Biochimica et Biophysica Acta

journal homepage: www.elsevier.com/locate/bbamem

Structural and functional evaluation of the palindromic alanine-rich antimicrobial peptide *Pa*-MAP2

Ludovico Migliolo [a,b], Mário R. Felício [c], Marlon H. Cardoso [a,b,h], Osmar N. Silva [a], Mary-Ann E. Xavier [d], Diego O. Nolasco [a,g], Adeliana Silva de Oliveira [e], Ignasi Roca-Subira [e], Jordi Vila Estape [e], Leandro D. Teixeira [a], Sonia M. Freitas [d], Anselmo J. Otero-Gonzalez [f], Sónia Gonçalves [c], Nuno C. Santos [c], Octavio L. Franco [a,b,h,*]

[a] Centro de Análises Proteômicas e Bioquímicas, Programa de Pós-Graduação em Ciências Genômicas e Biotecnologia, UCB, Brasília, DF, Brazil
[b] S-inova Biotech, Programa de Pós-Graduação em Biotecnologia, Universidade Católica Dom Bosco, Campo Grande, MS, Brazil
[c] Instituto de Medicina Molecular, Faculdade de Medicina, Universidade de Lisboa, Lisbon, Portugal
[d] Departamento de Biologia Celular, Laboratório de Biofísica, UnB, Brasília, DF, Brazil
[e] Instituto de Salud Global, CRESIB — Hospital Clinic, Universitat de Barcelona, Barcelona, Spain
[f] Laboratorio de Immunoanalitica y péptidos antimicrobianos, Faculdad de Biología, Centro de estudios de Proteínas, Universidad de La Habana, Cuba
[g] Research Laboratory of Electronics, Massachusetts Institute of Technology — MIT, Cambridge, MA, United States
[h] Programa de Pós-Graduação em Patologia Molecular, Faculdade de Medicina, Universidade de Brasília, Brasília, DF, Brazil

ARTICLE INFO

Article history:
Received 7 December 2015
Received in revised form 22 March 2016
Accepted 5 April 2016
Available online 8 April 2016

Keywords:
Pleuronectes americanus
Synthetic palindromic peptide
Pa-MAP2
Secondary structure
Molecular dynamics

ABSTRACT

Recently, several peptides have been studied regarding the defence process against pathogenic microorganisms, which are able to act against different targets, with the purpose of developing novel bioactive compounds. The present work focuses on the structural and functional evaluation of the palindromic antimicrobial peptide *Pa*-MAP2, designed based on the peptide *Pa*-MAP from *Pleuronectes americanus*.
For a better structural understanding, molecular modelling analyses were carried out, together with molecular dynamics and circular dichroism, in different media. Antibacterial activity against Gram-negative and positive bacteria was evaluated, as well as cytotoxicity against human erythrocytes, RAW 264.7, Vero and L6 cells. *In silico* docking experiments, lipid vesicle studies, and atomic force microscopy (AFM) imaging were carried out to explore the activity of the peptide. *In vivo* studies on infected mice were also done.
The palindromic primary sequence favoured an α-helix structure that was pH dependent, only present on alkaline environment, with dynamic N- and C-terminals that are stabilized in anionic media. *Pa*-MAP2 only showed activity against Gram-negative bacteria, with a MIC of 3.2 μM, and without any cytotoxic effect. *In silico*, lipid vesicles and AFM studies confirm the preference for anionic lipids (POPG, POPS, DPPE, DPPG and LPS), with the positively charged lysine residues being essential for the initial electrostatic interaction. *In vivo* studies showed that *Pa*-MAP2 increases to 100% the survival rate of mice infected with *Escherichia coli*.
Data here reported indicated that palindromic *Pa*-MAP2 could be an alternative candidate for use in therapeutics against Gram-negative bacterial infections.

1. Introduction

One of the main tasks of peptide designers is clearly connecting the primary structure proposed with an efficient desired function. In this context, the knowledge of sequence–structure relation in peptides has improved in recent decades. Among such peptides with biotechnological potential, the rational methods for peptide design have been applied to yield novel antimicrobial peptides (AMPs) with activity toward human target pathogens [1–3]. The search for alternatives in the development of antibiotics for control and prevention has gained importance, due to the rising incidence of antimicrobial resistance mechanisms developed by microbial pathogens, being nowadays a threat to Public health [4]. The diseases provoked by these microorganisms have been especially severe for those patients where the treatment with the currently available drugs has become less efficient [5,6]. Due to all these facts, antimicrobial peptides, which are widespread in nature, have become extremely attractive for their efficient control of natural resistance episodes in microorganisms, mainly because of the low resistance developed toward them [7,8]. This activity has been documented for different types of pathogens, including bacteria, viruses, fungi and also cancer cells, either inducing cell death or having immunomodulatory properties [9–12]. Those bioactive molecules that exhibit other functions, in addition to antimicrobial activities, have been isolated

* Corresponding author at: Centro de Análises Proteômicas e Bioquímicas, Programa de Pós-Graduação em Ciências Genômicas e Biotecnologia, UCB, Brasília, DF, Brazil.
E-mail address: ocfranco@gmail.com (O.L. Franco).

http://dx.doi.org/10.1016/j.bbamem.2016.04.003
0005-2736/

Artigo 8

Pesticide Biochemistry and Physiology 143 (2017) 14–25

Contents lists available at ScienceDirect

Pesticide Biochemistry and Physiology

journal homepage: www.elsevier.com/locate/pest

The rescue of botanical insecticides: A bioinspiration for new niches and needs

Jannaina Velasques[a,1], Marlon Henrique Cardoso[a,b,c,1], Guilherme Abrantes[a], Breno Emanuel Frihling[a], Octávio Luiz Franco[a,b,c], Ludovico Migliolo[a,*]

[a] S-Inova Biotech, Programa de Pós-Graduação em Biotecnologia, Universidade Católica Dom Bosco, Campo Grande, MS, Brazil
[b] Programa de Pós Graduação em Patologia Molecular, Faculdade de Medicina, Universidade de Brasília, Brasília, DF, Brazil
[c] Centro de Análises Proteômicas e Bioquímicas, Pós-Graduação em Ciências Genômicas e Biotecnologia, Universidade Católica de Brasília, Brasília, DF, Brazil

ARTICLE INFO

Keywords:
Plant metabolites
Defensive proteins
Insect control
Agriculture
Plant biotechnology

ABSTRACT

Crop protection is the basis of plant production and food security. Additionally, there are many efforts focused on increasing defensive mechanisms in order to avoid the damaging effects of insects, which still represent significant losses worldwide. Plants have naturally evolved different mechanisms to discourage herbivory, including chemical barriers such as the induction of defensive proteins and secondary metabolites, some of which have a historical link with bio-farming practices and others that are yet to be used. In the context of global concern regarding health and environmental impacts, which has been translated into political action and restrictions on the use of synthetic pesticides, this review deals with a description of some historical commercial phytochemicals and promising proteinaceous compounds that plants may modulate to defeat insect attacks. We present a broader outlook on molecular structure and mechanisms of action while we discuss possible tools to achieve effective methods for the biological control of pests, either by the formulation of products or by the development of new plant varieties with enhanced chemical defenses.

1. Background

Plants can synthesize a number of chemical compounds derived from primary metabolism, and although most of them are for essential functions such as growth, physiologic development and reproduction, there is still a small fraction that can be allocated as a substrate for secondary compound pathways [1]. Among a wide range of products, some classes deserve special attention due to their role in adaptation processes and defense mechanisms: the proteinaceous compounds and the secondary metabolites. Both classes can be produced for different purposes. As constitutive substances they can reduce the digestibility of plant tissues or cause direct toxicity, and as inducible substances they are synthesized in response to tissue damage. From an evolutionary perspective, those compounds have a close relationship to the protective apparatus that allowed plants to resist insect attack successfully, and they have also influenced their nutritional ecology. Therefore, these compounds can be toxic to a range of species while offering a potentially benign method of pest control [2].

Itis not possible to describe the exact moment in when humans started using plants and their products to control insects and microorganisms, but it has been historically associated with the onset of agriculture. If initially the use of botanicals was restricted to intuitive and naturalist procedures, the knowledge has spread and survived through different civilizations until the 19th century, when the first scientific observations associated with empirical practices allowed the significant use of botanical extracts as pesticides [3]. In the same period the identification and characterization of some plant secondary compounds enabled their use and description as repellents and biocides, mostly alkaloids such as nicotine and its isomer anabasine. But two other important classes also came to change the way of synthesizing natural compounds, bringing bioinspiration to laboratories; these are rotenones and pyrethrins, which have influenced several synthetic analogue formulas.

Until World War II, botanical pesticides were widely used for insect control in agriculture. However, at the end of 1930s they were largely replaced by synthetic organic compounds, more persistent and less selective, such as HCH ($C_6H_6Cl_6$); DDT ($C_{14}H_9Cl_5$); aldrin ($C_{12}H_8Cl_6$), dieldrin ($C_{12}H_8Cl_6O$) and chlordane ($C_{10}H_6Cl_8$) [4]. Organochlorines ruled the agricultural scene until the 1970s, when some questions concerning selectivity and environmental persistence were trigged by a

* Corresponding author at: PPG Biotecnologia/UCDB, Avenida Tamandaré 6000, Jardim Seminário, CEP 79117-900 Campo Grande, MS, Brazil.
E-mail address: ludovico@ucdb.br (L. Migliolo).
[1] These authors equally contributed to this article.

http://dx.doi.org/10.1016/j.pestbp.2017.10.003
Received 18 June 2017; Received in revised form 12 September 2017; Accepted 4 October 2017
Available online 10 October 2017
0048-3575/

www.nature.com/scientificreports

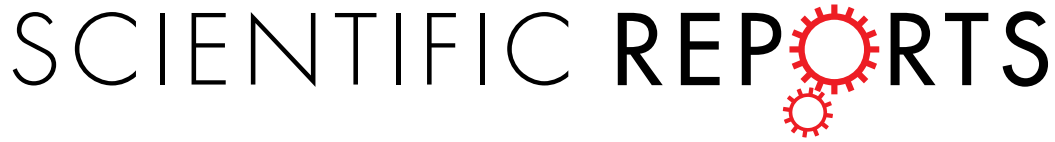

OPEN

Received: 4 January 2017
Accepted: 10 May 2017
Published online: 23 June 2017

Comparative NanoUPLC-MS^E analysis between magainin I-susceptible and -resistant *Escherichia coli* strains

Marlon H. Cardoso[1,2,4], Keyla C. de Almeida[1,2], Elizabete de S. Cândido[1,4], André M. Murad[3], Simoni C. Dias[1] & Octávio L. Franco[1,2,4]

In recent years the antimicrobial peptides (AMPs) have been prospected and designed as new alternatives to conventional antibiotics. Indeed, AMPs have presented great potential toward pathogenic bacterial strains by means of complex mechanisms of action. However, reports have increasingly emerged regarding the mechanisms by which bacteria resist AMP administration. In this context, we performed a comparative proteomic study by using the total bacterial lysate of magainin I-susceptible and –resistant *E. coli* strains. After nanoUPLC-MS^E analyses we identified 742 proteins distributed among the experimental groups, and 25 proteins were differentially expressed in the resistant strains. Among them 10 proteins involved in bacterial resistance, homeostasis, nutrition and protein transport were upregulated, while 15 proteins related to bacterial surface modifications, genetic information and β-lactams binding-protein were downregulated. Moreover, 60 exclusive proteins were identified in the resistant strains, among which biofilm and cell wall formation and multidrug efflux pump proteins could be observed. Thus, differentially from previous studies that could only associate single proteins to AMP bacterial resistance, data here reported show that several metabolic pathways may be related to *E. coli* resistance to AMPs, revealing the crucial role of multiple "omics" studies in order to elucidate the global molecular mechanisms involved in this resistance.

The abusive usage of antibiotics has been considered one of the most important factors that has led to the emergence, positive selection and dissemination of bacterial pathogens resistant to a wide variety of conventional antibiotics applied in animal and human therapies[1]. Both Gram-positive and -negative bacteria have been commonly associated with nosocomial infections in healthcare units. However, even considering the pharmacological and social importance of both groups, the Gram-negative bacteria from clinical isolates have demonstrated an impressive increase antibiotic resistance, mainly the Enterobacteriaceae members such as *Escherichia coli* and *Klebsiella pneumoniae*, which have been related to 95% of infections in healthcare units[2,3].

Bacteria have demonstrated diverse biological mechanisms of resistance, which are divided into intrinsic (natural) or acquired[1,2]. Among them we can cite the direct action of β-lactamase, as well as modified bacterial enzymes in the inactivation of cephalosporin, penicillin, aminoglycosides, gentamicin and streptomycin[2]. In Gram-negative bacteria, studies have shown mechanisms that target the way the drugs are transported, including the selective activity of porins, drug penetration blockage and efflux pumps[4–6]. Moreover, in resistant bacteria the existence has been reported of multi-resistant regions composed of mobile elements such as integrons and transposons, which, once combined, can contribute actively to bacterial resistance[7,8].

One of the proposed strategies to avoid the bacterial resistance phenomenon includes the usage of antimicrobial peptides (AMPs). These well-known multifunctional molecules have been widely prospected from several

[1]Centro de Análises Proteômicas e Bioquímicas, Pós-Graduação em Ciências Genômicas e Biotecnologia, Universidade Católica de Brasília, Brasília-DF, 70.790-160, Brazil. [2]Programa de Pós-Graduação em Patologia Molecular, Faculdade de Medicina, Universidade de Brasília, Brasília-DF, 70.910-900, Brazil. [3]Embrapa Recursos Genéticos e Biotecnologia, Laboratório de Biologia Sintética, Parque Estação Biológica, Brasília-DF, 70.770-917, Brazil. [4]S-Inova Biotech, Pós-graduação em Biotecnologia, Universidade Católica Dom Bosco, Campo Grande-MS, 79.117-900, Brazil. Marlon H. Cardoso and Keyla C. de Almeida contributed equally to this work. Correspondence and requests for materials should be addressed to O.L.F. (email: ocfranco@gmail.com)

Artigo 10

Plant Science 270 (2018) 72–84

Contents lists available at ScienceDirect

Plant Science

journal homepage: www.elsevier.com/locate/plantsci

Review article

Review: Potential biotechnological assets related to plant immunity modulation applicable in engineering disease-resistant crops

Marilia Santos Silva[a,**,1], Fabrício Barbosa Monteiro Arraes[a,b,***,1], Magnólia de Araújo Campos[c], Maira Grossi-de-Sa[d], Diana Fernandez[d], Elizabete de Souza Cândido[e,f], Marlon Henrique Cardoso[e,f,g], Octávio Luiz Franco[e,f,g], Maria Fátima Grossi-de-Sa[a,b,e,g,*]

[a] Embrapa Recursos Genéticos e Biotecnologia (Embrapa Cenargen), Brasília, DF, Brazil
[b] Universidade Federal do Rio Grande do Sul (UFRGS), Post-Graduation Program in Molecular and Cellular Biology, Porto Alegre, RS, Brazil
[c] Universidade Federal de Campina Grande (UFCG), Center of Education and Health Cuité-PB, Brazil
[d] IRD, CIRAD, Univ. Montpellier, IPME, Montpellier, France
[e] Universidade Católica de Brasília (UCB), Post-Graduation Program in Genomic Science and Biotechnology, Brasília, DF, Brazil
[f] Universidade Católica Dom Bosco (UCDB), Campo Grande, MS, Brazil
[g] Universidade de Brasília (UnB), Brasília, DF, Brazil

ARTICLE INFO

Keywords:
Pathogen-associated molecular pattern-triggered immunity (PTI)
Effector-triggered susceptibility (ETS)
Effector-triggered immunity (ETI)
RNA interference
Genetically modified (GM) crop
Disease resistance

ABSTRACT

This review emphasizes the biotechnological potential of molecules implicated in the different layers of plant immunity, including, pathogen-associated molecular pattern (PAMP)-triggered immunity (PTI), effector-triggered susceptibility (ETS), and effector-triggered immunity (ETI) that can be applied in the development of disease-resistant genetically modified (GM) plants. These biomolecules are produced by pathogens (viruses, bacteria, fungi, oomycetes) or plants during their mutual interactions. Biomolecules involved in the first layers of plant immunity, PTI and ETS, include inhibitors of pathogen cell-wall-degrading enzymes (CWDEs), plant pattern recognition receptors (PRRs) and susceptibility (S) proteins, while the ETI-related biomolecules include plant resistance (R) proteins. The biomolecules involved in plant defense PTI/ETI responses described herein also include antimicrobial peptides (AMPs), pathogenesis-related (PR) proteins and ribosome-inhibiting proteins (RIPs), as well as enzymes involved in plant defensive secondary metabolite biosynthesis (phytoanticipins and phytoalexins). Moreover, the regulation of immunity by RNA interference (RNAi) in GM disease-resistant plants is also considered. Therefore, the present review does not cover all the classes of biomolecules involved in plant innate immunity that may be applied in the development of disease-resistant GM crops but instead highlights the most common strategies in the literature, as well as their advantages and disadvantages.

1. Introduction

Plant pathogens, including viruses, bacteria, fungi, and oomycetes are a primary concern in agribusiness [1–3]. The diseases caused by these organisms in plants represent an important and persistent threat to food supplies worldwide [4]. The development of disease-resistant plants through biotechnological approaches aims to obtain economically important crops through elite genetically modified (GM) lines that not only display durable and broad-spectrum resistance to multiple phytopathogens, but that are also biosafe to the environment and consumers. To achieve this goal, several challenges related to transgene must be overcome, such as fine-tuning the choice, origin (i.e., heterologous species and/or non-host plant) and the number of genes to be employed and stacked, as well as gene expression control (e.g., by signal peptides, gene silencing and gene promoters). The current knowledge of the molecular mechanisms involved in plant-pathogen interactions has now provided a large set of biomolecules that can be applied in the development of GM disease-resistant/less susceptible crops.

Plant-pathogen interactions involve a two-way communication process, whereby plants can recognize and induce defense strategies against pathogens, while pathogens can threaten plant functional

* Corresponding authors at: Embrapa Recursos Genéticos e Biotecnologia (Cenargen), Brasília, DF, Brazil.
** Corresponding author.
*** Corresponding author at: Universidade Federal do Rio Grande do Sul (UFRGS), Post-Graduation Program in Molecular and Cellular Biology, Porto Alegre, RS, Brazil.
E-mail addresses: marilia.silva@embrapa.br (M.S. Silva), fabricio.arraes@gmail.com (F.B.M. Arraes), fatima.grossi@embrapa.br (M.F. Grossi-de-Sa).
[1] These authors contributed equally.

https://doi.org/10.1016/j.plantsci.2018.02.013
Received 9 October 2017; Received in revised form 1 February 2018; Accepted 4 February 2018
Available online 14 February 2018

www.nature.com/scientificreports

SCIENTIFIC REPORTS

OPEN

An acidic model pro-peptide affects the secondary structure, membrane interactions and antimicrobial activity of a crotalicidin fragment

Received: 16 March 2018
Accepted: 2 July 2018
Published online: 24 July 2018

Nelson G. O. Júnior[1,2,3], Marlon H. Cardoso[1,3,4], Elizabete S. Cândido[1,4], Daniëlle van den Broek[2], Niek de Lange[2], Nadya Velikova[5], J. Mieke Kleijn[2], Jerry M. Wells[5], Taia M. B. Rezende[1,6], Octávio Luiz Franco[1,3,4] & Renko de Vries[2]

In order to study how acidic pro-peptides inhibit the antimicrobial activity of antimicrobial peptides, we introduce a simple model system, consisting of a 19 amino-acid long antimicrobial peptide, and an N-terminally attached, 10 amino-acid long acidic model pro-peptide. The antimicrobial peptide is a fragment of the crotalicidin peptide, a member of the cathelidin family, from rattlesnake venom. The model pro-peptide is a deca (glutamic acid). Attachment of the model pro-peptide only leads to a moderately large reduction in the binding to- and induced leakage of model liposomes, while the antimicrobial activity of the crotalicidin fragment is completely inhibited by attaching the model pro-peptide. Attaching the pro-peptide induces a conformational change to a more helical conformation, while there are no signs of intra- or intermolecular peptide complexation. We conclude that inhibition of antimicrobial activity by the model pro-peptide might be related to a conformational change induced by the pro-peptide domain, and that additional effects beyond induced changes in membrane activity must also be involved.

Many proteins are synthetized as zymogens, precursor proteins that are inactive due to the presence of pro-peptide domains[1]. This also holds for antimicrobial peptides and proteins such as mammalian defensins[2], cathelicidins[3] and RegIII family proteins[4,5]. These are often synthesized and stored in inactive form, to protect host cells from potential cytotoxic effects as well as protecting the peptides and proteins and protected them from enzymatic degradation[6–8]. Understanding how pro-peptides control the activity of antimicrobial peptides is not only important in biology, but also for applications of antimicrobial peptides as pharmaceutical compounds. Biotechnologists have exploited fusion of antimicrobial peptides with pro-peptides to allow for the efficient production of antimicrobial peptides in bacterial hosts[9]. Pro-peptides can also be part of a pro-drug strategy for antimicrobial peptides, for example by arranging pro-peptide removal to be induced by the presence of a specific bacterial pathogen[10].

Explicit demonstration that pro-peptides inactivate the biological activity of antimicrobial peptides has been given for a number of cases, such as for defensins[6–8] but molecular mechanisms for inactivation have not yet been investigated. Very often, pro-peptide domains of antimicrobial peptides are highly acidic, and have charge densities that precisely neutralize the positive charge of the antimicrobial peptides. This suggests that electrostatic neutralization somehow plays an important role in inactivation by pro-peptides, but is unclear in what way. Ganz and co-workers[6,7] go one step further by hypothesizing that (at least for defensins) inactivation is due to

[1]Centro de Análises Proteômicas e Bioquímicas, Programa de Pós-Graduação em Ciências Genômicas e Biotecnologia, Universidade Católica de Brasília, Brasília-DF, Brazil. [2]Physical Chemistry and Soft Matter, Wageningen University, Stippeneng 4, 6708 WE, Wageningen, The Netherlands. [3]Programa de Pós-Graduação em Patologia Molecular, Faculdade de Medicina, Universidade de Brasília, Brasília-DF, Brazil. [4]S-inova Biotech, Programa de Pós-Graduação em Biotecnologia, Universidade Católica Dom Bosco, Campo Grande, MS, Brazil. [5]Host-Microbe Interactomics, Wageningen University, P.O. Box 338, 6700AH, Wageningen, The Netherlands. [6]Curso de Odontologia, Universidade Católica de Brasília, Brasília-DF, Brazil. Correspondence and requests for materials should be addressed to R.d.V. (email: renko.devries@wur.nl)

NJC

PAPER

Cite this: *New J. Chem.*, 2018, **42**, 13948

Synthesis and cytotoxic characteristics displayed by a series of Ag(I)-, Au(I)- and Au(III)-complexes supported by a common N-heterocyclic carbene†

Lalmohan Jhulki,[a] Parul Dutta,[b] Manas Kumar Santra,[b] Marlon H. Cardoso,[cde] Karen G. N. Oshiro,[ce] Octávio L. Franco,[cde] Valerio Bertolasi,[f] Anvarhusein A. Isab,[g] Christopher W. Bielawski[hi] and Joydev Dinda*[j]

Received 25th April 2018,
Accepted 13th July 2018

DOI: 10.1039/c8nj02008f

rsc.li/njc

The synthesis, structures and anticancer studies of a series of precious metal complexes supported by 1-methyl-2-(phenyl)imidazo[1,5-*a*]pyridine-2-ylidene (**1**) have been highlighted. The Ag(I) (**2**), Au(I) (**3**) and Au(III) (**4**) complexes were prepared using standard methods and characterized by a range of techniques, including NMR spectroscopy, X-ray crystallography and elemental analyses. The *in vitro* cytotoxicity activities displayed by **2–4** were explored against human colon adenocarcinoma (HCT116), lung cancer (A549) and breast cancer (MCF7) cell lines. A series of assays showed that all of the complexes exhibited significant growth inhibition in the aforementioned cell lines. Inspection of the data collected revealed that the Au(I) and Ag(I) complexes were more potent than their Au(III) congener, a trend that was found to be consistent with molecular docking studies that utilized BCL-2 as a model as this protein regulates cell death through apoptosis.

Introduction

The N-heterocyclic carbenes (NHCs) have emerged as an important class of ancillary ligands for a broad range of transition metals.[1] When compared to their phosphine analogues, metal complexes supported by NHCs often exhibit increased stabilities toward elevated temperatures, oxygen, and water, which frequently facilitates practicality.[2] Silver(I) complexes bearing NHCs, in particular, have attracted significant attention for their chemical,[3] structural[4] and photophysical properties.[5] More recently, the biological applications[6] displayed by Ag(I) and Au(I)–NHC complexes have steadily gained interest for their potential as new classes of metal-based drugs,[7] especially for the treatment of cancer and drug-resistant pathogens.[8,9] Although several reviews describe the utilities of Ag(I)–NHC complexes against various cancer lines, analogous Au(I) complexes may hold greater potential.[10] Gold has a long history of use as a medicine in ancient China and numerous gold-based drugs are being investigated for their activities against various ailments (*e.g.*, auranofin as an anti-rheumatic agent), including cancer.[11] Unfortunately, many of these complexes are readily metabolized *in vivo* by thiols,[12] which significantly reduces their activities. To overcome this limitation, gold-complexes bearing stabilizing NHCs have been explored as alternatives, often with good results.[13] For example, Panda and Ghosh reported[14] that Au(I)–NHC complex, [1-benzyl-3-*t*butylimidazol-2-ylidene]AuCl, exhibited excellent efficiency against the proliferation of HeLa cells (1.7% proliferation at $[Au]_0$ = 10 μM). Ott and co-workers discovered[15] that Au(I)–NHC-based thiotetrazolates are effective thioredoxin reductase inhibitors and antiproliferative agents against breast and colon carcinoma cells. Likewise, Berners-Price and Filipovska described[16] a new approach to based antitumor agents, where selective mitochondria targeting and thioredoxin by Picquet and Casini as anticancer agents against human

[a] *School of Applied Science, Haldia Institute of Technology, Haldia 721657, West Bengal, India*
[b] *National Centre for Cell Science, Pune 411007, Maharastra, India*
[c] *Programa de Pós-Graduação em Patologia Molecular, Faculdade de Medicina, Universidade de Brasília, Brasília-DF, Brazil*
[d] *Centro de Análises Proteômicas e Bioquímicas, Programa de Pós-Graduação em Ciências Genômicas e Biotecnologia, Universidade Católica de Brasília, Brasília-DF, Brazil*
[e] *Biotecnologia, Universidade Católica de Brasília, Brasília-DF, Brazil*
[f] *Dipartimento di Scienze Chimiche e Farmaceutiche, Centro di Strutturistica Diffrattometrica, Universita' di Ferrara, Via L. Borsari, 46, Italy*
[g] *Department of Chemistry, King Fahd University of Petroleum and Minerals, Dhahran 31261, Saudi Arabia*
[h] *Center for Multidimensional Carbon Materials (CMCM), Institute for Basic Science (IBS), Ulsan 44919, Republic of Korea*
[i] *Department of Chemistry and Department of Energy Engineering, Ulsan National Institute of Science and Technology (UNIST), Ulsan 44919, Republic of Korea*
[j] *Department of Chemistry, Utkal University, Vani Bihar, Bhubaneswar 751004, Odisha, India. E-mail: joydevdinda@gmail.com, dindajoy@yahoo.com*

† Electronic supplementary information (ESI) available: Crystallographic data for the complexes **2**, **3** and **4** in CIF format. CCDC 1562513–1562515. For ESI and crystallographic data in CIF or other electronic format see DOI: 10.1039/c8nj02008f

MICROBIOLOGY

RESEARCH ARTICLE
Cardoso *et al.*, *Microbiology*
DOI 10.1099/mic.0.000725

MICROBIOLOGY SOCIETY

Comparative transcriptome analyses of magainin I-susceptible and -resistant *Escherichia coli* strains

Marlon H. Cardoso,[1,2,3]† Keyla C. de Almeida,[1,2]† Elizabete S. Cândido,[1,3] Gabriel da R. Fernandes,[1,4] Simoni C. Dias,[1,5] Sérgio A. de Alencar[1] and Octávio L. Franco[1,2,3,*]

Abstract

Antimicrobial peptides (AMPs) have attracted considerable attention because of their multiple and complex mechanisms of action toward resistant bacteria. However, reports have increasingly highlighted how bacteria can escape AMP administration. Here, the molecular mechanisms involved in *Escherichia coli* resistance to magainin I were investigated through comparative transcriptomics. Sub-inhibitory concentrations of magainin I were used to generate four experimental groups, including magainin I-susceptible *E. coli*, in the absence (C) and presence of magainin I (CM); and magainin I-resistant *E. coli* in the absence (R) and presence of magainin I (RM). The total RNA from each sample was extracted; cDNA libraries were constructed and further submitted for Illumina MiSeq sequencing. After RNA-seq data pre-processing and functional annotation, a total of 103 differentially expressed genes (DEGs) were identified, mainly related to bacterial metabolism. Moreover, down-regulation of cell motility and chaperone-related genes was observed in CM and RM, whereas cell communication, acid tolerance and multidrug efflux pump genes (ABC transporter, major facilitator and resistance-nodulation cell division superfamilies) were up-regulated in these same groups. DEGs from the C and R groups are related to basal levels of expression of homeostasis-related genes compared to CM and RM, suggesting that the presence of magainin I is required to change the transcriptomics panel in both C and R *E. coli* strains. These findings show the complexity of *E. coli* resistance to magainin I through the rearrangement of several metabolic pathways involved in bacterial physiology and drug response, also providing information on the development of novel antimicrobial strategies targeting resistance-related transcripts and proteins herein described.

INTRODUCTION

Antimicrobial agents have long been developed as a flagship in medical modernization. During the mid-20th century, more precisely starting from 1940, the golden era of antibiotic discovery and application was established [1]. However, since the 1970s this reality has gone from boom to bust [1]. Bacterial resistance has gained huge ground over the years, and difficult-to-treat infections are among the greatest threats to human health [2]. In the United States, it is estimated that 23 000 people die annually due to multidrug-resistant bacterial infections, and more than two million require hospital treatment [1]. In addition, looking from another perspective, the bacterial resistance crisis is estimated to impact the global economy by up to US$100 trillion [1]. In this scenario, a race to comprehend the molecular panel involved in bacterial resistance to antibiotics has been in progress.

Received 24 February 2018; Accepted 6 September 2018
Author affiliations: [1]Pós-Graduação em Ciências Genômicas e Biotecnologia, Centro de Análises Proteômicas e Bioquímicas, Universidade Católica de Brasília, Brasília- DF, Brazil; [2]Programa de Pós-Graduação em Patologia Molecular, Faculdade de Medicina, Universidade de Brasília, Brasília-DF, Brazil; [3]S-Inova Biotech, Pós-graduação em Biotecnologia, Universidade Católica Dom Bosco, Campo Grande-MS, Brazil; [4]Oswaldo Cruz Foundation, René Rachou Research Center, Belo Horizonte, MG, Brazil; [5]Programa de Pós Graduação em Biologia Animal, Universidade de Brasília, Brasília, Brazil.
***Correspondence:** Octávio L. Franco, ocfranco@gmail.com
Keywords: RNA-seq; antimicrobial peptides; bacterial resistance; magainin I; comparative transcriptomics.
Abbreviations: AcrA and B, multidrug efflux pump subunit; *adk*, adenilate kinase; C, magainin I-susceptible *E. coli* in the absence of magainin I; CM, magainin I-susceptible *E. coli* in the presence of magainin I; CysA, P, U and W, sulfate/thiosulfate import ATP-binding protein; *cysG*, siroheme synthase; DEG, Differentially expressed genes; DNA *gyrB*, gyrase subunit B; dicF, small regulatory RNA; FlgF, H, G and K, flagellar hook-associated proteins; *frr*, ribosome recycling factor; *fumC*, fumarate hydratase; GadA, B and C, glutamate decarboxylase alpha, beta and gamma-aminobutyrate, respectively; *gyrA*, DNA gyrase subunit A; IbpA and B, small heat shock proteins; KEGG, Kyoto Encyclopedia of Genes and Genomes; MacAB, macrolide export ATP-binding/permease protein; *metG*, methionyl-tRNA synthetase; MIC, minimum inhibitory concentration; MqsR, mRNA interferase toxin; MSF, major facilitator superfamily; mtr, tryptophan-specific transport protein; PrpB, methylisocitrate lyase; PrpC, 2-methylcitrate synthase; PrpD, 2-methylcitrate dehydratase; PrpE, propionyl-CoA synthetase; R, magainin I-resistant *E. coli* in the absence of magainin I; *recA*, DNA recombination and repair protein; RM, magainin I-resistant *E. coli* in the presence of magainin I; RND, resistance-nodulation cell division; SecM, secretion monitor; SRP, signal recognition particle receptor; TolC, outer membrane protein channel; ZraP, R and S, zinc-associated proteins.
†These authors contributed equally to this work.
Four supplementary tables are available with the online version of this article.

ACS Infectious Diseases

Article

Cite This: ACS Infect. Dis. 2018, 4, 1727−1736

pubs.acs.org/journal/aidcbc

A Computationally Designed Peptide Derived from *Escherichia coli* as a Potential Drug Template for Antibacterial and Antibiofilm Therapies

Marlon H. Cardoso,[†,‡,§,∥] Elizabete S. Cândido,[‡,§] Lai Y. Chan,[∥] Marcelo Der Torossian Torres,[⊥,#,∇] Karen G. N. Oshiro,[†,§] Samilla B. Rezende,[§] William F. Porto,[‡,§,⊗] Timothy K. Lu,[⊥,#] Cesar de la Fuente-Nunez,[⊥,#] David J. Craik,[∥] and Octávio L. Franco*[,†,‡,§]

[†]Programa de Pós-Graduação em Patologia Molecular, Faculdade de Medicina, Universidade de Brasília, Campus Darcy Ribeiro, Asa Norte, Brasília, DF 70910900, Brazil

[‡]Centro de Análises Proteômicas e Bioquímicas, Pós-Graduação em Ciências Genômicas e Biotecnologia, Universidade Católica de Brasília, SGAN 916 Módulo B, Asa Norte, Brasília, DF 70790160, Brazil

[§]S-inova Biotech, Programa de Pós-Graduação em Biotecnologia, Universidade Católica Dom Bosco Avenida Tamandaré 6000, Campo Grande, MS 79117900, Brazil

[∥]Institute for Molecular Bioscience, The University of Queensland, 306 Carmody Road, Brisbane, QLD 4072, Australia

[⊥]Synthetic Biology Group, MIT Synthetic Biology Center; The Center for Microbiome Informatics and Therapeutics; Research Laboratory of Electronics, Department of Biological Engineering, and Department of Electrical Engineering and Computer Science, Massachusetts Institute of Technology, Cambridge, Massachusetts 02139, United States

[#]Broad Institute of MIT and Harvard, Cambridge, Massachusetts 02139, United States

[∇]Centro de Ciências Naturais e Humanas, Universidade Federal do ABC, Santo André, SP 09210170, Brazil

[⊗]Porto Reports, Brasília, DF 70790160, Brazil

Supporting Information

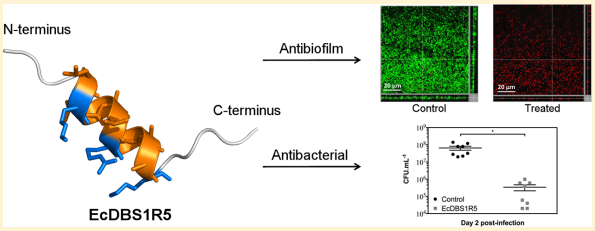

ABSTRACT: Computer-aided screening of antimicrobial peptides (AMPs) is a promising approach for discovering novel therapies against multidrug-resistant bacterial infections. Here, we functionally and structurally characterized an *Escherichia coli*-derived AMP (EcDBS1R5) previously designed through pattern identification [α-helical set (KK[ILV]$_{(3)}$[AILV])], followed by sequence optimization. EcDBS1R5 inhibited the growth of Gram-negative and Gram-positive, susceptible and resistant bacterial strains at low doses (2−32 μM), with no cytotoxicity observed against non-cancerous and cancerous cell lines in the concentration range analyzed (<100 μM). Furthermore, EcDBS1R5 (16 μM) acted on *Pseudomonas aeruginosa* pre-formed biofilms by compromising the viability of biofilm-constituting cells. The *in vivo* antibacterial potential of EcDBS1R5 was confirmed as the peptide reduced bacterial counts by two-logs 2 days post-infection using a skin scarification mouse model. Structurally, circular dichroism analysis revealed that EcDBS1R5 is unstructured in hydrophilic environments, but has strong helicity in 2,2,2-trifluoroethanol (TFE)/water mixtures (v/v) and sodium dodecyl sulfate (SDS) micelles. The TFE-induced nuclear magnetic resonance structure of EcDBS1R5 was determined and showed an amphipathic helical segment with flexible termini. Moreover, we observed that the amide protons for residues Met2-Ala8, Arg10, Ala13-Ala16, and Trp19 in EcDBS1R5 are protected from the solvent, as their temperature coefficients values are more positive than −4.6 ppb·K^{-1}. In summary, this study reports a novel dual-antibacterial/antibiofilm α-helical peptide with therapeutic potential *in vitro* and *in vivo* against clinically relevant bacterial strains.

KEYWORDS: *antimicrobial peptides, bacterial resistance, bacterial biofilm, skin infection, biophysics*

Multidrug bacterial resistance is among the most significant health threats of the 21st century.[1] Approximately 15 million deaths were associated with bacterial infections in 2010, and

Received: August 24, 2018
Published: October 22, 2018

DOI: 10.1021/acsinfecdis.8b00219
ACS Infect. Dis. 2018, 4, 1727−1736

The Journal of Antibiotics
https://doi.org/10.1038/s41429-018-0126-z

JARA Japan Antibiotics Research Association
The Society for Actinomycetes Japan

ARTICLE

Identification, molecular characterization, and structural analysis of the bla_{NDM-1} gene/enzyme from NDM-1-producing *Klebsiella pneumoniae* isolates

Jhessyca Leal Melgarejo[1] · Marlon Henrique Cardoso[1,2,3] · Ingrid Batista Pinto[1] · Célio Faria-Junior[4] · Sónia Mendo[5] · Carina Elisei de Oliveira[1] · Octavio Luiz Franco[1,2,3]

Received: 7 August 2018 / Revised: 18 October 2018 / Accepted: 5 November 2018

Abstract

NDM-1 comprises a carbapenemase that was first detected in 2008 in New Delhi, India. Since then, NDM-1-producing *Klebsiella pneumoniae* strains have been reported in many countries and usually associated with intra and inter-hospital dissemination, along with travel-related epidemiological links. In South America, Brazil represents the largest reservoir of NMD-1-producing *K. pneumoniae*. Here, we focused on the detection and molecular/structural characterization of the bla_{NDM-1} resistance gene/enzyme from 24 *K. pneumoniae* clinical isolates in the Midwest region of Brazil. Antimicrobial susceptibility assays showed that all isolates are resistant to carbapenems. Molecular typing of the isolates revealed seven clonal groups among the *K. pneumoniae* isolates, which may indicate intra or inter-hospital dissemination. Moreover, the bla_{NDM-1} gene was detected in all 24 *K. pneumoniae* isolates and the full bla_{NDM-1} gene was cloned. Bioinformatics analysis showed that the NDM-1 enzyme sequence found in our isolates is highly conserved when compared to other NDM-1 enzymes. In addition, molecular docking studies indicate that the NDM-1 identified binds to different carbapenems through hydrogen and zinc coordination bonds. In summary, we present the molecular characterization of NDM-1-producing *K. pneumoniae* strains isolated from different hospitals, also providing atomic level insights into molecular complexes NDM-1/carbapenem antibiotics.

Introduction

Klebsiella pneumoniae is a Gram-negative bacterium belonging to the Enterobacteriaceae family. This bacterium is a major pathogen associated with nosocomial infections and, for this reason, it is part of the so-called ESKAPE group (*Enterococcus faecium*, *Staphylococcus aureus*, *Klebsiella pneumoniae*, *Acinetobacter baumannii*, *Pseudomonas aeruginosa* and *Enterobacter* species), as an analogy to "escape" from the lethal action of antibiotics [1]. *K. pneumoniae* can be an opportunistic pathogen causing pulmonary, urinary tract, and bloodstream infections, as well as septicemia [2, 3]. Drug-resistant *K. pneumoniae* isolates are rapidly spreading and have become an important clinical challenge [4]. Carbapenems are last resort β-Lactam drugs used to treat serious bacterial infections [5]. Yet, diverse β-lactamases produced by bacteria can degrade β-lactam antibiotics by cleaving the β-lactam ring (CO–N bond), rendering them inactive [6, 7].

β-Lactamases can be classified according to their primary structure (classes A–D) or their biological function (groups

Electronic supplementary material The online version of this article (https://doi.org/10.1038/s41429-018-0126-z) contains supplementary material, which is available to authorized users.

✉ Octavio Luiz Franco
ocfranco@gmail.com

[1] S-Inova Biotech, Programa de Pós-Graduação em Biotecnologia, Universidade Católica Dom Bosco, Campo Grande, MS, Brazil

[2] Programa de Pós-Graduação em Patologia Molecular, Faculdade de Medicina, Universidade de Brasília, Brasília, DF, Brazil

[3] Centro de Análises Proteômicas e Bioquímicas, Programa de Pós-Graduação em Ciências Genômicas e Biotecnologia, Universidade Católica de Brasília, Brasília, DF, Brazil

[4] Núcleo de Bacteriologia, Laboratório Central de Saúde Pública do Distrito Federal, Brasília, DF, Brazil

[5] CESAM and Department of Biology, University of Aveiro, Campus de Santiago, Aveiro, Portugal

Published online: 27 November 2018

Artigo 16

ARTICLE IN PRESS
JPT-07296; No of Pages 20
Pharmacology & Therapeutics xxx (xxxx) xxx
Contents lists available at ScienceDirect
Pharmacology & Therapeutics
journal homepage: www.elsevier.com/locate/pharmthera

Neuropeptide receptors as potential pharmacological targets for obesity

Beatriz T. Meneguetti [a], Marlon H. Cardoso [a,b,c], Camila F.A. Ribeiro [a], Mário R. Felício [d], Ingrid B. Pinto [a], Nuno C. Santos [d], Cristiano M.E. Carvalho [a], Octávio L. Franco [a,b,c,*]

[a] S-Inova Biotech, Programa de Pós-Graduação em Biotecnologia, Universidade Católica Dom Bosco, Campo Grande, MS, Brazil
[b] Centro de Análises Proteômicas e Bioquímicas, Pós-Graduação em Ciências Genômicas e Biotecnologia, Universidade Católica de Brasília, Brasília, DF, Brazil
[c] Programa de Pós-Graduação em Patologia Molecular, Faculdade de Medicina, Universidade de Brasília, Brasília, DF, Brazil
[d] Instituto de Medicina Molecular, Faculdade de Medicina, Universidade de Lisboa, Lisbon, Portugal

ARTICLE INFO

Keywords:
Food intake
GPCRs
Hypothalamus
Neuropeptides
Peptide hormones
Obesity

ABSTRACT

Obesity is a chronic multifactorial disease, characterized by an excessive accumulation of adipose tissue. It is usually the result of excessive food intake and/or low energy expenditure. Obesity can be triggered by lifestyle, nutritional, genetic, environmental, hormonal and psychological factors. Several strategies are used to treat obesity, including dietary reeducation, with balanced food intake, increased physical exercise, in order to promote energy expenditure and to overcome the insufficiency in weight reduction by other strategies, and administration of drugs. However, these medications are associated to undesirable side effects, resulting in a high withdrawal rate. Several studies have been focused on the development of compounds that act in the hypothalamic region where the center of the regulation of hunger and satiety is located. Some of them target the activity of endogenous peptides, such as ghrelin pancreatic polypeptide, peptide YY and neuropeptide Y, as well as their receptors. This review addresses the importance of understanding the neuropeptide/peptide hormones and their receptors for the development of novel anti-obesity compounds that may aid in weight reduction as a promising alternative for the treatment of obesity.

Contents

1. Introduction . . . 0
2. Neuroendocrine regulation of hunger and satiety . . . 0
3. Conventional drug treatment in obesity . . . 0
4. The PP-fold neuropeptide family . . . 0
5. GPCRs and their relevance in obesity . . . 0
6. Conclusion and prospects . . . 0
Conflicts of interest statement . . . 0
Acknowledgments . . . 0
References . . . 0

Abbreviations: 5-HT, 5-hydroxytryptamine receptors; AgRP, agouti-related peptide; ARC, arcuate nucleus; BMI, body mass index; CART, cocaine and amphetamine-regulated transcript; CNS, central nervous system; FDA, Food and Drug Administration; GABA, γ-aminobutyric acid; GALP, galanin-like peptide; GLP-1, glucagon-like peptide-1; GPCRs, G-protein coupled receptors; LHA, lateral hypothalamic area; MCH, melanin-concentrating hormone; MCR, melanocortin receptors; NPY, neuropeptide Y; OX1, orexin 1; OX2, orexin 2; POMC, pro-opiomelanocortin; PP, pancreatic polypeptide; PVN, paraventricular nucleus; PYY, Peptide YY; RYGB, Roux-en-Y gastric bypass; TAG, triacylglycerol; TM, transmembrane helices; TRH, thyrotropin-releasing hormone; VMH, ventromedial hypothalamus; α-MSH, melanocyte-stimulating hormones.

* Corresponding author at: Universidade Católica Dom Bosco, Pós-Graduação em Biotecnologia, S-Inova Biotech - Av. Tamandaré 6000, Jardim Seminário, 79117-900 Campo Grande, MS, Brazil.
E-mail address: ocfranco@gmail.com (O.L. Franco).

1. Introduction

Obesity is a multifactorial disease that can be considered one of the major public health problems, due to its high prevalence worldwide, being characterized as a global pandemic (Ng et al., 2014; Popkin et al., 2012; Swinburn et al., 2011). Obesity is characterized by excessive weight and abnormal or excessive fat accumulation, which can cause the development of several diseases (WHO, 2000), such as type 2 diabetes, insulin resistance, hypertension, cardiovascular diseases (Kopelman, 2000), hyperlipidemia, osteoarthritis, sleep apnea, non-alcoholic hepatic steatosis

https://doi.org/10.1016/j.pharmthera.2018.11.002
0163-7258/

Please cite this article as: B.T. Meneguetti, M.H. Cardoso, C.F.A. Ribeiro, et al., Neuropeptide receptors as potential pharmacological targets for obesity, Pharmacology & Therapeutics, https://doi.org/10.1016/j.pharmthera.2018.11.002

Artigo 17

COMMUNICATIONS BIOLOGY

ARTICLE

DOI: 10.1038/s42003-018-0224-2 OPEN

Structure-function-guided exploration of the antimicrobial peptide polybia-CP identifies activity determinants and generates synthetic therapeutic candidates

Marcelo D.T. Torres[1,2,3], Cibele N. Pedron[3], Yasutomi Higashikuni et al.[#]

Antimicrobial peptides (AMPs) constitute promising alternatives to classical antibiotics for the treatment of drug-resistant infections, which are a rapidly emerging global health challenge. However, our understanding of the structure-function relationships of AMPs is limited, and we are just beginning to rationally engineer peptides in order to develop them as therapeutics. Here, we leverage a physicochemical-guided peptide design strategy to identify specific functional hotspots in the wasp-derived AMP polybia-CP and turn this toxic peptide into a viable antimicrobial. Helical fraction, hydrophobicity, and hydrophobic moment are identified as key structural and physicochemical determinants of antimicrobial activity, utilized in combination with rational engineering to generate synthetic AMPs with therapeutic activity in a mouse model. We demonstrate that, by tuning these physicochemical parameters, it is possible to design nontoxic synthetic peptides with enhanced sub-micromolar antimicrobial potency in vitro and anti-infective activity in vivo. We present a physicochemical-guided rational design strategy to generate peptide antibiotics.

. Correspondence and requests for materials should be addressed to V.X.O.J. (email: vani.junior@ufabc.edu.br) or to T.K.L. (email: timlu@mit.edu) or to C.d.l.F.-N. (email: cfuente@mit.edu). [#]A full list of authors and their affliations appears at the end of the paper.

PATHOGENS AND GLOBAL HEALTH
https://doi.org/10.1080/20477724.2018.1559489

Adevonin, a novel synthetic antimicrobial peptide designed from the *Adenanthera pavonina* trypsin inhibitor (ApTI) sequence

Mayara S. Rodrigues[a], Caio F. R. de Oliveira[b], Luís H. O. Almeida[a], Simone M. Neto[a], Ana Paula A. Boleti[b], Edson L. dos Santos[b], Marlon H. Cardoso[c,d,e], Suzana M. Ribeiro[b,e], Octávio L. Franco[c,d,e], Fernando S. Rodrigues[f], Alexandre J. Macedo[g], Flávia R. Brust[g] and Maria Lígia R. Macedo[a]

[a]Faculdade de Ciências Farmacêuticas, Alimentos e Nutrição, Universidade Federal de Mato Grosso do Sul, Campo Grande, Brazil; [b]Faculdade de Ciências Biológicas e Ambientais, Universidade Federal da Grande Dourados, Dourados, Brazil; [c]Centro de Análises Proteômicas e Bioquímicas, Programa de Pós-Graduação em Ciências Genômicas e Biotecnologia, Universidade Católica de Brasília, Brasília, Brazil; [d]Programa de Pós-Graduação em Patologia Molecular, Faculdade de Medicina, Universidade de Brasília, Brasília, Brazil; [e]S-inova Biotech, Programa de Pós-Graduação em Biotecnologia, Universidade Católica Dom Bosco, Campo Grande, Brazil; [f]Programa de Pós Graduação em Medicina Veterinária, Universidade Federal de Santa Maria, Santa Maria, Brazil; [g]Faculdade de Farmácia e Centro de Biotecnologia, Universidade Federal do Rio Grande do Sul, Porto Alegre, Brazil

ABSTRACT

The biological activities and the structural arrangement of adevonin, a novel antimicrobial peptide, were investigated. The trypsin inhibitor ApTI, isolated from *Adenanthera pavonina* seeds, was used as a template for screening 18-amino acid peptides with predicted antimicrobial activity. Adevonin presented antimicrobial activity and minimum inhibitory concentrations (MIC) ranging from 1.86 to 7.35 μM against both Gram-positive and – negative bacterial strains. Moreover, adevonin exerted time-kill effects within 10 min and both susceptible and drug-resistant bacterial strains were affected by the peptide. *In vitro* and *in vivo* assays showed that, at MIC concentration, adevonin did not affect human fibroblasts (MRC-5) viability or *Galleria mellonella* survival, respectively. Hemolytic activity was observed only at high peptide concentrations. Additionally, nucleic acid efflux assays, gentian violet uptake and time-kill kinetics indicate that the antimicrobial activity of adevonin may be mediated by bacterial membrane damage. Furthermore, molecular dynamic simulation in the presence of SDS micelles and anionic membrane bilayers showed that adevonin acquired a stable α-helix secondary structure. Further studies are encouraged to better understand the mechanism of action of adevonin, as well as to investigate the anti-infective activity of this peptide.

KEYWORDS

Adenanthera pavonina; antimicrobial peptide; rational design; α-helical

1. Introduction

The emergence and spreading of multidrug-resistant bacteria strains have increased in recent decades. Known as 'superbugs' [1,2], these bacteria strains display resistance against different antibiotic classes and their appearance has spread at alarming rates. High bacterial resistance levels present a potential public health risk difficulting infectious diseases control that further aggravating clinical conditions. In order to address this global threat, research and development of new antimicrobial drugs with mechanisms of action that differ from traditional antibiotics are of great importance [3]. In this context, antimicrobial peptides (AMPs) represent a potential class of molecules to be used in the prevention and control of bacterial infections.

AMPs are a class of antimicrobials with broad-spectrum activities, usually composed of 10 to 50 amino acids, also presenting an overall positive charge and large hydrophobic patches [4–6]. They are classified into 4 major structural categories, according to the secondary structure adopted during the interaction with the bacterial membrane, including α-helix, β-sheet, loop coil, and extended structural arrangements [7]. In addition to the AMPs obtained from natural sources, numerous AMPs have been designed based on natural peptides [8]. As a result of knowledge derived from natural peptides and database screening, shorter and more specific AMPs have been designed. The rational design and chemical synthesis of AMPs may overcome issues related to stability, bioavailability and their resistance to proteolysis [9]. For AMPs to become a therapeutic option several challenges must be overcome, including antibacterial effectiveness *in vitro* and *in vivo*, along with low toxicity rates at the therapeutic dose [10]. The use of innovative rational and computational design strategies have the potential to increase the discovery of novel therapeutic peptides at a lower cost, with enhanced effectiveness and broad-spectrum activities [10,11].

Here we report the rational design of a new AMP derived from the *Adenanthera pavonina* trypsin inhibitor

CONTACT Maria Lígia R. Macedo ligiamacedo18@gmail.com Faculdade de Ciências Farmacêuticas, Alimentos e Nutrição, Universidade Federal de Mato Grosso do Sul, Campo Grande, Brazil
Supplemental data can be accessed here.

Capítulo de livro 1

Proteinaceous Plant Toxins with Antimicrobial and Antitumor Activities

Elizabete de Souza Cândido, Marlon Henrique Cardoso, Daniel Amaro Sousa, Karina Castellanos Romero and Octávio Luiz Franco

Contents

Introduction 2
Non-usual Plant Toxin Classes 3
β-Momorcharin 3

E.S. Cândido
Centro de Análises Proteômicas e Bioquímicas, Programa de Pós-Graduação em Ciências Genômicas e Biotecnologia, Universidade Católica de Brasília, Brasília, Distrito Federal, Brazil
e-mail: betty.souza@gmail.com

M.H. Cardoso • D.A. Sousa
Centro de Análises Proteômicas e Bioquímicas, Programa de Pós-Graduação em Ciências Genômicas e Biotecnologia, Universidade Católica de Brasília, Brasília, Distrito Federal, Brazil

Programa de Pós-Graduação em Patologia Molecular, Universidade de Brasília, Brasília, Distrito Federal, Brazil
e-mail: marlonhenrique6@gmail.com; amarods@gmail.com

K.C. Romero
Programa de Pós-Graduação em Genética e Biotecnologia, Departamento de Genética e Biotecnologia, Instituto de Ciências Biológicas, Universidade Federal de Juiz de Fora, Campus Universitário, Juiz de Fora, Minas Gerais, Brazil
e-mail: karinaicr@yahoo.es

O.L. Franco (✉)
Centro de Análises Proteômicas e Bioquímicas, Programa de Pós-Graduação em Ciências Genômicas e Biotecnologia, Universidade Católica de Brasília, Brasília, Distrito Federal, Brazil

Programa de Pós-Graduação em Patologia Molecular, Universidade de Brasília, Brasília, Distrito Federal, Brazil

Programa de Pós-Graduação em Genética e Biotecnologia, Departamento de Genética e Biotecnologia, Instituto de Ciências Biológicas, Universidade Federal de Juiz de Fora, Campus Universitário, Juiz de Fora, Minas Gerais, Brazil

S-Inova Biotech, Programa de Pós-Graduação em Biotecnologia, Universidade Catolica Dom Bosco, Campo Grande, Mato Grosso do Sul, Brazil
e-mail: ocfranco@gmail.com

P. Gopalakrishnakone et al. (eds.), *Plant Toxins*, Toxinology,
DOI 10.1007/978-94-007-6728-7_12-1

Capítulo de livro 2

Peptides containing D-amino acids and retro-inverso peptides: General applications and special focus on antimicrobial peptides

5

Marlon H. Cardoso[1,2,3], Elizabete S. Cândido[2,3], Karen G.N. Oshiro[3], Samilla B. Rezende[3] and Octávio L. Franco[1,2,3]
[1]University of Brasília, Brasília, Brazil, [2]Catholic University of Brasília, Brasília, Brazil, [3]Catholic University Dom Bosco, Campo Grande, Brazil

5.1 Introduction and overview

According to the central dogma established by classical naturalists and biologists, proteins/peptides were expected to be exclusively constituted by 20 building blocks, including 19 L-amino acids (L-AAs) and glycine, which is not chiral. At that time, special cases were reported for D-amino acids (D-AAs) containing proteins/peptides such as the presence of D-alanine in octopine derivatives from octopus [1]. Over the years, however, increasing reports were published revealing the natural occurrence of D-AAs in several organisms [2,3]. Since there is no codon for D-AAs synthesis, a gap regarding the biogenesis of D-AAs containing proteins/peptides encouraged further studies, which have led to diverse hypotheses. Among them, we can cite the incorporation of D-AAs during the translation of L-proteins/peptides, the isomerization of L-AAs within polypeptide chains by nonenzymatic pathways, as well as by the action of specific isomerases [4]. From a functional point of view, these post-translational and chemical modifications in D-AAs containing proteins/peptides confer on them an unusual stereochemistry mostly related to enhanced resistance to enzyme-catalyzed breakdown, which is indicated as a desirable property when it comes to pharmacological investments.

Structurally, apart from the conserved physicochemical properties between L- and D-enantiomers, each enantiomer rotates plane-polarized light in opposite directions. In other words, it means that in α-helical peptides, for example, the left-handed helix of the parent L-peptide could be presented as a right-handed helix in the D-peptide analogues [5]. Interestingly, experimental structural analyses have shown that D-AAs may act as α-helical and β-sheet breakers in D-AAs containing peptides, contributing to a completely opposite spatial orientation when compared to their parent L-peptides, thus favoring proteolytic stability and, consequently, bioavailability in vivo [6]. On the other hand, there are suggestions indicating that D-AAs stabilize turns, for example, in the $(i + 1)$ or $(i + 2)$ positions of types II' and II β-turns, respectively [7]. In addition, more recently, Makwana and Mahalakshmi

Peptide Applications in Biomedicine, Biotechnology and Bioengineering.
DOI: http://dx.doi.org/10.1016/B978-0-08-100736-5.00005-3

CHAPTER TEN

The Structure/Function Relationship in Antimicrobial Peptides: What Can we Obtain From Structural Data?

Marlon H. Cardoso[*,†,‡,2], **Karen G.N. Oshiro**[‡,2], **Samilla B. Rezende**[‡], **Elizabete S. Cândido**[†,‡], **Octávio L. Franco**[*,†,‡,1]

*Programa de Pós-Graduação em Patologia Molecular, Faculdade de Medicina, Universidade de Brasília, Brasília, Brazil
†Centro de Análises Proteômicas e Bioquímicas, Programa de Pós-Graduação em Ciências Genômicas e Biotecnologia, Universidade Católica de Brasília, Brasília, Brazil
‡S-inova Biotech, Programa de Pós-Graduação em Biotecnologia, Universidade Católica Dom Bosco, Campo Grande, Brazil
[1]Corresponding author: e-mail address: ocfranco@gmail.com

Contents

1. Introduction 360
2. Experimental Approaches for the Structural Elucidation of AMPs 361
   2.1 Solution NMR 361
   2.2 Solid-State NMR 367
   2.3 X-Ray Crystallography 369
   2.4 Cryo-Electron Microscopy 372
3. Computational Approaches for AMPs Structure Prediction 374
   3.1 Molecular Modeling, Dynamics, and Docking 374
4. Outlook 377
References 379

Abstract

Antimicrobial peptides (AMPs) have been widely isolated from most organisms in nature. This class of antimicrobials may undergo changes in their sequence for improved physicochemical properties, including charge, hydrophobicity, and hydrophobic moment. It is known that such properties may be directly associated with AMPs' structural arrangements and, consequently, could interfere in their modes of action against microorganisms. In this scenario, biophysical methodologies, such as nuclear magnetic resonance spectroscopy, X-ray crystallography, and cryo-electron

[2] These authors contributed equally.

Advances in Protein Chemistry and Structural Biology, Volume 112
ISSN 1876-1623
https://doi.org/10.1016/bs.apcsb.2018.01.008

Artigo em conferência 1

library for activity in the presence of RBCs. We present data from preliminary screening that indicates our new library contains peptides that retain activity in the presence of RBCs; greatly outperforming the template peptide. Additionally, we show data on two peptides discovered in our preliminary screens that have been characterized and compared to the template sequence. Both of the peptides discovered show reduced antimicrobial potency as compared to the parent sequence when RBCs are not present, but increased efficacy in the presence of concentrated erythrocytes. As these peptides were discovered in a small screen of only 2000 library sequences, we believe the library contains peptides that will retain potent activity in the presence of RBCs. Finally, we present a revised screening approach that will be employed for a full-scale screen of the library with the intention of retaining the high antibiotic potency characteristic of the parent peptide while selecting for minimal interaction with and toxicity toward eukaryotic cells.

405-Pos Board B185
Molecular Dynamics Simulation of Passive Transport of Neurotoxicant Antidotes through the Blood-Brain Barrier
Yukun Wang, Peter C. Searson, Martin Ulmschneider.
Department of Materials Science and Engineering, Johns Hopkins University, Baltimore, MD, USA.
Systemic delivery of neurotoxicant antidotes into the brain is controlled by the blood-brain barrier. At present the atomic detail mechanisms of molecular transport across the blood brain barrier are poorly understood, hindering optimization of delivery properties of next-generation antidotes. Here we study the mechanisms of passive molecular transport of a number of oximes and other small molecules across the blood-brain barrier. For this purpose, we have built atomic detail molecular models of the apical and basolateral lipid bilayer membranes of human brain microvascular endothelial cells. Lipid bilayer properties were validated against experimental data. Subsequently the diffusive transport of oximes and other small molecules across the apical and basolateral lipid bilayer was simulated using atomic detail molecular dynamics simulations. This allowed measurement of transbilayer permeation rates, which can be directly compared to experimental data, as well as providing atomic detail insights into the mechanisms of drug transport. The simulations reveal how individual drug chemistry (e.g. lipophilicity, polarity, hydrogen bonds) affects drug-bilayer interactions, and ultimately the rate of passive diffusion across the bilayer.

406-Pos Board B186
A Comparative Study on Techniques for the Determination of Permeabilization Events on Charged and Uncharged Lipid Bilayers
Laura Paulowski[1], Nadine Gebauer[1], Julia Wernecke[2], Bruce A. Cornell[3], Thomas Gutsmann[1].
[1]Research Center Borstel, Borstel, Germany, [2]Deutsches Elektronen Synchrotron DESY, Hamburg, Germany, [3]SDx Tethered Membranes, Sydney, Australia.
Host defense peptides (HDPs) are small effector molecules of the innate immune system building up the first defense barrier when it comes to infections. Infectious diseases are commonly treated with antibiotics leading to an increase in antibiotic resistances among clinically relevant pathogens. Therefore, understanding the mode of function of alternative agents with antibiotic function is undeniable for the successful development of new antibiotics opening new treatment options. To understand recognition-, recruiting- and permeabilization-processes on membrane surfaces a set of structurally diverse peptides is investigated regarding their membrane active function on charged and uncharged model membranes. Lipid bilayers are reconstituted from pure DOPC to mimic uncharged membranes and from POPE/POPG in a ratio of 4:1 to mimic the inner leaflet of the bactericidal cell envelope with an overall negative surface charge. Permeabilization events induced by the antimicrobial peptides LL32, Arenicin-1 and hBD3-l as well as the ionophore Nonactin and α-Hemolysin of *Staphylococcus aureus* are investigated with respect to the membrane systems stated above, buffer composition (high-salt vs. low-salt) and temperature conditions. A combination of a complex array of biophysical techniques is taken into account for studying permeabilization events with nearly no limitations - MONTAL-MUELLER-Setup for planar lipid bilayers, tethered membrane technology for supported bilayers, liposome-based assays (Calcein release assay, potassium iodide quenching, FRET-intercalation assay) and a chip-based pore spanning dye release assay. These methods allow to investigate the whole spectrum ranging from single pore characterization to the statistical analysis of either large membrane areas or a huge number of single membranes.

407-Pos Board B187
Localisation of the Antimicrobial Peptide Maculatin 1.1 in Lipid Bilayers using Solid-State NMR
Marc-Antoine Sani, Frances Separovic.
School of Chemistry Bio21 institute, Univeristy of Melbourne, parkville, Australia.
Antimicrobial peptides that target membranes are an attractive alternative to classic antibiotics, since they do not require internalization nor target a specific stereo-structure, thus limiting development of bacterial resistance. Their mode of action involves the disruption of lipid membranes, leading to growth inhibition and ultimately death of the bacteria. However, the molecular details of the killing mechanism and, more particularly, the difference in potency observed between different bacterial strains, remain unclear. Structural information is crucial for defining the molecular mechanism by which these peptides recognize and interact with a particular lipid membrane. Solid-state NMR is a non-invasive tool that allows study of the structural details of lipid-peptide interactions. Explicitly, we have combined ^{2}H, ^{31}P, $\{^{19}F\}^{13}C$ and $\{^{31}P\}^{13}C$ REDOR solid-state NMR experiments to obtain the localisation of the antimicrobial peptide maculatin 1.1 (Mac1) in anionic lipid bilayers (PC/PG 3:1). Mac1 showed reduced dynamics of d_{54}-DMPG acyl chain compared to d_{54}-DMPC. ^{31}P NMR experiments also showed more pronounced effect on DMPG than neutral DMPC headgroups. Penetration depth of the peptide was further probed by REDOR experiments where the distance between the ^{13}C labelled peptide and the acyl chain mono-fluorinated DPPC lipid or the phosphorous headgroup was measured. Furthermore, solution NMR using isotropic bicelles with similar lipid composition showed a helical peptide structure for Mac1 and addition of paramagnetic agents confirmed a transmembrane insertion. Overall, Mac1 showed a greater affinity for the anionic DMPG, recruiting the lipid while spaning the bilayer in a transmembrane orientation.

408-Pos Board B188
Pa-MAP 1.5 and 1.9: Mechanisms of Action of two Antimicrobial Peptides
Mário R. Felício[1], Octavio L. Franco[2], Marlon H. Cardoso[2], Ludovico Migliolo[2], Nuno C. Santos[1], Sónia Gonçalves[1].
[1]Nuno Santos Lab, Instituto de Medicina Molecular, Lisbon, Portugal, [2]S-inova, Programa de Pós-Graduação em Biotecnologia, Universidade Católica Dom Bosco, Campo Grande, MS, Brazil.
Increased resistance to conventional antibiotics has become a major problem worldwide. Existing antibiotics are increasingly ineffective, as a result of resistance, becoming imperative to find new antibacterial strategies. One of the most promising possibilities is the use of antimicrobial peptides (AMPs), which play an important role in the innate immune response of different organisms. Some of these peptides can also act against cancer cells (anticancer peptides, ACPs). AMPs are small cationic amphipathic molecules. Their mechanisms of action are not fully understood, but their physicochemical properties are determinant, namely their amphipathic conformation upon interaction with biomembranes and their positive net charge, which allows them to interact preferentially with negatively charged biomembranes, like those of Gram-negative bacteria. Until now, AMPs demonstrate a low propensity for drug resistance development.
Two different AMPs (*Pa*-MAP 1.5 and 1.9) were synthetically created based on an antifreezing peptide from the Antarctic fish *Pleuronectes americanus*. Both peptides showed promising therapeutic results against bacteria and cancer cells. Membrane leakage tests using lipid vesicles to mimic bacteria and cancer cells have shown that these two AMPs efficiently induce membrane disruption. Dynamic light scattering, surface plasmon resonance and zeta-potential studies confirmed the interaction of the peptides with the membranes. Studies using fluorescent probes that report different aspects of peptide-membrane interaction (DPH, TMA-DPH, di-8-ANEPPS and Laurdan) were also conducted, either using model vesicles or with *Escherichia coli*. Atomic force microscopy imaging of the AMPs effects on live cells and flow cytometry measurements confirmed the results obtained with lipid vesicles. The results obtained show that, although these two AMPs have several similarities, they act through different mechanisms of action.

Patente 1

UNIVERSIDADE CATÓLICA DOM BOSCO
Inspira o futuro

DECLARAÇÃO DE TRÂMITE PROCESSUAL

Declaro, para os devidos fins, que a Srta. **KAREN GARCIA NOGUEIRA OSHIRO** junto dos inventores, **MARLON HENRIQUE E SILVA CARDOSO, ELIZABETE DE SOUZA CÂNDIDO, SILVIA GOMES RODRIGUES, SUZANA MEIRA RIBEIRO, WILLIAN FARIAS PORTO e OCTÁVIO LUIZ FRANCO** apresentaram ao Núcleo de Inovação Tecnológica da Universidade Católica Dom Bosco o projeto de pesquisa e inovação resultante no processo de Pedido de Depósito de Patente (NIT/S-INOVA/UCDB nº01.2017-10), sob o título "**R1 E R5, PEPTÍDEOS SINTÉTICOS COM AÇÃO ANTIBACTERIANA**", o qual encontra-se em trâmite processual interno de depósito de patente junto ao Instituto Nacional de Propriedade Industrial – INPI, sob o protocolo **BR10 2018 0005359.**

Campo Grande/MS, 25 de Janeiro de 2017.

NEILA FARIAS LOPES
Diretora de Inovação
Agência de Inovação e Empreendedorismo S-INOVA
Universidade Católica Dom Bosco - UCDB

MISSÃO SALESIANA DE MATO GROSSO - UNIVERSIDADE CATÓLICA DOM BOSCO
Av. Tamandaré, 6000 - Jardim Seminário - CEP: 79117-900 - CAMPO GRANDE - MS - BRASIL
CNPJ/MF: 03.226.149/0015-87 - Fone: 55 67 3312 3300 - Fax: 55 67 3312 3301 - www.ucdb.br

10. REFERÊNCIA BIBLIOGRÁFICAS

ABRAHAM, E. P.; CHAIN, E. An enzyme from bacteria able to destroy penicillin. 1940. **Rev Infect Dis,** v. 10, n. 4, p. 677-8, 1988.

AFACAN, N. J. et al. Therapeutic potential of host defense peptides in antibiotic-resistant infections. **Curr Pharm Des,** v. 18, n. 6, p. 807-19, 2012.

ALEKSHUN, M. N.; LEVY, S. B. Molecular mechanisms of antibacterial multidrug resistance. **Cell,** v. 128, n. 6, p. 1037-50, 2007.

ALVES, A. C. et al. Biophysics in cancer: The relevance of drug-membrane interaction studies. **Biochim Biophys Acta,** v. 1858, n. 9, p. 2231-44, 2016.

ANDERSON, A. C. The process of structure-based drug design. **Chem Biol,** v. 10, n. 9, p. 787-97, 2003.

ANDRESEN, L.; TENSON, T.; HAURYLIUK, V. Cationic bactericidal peptide 1018 does not specifically target the stringent response alarmone (p)ppGpp. **Sci Rep,** v. 6, p. 36549, 2016.

ARIAS, C. A.; MURRAY, B. E. A new antibiotic and the evolution of resistance. **N Engl J Med,** v. 372, n. 12, p. 1168-70, 2015.

BAKER-AUSTIN, C. et al. Co-selection of antibiotic and metal resistance. **Trends Microbiol,** v. 14, n. 4, p. 176-82, 2006.

BALABAN, N. et al. Use of the quorum-sensing inhibitor RNAIII-inhibiting peptide to prevent biofilm formation *in vivo* by drug-resistant *Staphylococcus epidermidis*. **J Infect Dis,** v. 187, n. 4, p. 625-30, 2003.

BALESTRINO, D. et al. Characterization of type 2 quorum sensing in *Klebsiella pneumoniae* and relationship with biofilm formation. **J Bacteriol,** v. 187, n. 8, p. 2870-80, 2005.

BALTZER, S. A.; BROWN, M. H. Antimicrobial peptides: promising alternatives to conventional antibiotics. **J Mol Microbiol Biotechnol,** v. 20, n. 4, p. 228-35, 2011.

BECHINGER, B. Membrane insertion and orientation of polyalanine peptides: a (15)N solid-state NMR spectroscopy investigation. **Biophys J,** v. 81, n. 4, p. 2251-6, 2001.

BESSA, L. J. et al. Synergistic and antibiofilm properties of ocellatin peptides against multidrug-resistant *Pseudomonas aeruginosa*. **Future Microbiol,** v. 13, p. 151-63, 2018.

BHARDWAJ, A. K.; VINOTHKUMAR, K.; RAJPARA, N. Bacterial quorum sensing inhibitors: attractive alternatives for control of infectious pathogens showing multiple drug resistance. **Recent Pat Antiinfect Drug Discov,** v. 8, n. 1, p. 68-83, 2013.

BILLAL, D. S. et al. Whole genome analysis of linezolid resistance in *Streptococcus pneumoniae* reveals resistance and compensatory mutations. **BMC Genomics,** v. 12, p. 512, 2011.

BJARNSHOLT, T. et al. Applying insights from biofilm biology to drug development - can a new approach be developed? **Nat Rev Drug Discov,** v. 12, n. 10, p. 791-808, 2013.

BLAIR, J. M. et al. Molecular mechanisms of antibiotic resistance. **Nat Rev Microbiol,** v. 13, n. 1, p. 42-51, 2015.

BLONDELLE, S.; LOHNER, K. Optimization and high-throughput screening of antimicrobial peptides. **Curr Pharm Des,** v. 16, n. 28, p. 3204-11, 2010.

BOUCHER, H. W. et al. Progress development of new drugs active against gram-negative bacilli: an update from the Infectious Diseases Society of America. **Clin Infect Dis,** v. 56, n. 12, p. 1685-94, 2013.

BRACKMAN, G.; COENYE, T. Quorum sensing inhibitors as anti-biofilm agents. **Curr Pharm Des,** v. 21, n. 1, p. 5-11, 2015.

BRANCATISANO, F. L. et al. Inhibitory effect of the human liver-derived antimicrobial peptide hepcidin 20 on biofilms of polysaccharide intercellular adhesin (PIA)-positive and PIA-negative strains of *Staphylococcus epidermidis*. **Biofouling,** v. 30, n. 4, p. 435-46, 2014.

CANDIDO, E. D. et al. The use of versatile plant antimicrobial peptides in agribusiness and human health. **Peptides,** v. 55, p. 65-78, 2014.

CARDOSO, M. H. et al. A computationally designed peptide derived from *Escherichia coli* as a potential drug template for antibacterial and antibiofilm therapies. **ACS Infect Dis,** v. 4, n. 12, p. 1727-36, 2018.

CARDOSO, M. H. et al. Comparative transcriptome analyses of magainin I-susceptible and -resistant *Escherichia coli* strains. **Microbiology,** v. 164, n. 11, p. 1383-93, 2018.

CARDOSO, M. H. et al. The structure/function relationship in antimicrobial peptides: What can we obtain from structural data? **Adv Protein Chem Struct Biol,** v. 112, p. 359-84, 2018.

CARDOSO, M. H. et al. A polyalanine peptide derived from polar fish with anti-infectious activities. **Sci Rep,** v. 6, p. 21385, 2016.

CHEN, Y. et al. Rational design of alpha-helical antimicrobial peptides with enhanced activities and specificity/therapeutic index. **J Biol Chem,** v. 280, n. 13, p. 12316-29, 2005.

CHERNYSH, S.; GORDYA, N.; SUBOROVA, T. Insect antimicrobial peptide complexes prevent resistance development in bacteria. **PLoS One,** v. 10, n. 7, p. e0130788, 2015.

CHUA, S. L. et al. C-di-GMP regulates *Pseudomonas aeruginosa* stress response to tellurite during both planktonic and biofilm modes of growth. **Sci Rep,** v. 5, p. 10052, 2015.

CONGREVE, M.; MURRAY, C. W.; BLUNDELL, T. L. Structural biology and drug discovery. **Drug Discov Today,** v. 10, n. 13, p. 895-907, 2005.

COSTA, F. et al. Covalent immobilization of antimicrobial peptides (AMPs) onto biomaterial surfaces. **Acta Biomater,** v. 7, n. 4, p. 1431-40, 2011.

COSTERTON, J. W.; STEWART, P. S.; GREENBERG, E. P. Bacterial biofilms: a common cause of persistent infections. **Science,** v. 284, n. 5418, p. 1318-22, 1999.

D'ANGELO, I. et al. Overcoming barriers in *Pseudomonas aeruginosa* lung infections: Engineered nanoparticles for local delivery of a cationic antimicrobial peptide. **Colloids Surf B Biointerfaces,** v. 135, p. 717-25, 2015.

DAVIES, A.; SHAMU, C. An introduction to high content screening: imaging technology, assay development, and data analysis in biology and drug discovery. John Wiley & Sons, 2014. ISBN-1118859413.

DAVIES, D. Understanding biofilm resistance to antibacterial agents. **Nat Rev Drug Discov,** v. 2, n. 2, p. 114-22, 2003.

DE LA FUENTE-NUNEZ, C. et al. Synthetic antibiofilm peptides. **Biochim Biophys Acta,** v. 1858, n. 5, p. 1061-9, 2016.

DE LA FUENTE-NUNEZ, C. et al. Bacterial biofilm development as a multicellular adaptation: antibiotic resistance and new therapeutic strategies. **Curr Opin Microbiol,** v. 16, n. 5, p. 580-9, 2013.

DE LA FUENTE-NUNEZ, C. et al. Broad-spectrum anti-biofilm peptide that targets a cellular stress response. **PLoS Pathog,** v. 10, n. 5, p. e1004152, 2014.

DE LA FUENTE-NUNEZ, C. et al. D-enantiomeric peptides that eradicate wild-type and multidrug-resistant biofilms and protect against lethal *Pseudomonas aeruginosa* infections. **Chem Biol,** v. 22, n. 2, p. 196-205, 2015.

DI LUCA, M. et al. BaAMPs: the database of biofilm-active antimicrobial peptides. **Biofouling,** v. 31, n. 2, p. 193-9, 2015.

DI LUCA, M.; MACCARI, G.; NIFOSI, R. Treatment of microbial biofilms in the post-antibiotic era: prophylactic and therapeutic use of antimicrobial peptides and their design by bioinformatics tools. **Pathog Dis,** v. 70, n. 3, p. 257-70, 2014.

DOLEJSKA, M. et al. Complete sequencing of an IncHI1 plasmid encoding the carbapenemase NDM-1, the ArmA 16S RNA methylase and a resistance-nodulation-cell division/multidrug efflux pump. **J Antimicrob Chemother,** v. 68, n. 1, p. 34-9, 2013.

DRENKARD, E.; AUSUBEL, F. M. *Pseudomonas* biofilm formation and antibiotic resistance are linked to phenotypic variation. **Nature,** v. 416, n. 6882, p. 740-3, 2002.

EISENBERG, D.; WEISS, R. M.; TERWILLIGER, T. C. The hydrophobic moment detects periodicity in protein hydrophobicity. **Proc Natl Acad Sci USA,** v. 81, n. 1, p. 140-4, 1984.

FENSTERSEIFER, I. C. et al. Effects of cyclotides against cutaneous infections caused by *Staphylococcus aureus*. **Peptides,** v. 63, p. 38-42, 2015.

FERNANDES, F. C.; PORTO, W. F.; OCTÁVIO, L. F. A wide antimicrobial peptides search method using fuzzy modeling. In: (Ed.). Lecture Notes in Computer Science. Berlin, Heidelberg: Springer, 2009.

FIORONI, M. et al. Solvation phenomena of a tetrapeptide in water/trifluoroethanol and water/ethanol mixtures: a diffusion NMR, intermolecular NOE, and molecular dynamics study. **J Am Chem Soc,** v. 124, n. 26, p. 7737-44, 2002.

FISHER, R. A.; GOLLAN, B.; HELAINE, S. Persistent bacterial infections and persister cells. **Nat Rev Microbiol,** v. 15, n. 8, p. 453-64, 2017.

FJELL, C. D. et al. Designing antimicrobial peptides: form follows function. **Nat Rev Drug Discov,** v. 11, n. 1, p. 37-51, 2012.

FJELL, C. D. et al. Optimization of antibacterial peptides by genetic algorithms and cheminformatics. **Chem Biol Drug Des,** v. 77, n. 1, p. 48-56, 2011.

GAO, G. et al. The biocompatibility and biofilm resistance of implant coatings based on hydrophilic polymer brushes conjugated with antimicrobial peptides. **Biomaterials,** v. 32, n. 16, p. 3899-909, 2011.

GASPAR, D.; VEIGA, A. S.; CASTANHO, M. A. From antimicrobial to anticancer peptides. A review. **Front Microbiol,** v. 4, p. 294, 2013.

GIEDRAITIENE, A. et al. Antibiotic resistance mechanisms of clinically important bacteria. **Medicina (Kaunas),** v. 47, n. 3, p. 137-46, 2011.

HALE, J. D.; HANCOCK, R. E. Alternative mechanisms of action of cationic antimicrobial peptides on bacteria. **Expert Rev Anti Infect Ther,** v. 5, n. 6, p. 951-9, 2007.

HALL-STOODLEY, L.; COSTERTON, J. W.; STOODLEY, P. Bacterial biofilms: from the natural environment to infectious diseases. **Nat Rev Microbiol,** v. 2, n. 2, p. 95-108, 2004.

HANEY, E. F. et al. Computer-aided discovery of peptides that specifically attack bacterial biofilms. **Sci Rep,** v. 8, n. 1, p. 1871, 2018.

HANEY, E. F. et al. Solution NMR studies of amphibian antimicrobial peptides: linking structure to function? **Biochim Biophys Acta,** v. 1788, n. 8, p. 1639-55, 2009.

HANEY, E. F. et al. High throughput screening methods for assessing antibiofilm and immunomodulatory activities of synthetic peptides. **Peptides,** v. 71, p. 276-85, 2015.

HARRISON, J. J.; TURNER, R. J.; CERI, H. Persister cells, the biofilm matrix and tolerance to metal cations in biofilm and planktonic *Pseudomonas aeruginosa*. **Environ Microbiol,** v. 7, n. 7, p. 981-94, 2005.

HILPERT, K. et al. High-throughput generation of small antibacterial peptides with improved activity. **Nat Biotechnol,** v. 23, n. 8, p. 1008-12, 2005.

HISS, J.; HARTENFELLER, M.; SCHNEIDER, G. Concepts and applications of “natural computing” techniques in de novo drug and peptide design. **Curr Pharm Des,** v. 16, n. 15, p. 1656-65, 2010.

HOLLAND, J.; GOLDBERG, D. Genetic algorithms in search, optimization and machine learning. ed: Addison-Wesley, Reading, MA, 1989.

JACOBY, G. A.; MUNOZ-PRICE, L. S. The new β-lactamases. **N Engl J Med,** v. 352, n. 4, p. 380-91, 2005.

JEE, Y. et al. Antimicrobial resistance: a threat to global health. **Lancet Infect Dis,** v. 18, n. 9, p. 939-40, 2018.

JEFFERSON, K. K.; GOLDMANN, D. A.; PIER, G. B. Use of confocal microscopy to analyze the rate of vancomycin penetration through *Staphylococcus aureus* biofilms. **Antimicrob Agents Chemother,** v. 49, n. 6, p. 2467-73, 2005.

JENSSEN, H. et al. Evaluating different descriptors for model design of antimicrobial peptides with enhanced activity toward *P. aeruginosa*. **Chem Biol Drug Des,** v. 70, n. 2, p. 134-42, 2007.

KATAYAMA, Y.; ITO, T.; HIRAMATSU, K. A new class of genetic element, staphylococcus cassette chromosome mec, encodes methicillin resistance in *Staphylococcus aureus*. **Antimicrob Agents Chemother,** v. 44, n. 6, p. 1549-55, 2000.

KLIGER, Y. Computational approaches to therapeutic peptide discovery. **Peptide Science,** v. 94, n. 6, p. 701-10, 2010.

KOJIMA, S.; NIKAIDO, H. Permeation rates of penicillins indicate that *Escherichia coli* porins function principally as nonspecific channels. **Proc Natl Acad Sci USA,** v. 110, n. 28, p. E2629-34, 2013.

KOSTAKIOTI, M.; HADJIFRANGISKOU, M.; HULTGREN, S. J. Bacterial biofilms: development, dispersal, and therapeutic strategies in the dawn of the postantibiotic era. **Cold Spring Harb Perspect Med,** v. 3, n. 4, p. a010306, 2013.

KOTSIANTIS, S. B.; ZAHARAKIS, I.; PINTELAS, P. Supervised machine learning: A review of classification techniques. **Informatica**, v. 31, p. 249-68, 2007.

KOVACH, K. et al. Evolutionary adaptations of biofilms infecting cystic fibrosis lungs promote mechanical toughness by adjusting polysaccharide production. **NPJ Biofilms Microbiomes,** v. 3, p. 1, 2017.

KUMAR, N. et al. Crystal structure of the transcriptional regulator Rv1219c of *Mycobacterium tuberculosis*. **Protein Sci,** v. 23, n. 4, p. 423-32, 2014.

KYTE, J.; DOOLITTLE, R. F. A simple method for displaying the hydropathic character of a protein. **J Mol Biol,** v. 157, n. 1, p. 105-32, 1982.

LATA, S.; SHARMA, B. K.; RAGHAVA, G. P. Analysis and prediction of antibacterial peptides. **BMC Bioinformatics,** v. 8, p. 263, 2007.

LAVIGNE, J. P. et al. An adaptive response of Enterobacter aerogenes to imipenem: regulation of porin balance in clinical isolates. **Int J Antimicrob Agents,** v. 41, n. 2, p. 130-6, 2013.

LEVY, S. B. Active efflux mechanisms for antimicrobial resistance. **Antimicrob Agents Chemother,** v. 36, n. 4, p. 695-703, 1992.

LEVY, S. B.; MARSHALL, B. Antibacterial resistance worldwide: causes, challenges and responses. **Nat Med,** v. 10, n. 12 Suppl, p. S122-9, 2004.

LI, B.; WEBSTER, T. J. Bacteria antibiotic resistance: New challenges and opportunities for implant-associated orthopedic infections. **J Orthop Res,** v. 36, n. 1, p. 22-32, 2018.

LIM, K. et al. Immobilization studies of an engineered arginine-tryptophan-rich peptide on a silicone surface with antimicrobial and antibiofilm activity. **ACS Appl Mater Interfaces,** v. 5, n. 13, p. 6412-22, 2013.

LIU, L. P.; DEBER, C. M. Uncoupling hydrophobicity and helicity in transmembrane segments. Alpha-helical propensities of the amino acids in non-polar environments. **J Biol Chem,** v. 273, n. 37, p. 23645-8, 1998.

LIU, L. P. et al. Threshold hydrophobicity dictates helical conformations of peptides in membrane environments. **Biopolymers,** v. 39, n. 3, p. 465-70, 1996.

LLARRULL, L. I. et al. The future of the β-lactams. **Curr Opin Microbiol,** v. 13, n. 5, p. 551-7, 2010.

LOMBARDINO, J. G.; LOWE, J. A. The role of the medicinal chemist in drug discovery - then and now. **Nat Rev Drug Discov,** v. 3, n. 10, p. 853-62, 2004.

LOOSE, C. et al. A linguistic model for the rational design of antimicrobial peptides. **Nature,** v. 443, n. 7113, p. 867-9, 2006.

LOPEZ-ABARRATEGUI, C. et al. Cm-p5: an antifungal hydrophilic peptide derived from the coastal mollusk *Cenchritis muricatus* (Gastropoda: Littorinidae). **FASEB J,** v. 29, n. 8, p. 3315-25, 2015.

LYNCH, J. P., 3RD; CLARK, N. M.; ZHANEL, G. G. Evolution of antimicrobial resistance among Enterobacteriaceae (focus on extended spectrum β-lactamases and carbapenemases). **Expert Opin Pharmacother,** v. 14, n. 2, p. 199-210, 2013.

MARCONE, G. L. et al. Old and new glycopeptide antibiotics: From product to gene and back in the post-genomic era. **Biotechnol Adv,** v. 36, n. 2, p. 534-54, 2018.

MARION, D.; ZASLOFF, M.; BAX, A. A two-dimensional NMR study of the antimicrobial peptide magainin 2. **FEBS Lett,** v. 227, n. 1, p. 21-6, 1988.

MARTINEZ-SOLANO, L. et al. Chronic *Pseudomonas aeruginosa* infection in chronic obstructive pulmonary disease. **Clin Infect Dis,** v. 47, n. 12, p. 1526-33, 2008.

MAURICE, N. M.; BEDI, B.; SADIKOT, R. T. *Pseudomonas aeruginosa* biofilms: Host response and clinical implications in lung infections. **Am J Respir Cell Mol Biol,** v. 58, n. 4, p. 428-39, 2018.

MCKENNA, M. Antibiotic resistance: the last resort. **Nature,** v. 499, n. 7459, p. 394-6, 2013.

MEHRNEJAD, F.; NADERI-MANESH, H.; RANJBAR, B. The structural properties of magainin in water, TFE/water, and aqueous urea solutions: molecular dynamics simulations. **Proteins,** v. 67, n. 4, p. 931-40, 2007.

MIGLIOLO, L. et al. Structural and functional evaluation of the palindromic alanine-rich antimicrobial peptide *Pa*-MAP2. **Biochim Biophys Acta,** v. 1858, n. 7, p. 1488-98, 2016.

MIGLIOLO, L. et al. Structural and functional characterization of a multifunctional alanine-rich peptide analogue from *Pleuronectes americanus*. **PLoS One,** v. 7, n. 10, p. e47047, 2012.

MORGENSTERN, B. et al. Multiple sequence alignment with user-defined anchor points. **Algorithms Mol Biol,** v. 1, n. 1, p. 6, 2006.

NAPARSTEK, L. et al. Biofilm formation and susceptibility to gentamicin and colistin of extremely drug-resistant KPC-producing *Klebsiella pneumoniae*. **J Antimicrob Chemother,** v. 69, n. 4, p. 1027-34, 2014.

NASCIMENTO, J. M. et al. Elucidation of mechanisms of interaction of a multifunctional peptide Pa-MAP with lipid membranes. **Biochim Biophys Acta,** v. 1838, n. 11, p. 2899-909, 2014.

NGUYEN, L. T.; HANEY, E. F.; VOGEL, H. J. The expanding scope of antimicrobial peptide structures and their modes of action. **Trends in Biotechnology,** v. 29, n. 9, p. 464-72, 2011.

NICOLAS, P. Multifunctional host defense peptides: intracellular-targeting antimicrobial peptides. **FEBS J,** v. 276, n. 22, p. 6483-96, 2009.

OSBORN, A. M.; BOLTNER, D. When phage, plasmids, and transposons collide: genomic islands, and conjugative- and mobilizable-transposons as a mosaic continuum. **Plasmid,** v. 48, n. 3, p. 202-12, 2002.

OVERHAGE, J. et al. Human host defense peptide LL-37 prevents bacterial biofilm formation. **Infect Immun,** v. 76, n. 9, p. 4176-82, 2008.

PAGANO, L. et al. Carbapenemase-producing *Klebsiella pneumoniae* and hematologic malignancies. **Emerg Infect Dis,** v. 20, n. 7, p. 1235-6, 2014.

PALAVUTITOTAI, N. et al. Epidemiology and risk factors of extensively drug-resistant *Pseudomonas aeruginosa* infections. **PLoS One,** v. 13, n. 2, p. e0193431, 2018.

PELEGRINI, P. B. et al. Antibacterial peptides from plants: what they are and how they probably work. **Biochem Res Int,** v. 2011, p. 250349, 2011.

PERCIVAL, S. L. et al. A review of the scientific evidence for biofilms in wounds. **Wound Repair Regen,** v. 20, n. 5, p. 647-57, 2012.

PERRIN, B. S., JR. et al. High-resolution structures and orientations of antimicrobial peptides piscidin 1 and piscidin 3 in fluid bilayers reveal tilting, kinking, and bilayer immersion. **J Am Chem Soc,** v. 136, n. 9, p. 3491-504, 2014.

PLETZER, D.; COLEMAN, S. R.; HANCOCK, R. E. Anti-biofilm peptides as a new weapon in antimicrobial warfare. **Curr Opin Microbiol,** v. 33, p. 35-40, 2016.

PORTO, W. F. et al. Joker: An algorithm to insert patterns into sequences for designing antimicrobial peptides. **Biochim Biophys Acta Gen Subj,** v. 1862, n. 9, p. 2043-52, 2018.

PORTO, W. F.; FERNANDES, F. C.; FRANCO, O. L. An SVM Model Based on Physicochemical Properties to Predict Antimicrobial Activity from Protein Sequences with Cysteine Knot Motifs. **Adv Bioinformatics Comput Biol,** v. 6268, p. 59-62, 2010.

POULOU, A. et al. Outbreak caused by an ertapenem-resistant, CTX-M-15-producing *Klebsiella pneumoniae* sequence type 101 clone carrying an OmpK36 porin variant. **J Clin Microbiol,** v. 51, n. 10, p. 3176-82, 2013.

RAAGEL, H. et al. Cell-penetrating peptide secures an efficient endosomal escape of an intact cargo upon a brief photo-induction. **Cell Mol Life Sci,** v. 70, n. 24, p. 4825-39, 2013.

RESENDE, J. M. et al. Solution NMR structures of the antimicrobial peptides phylloseptin-1, -2, and -3 and biological activity: the role of charges and hydrogen bonding interactions in stabilizing helix conformations. **Peptides,** v. 29, n. 10, p. 1633-44, 2008.

RIBEIRO, S. M. et al. Understanding, preventing and eradicating *Klebsiella pneumoniae* biofilms. **Future Microbiol,** v. 11, n. 4, p. 527-38, 2016.

RIBEIRO, S. M. et al. Antibiofilm peptides increase the susceptibility of carbapenemase-producing *Klebsiella pneumoniae* clinical isolates to β-lactam antibiotics. **Antimicrob Agents Chemother,** v. 59, n. 7, p. 3906-12, 2015.

ROCCATANO, D. et al. Mechanism by which 2,2,2-trifluoroethanol/water mixtures stabilize secondary-structure formation in peptides: a molecular dynamics study. **Proc Natl Acad Sci USA,** v. 99, n. 19, p. 12179-84, 2002.

ROMLING, U.; BALSALOBRE, C. Biofilm infections, their resilience to therapy and innovative treatment strategies. **J Intern Med,** v. 272, n. 6, p. 541-61, 2012.

RONCEVIC, T. et al. Antibacterial activity affected by the conformational flexibility in glycine-lysine based alpha-helical antimicrobial peptides. **J Med Chem,** v. 61, n. 7, p. 2924-36, 2018.

SANTAJIT, S.; INDRAWATTANA, N. Mechanisms of antimicrobial resistance in ESKAPE pathogens. **Biomed Res Int,** v. 2016, p. 2475067, 2016.

SILVA, O. N. et al. Structural studies of a lipid-binding peptide from tunicate hemocytes with anti-biofilm activity. **Sci Rep,** v. 6, p. 27128, 2016.

SIRTORI, L. R.; MOTTA ADE, S.; BRANDELLI, A. Mode of action of antimicrobial peptide P45 on *Listeria monocytogenes*. **J Basic Microbiol,** v. 48, n. 5, p. 393-400, 2008.

SMITH, P. A. et al. Optimized arylomycins are a new class of Gram-negative antibiotics. **Nature,** v. 561, n. 7722, p. 189-94, 2018.

STREMPEL, N.; STREHMEL, J.; OVERHAGE, J. Potential application of antimicrobial peptides in the treatment of bacterial biofilm infections. **Curr Pharm Des,** v. 21, n. 1, p. 67-84, 2015.

SU, Y.; LI, S.; HONG, M. Cationic membrane peptides: atomic-level insight of structure-activity relationships from solid-state NMR. **Amino Acids,** v. 44, n. 3, p. 821-33, 2013.

TACHI, T. et al. Position-dependent hydrophobicity of the antimicrobial magainin peptide affects the mode of peptide-lipid interactions and selective toxicity. **Biochemistry,** v. 41, n. 34, p. 10723-31, 2002.

TEIXEIRA, L. D. et al. *In vivo* antimicrobial evaluation of an alanine-rich peptide derived from *Pleuronectes americanus*. **Peptides,** v. 42, p. 144-8, 2013.

THOMAS, S. et al. CAMP: a useful resource for research on antimicrobial peptides. **Nucleic Acids Res,** v. 38, p. D774-80, 2010.

TORRES, M. D. T. et al. Structure-function-guided exploration of the antimicrobial peptide polybia-CP identifies activity determinants and generates synthetic therapeutic candidates. **Commun Biol,** v. 1, p. 221, 2018.

TROEIRA HENRIQUES, S. et al. Redesigned spider peptide with improved antimicrobial and anticancer properties. **ACS Chem Biol,** v. 12, n. 9, p. 2324-34, 2017.

VAN ACKER, H.; VAN DIJCK, P.; COENYE, T. Molecular mechanisms of antimicrobial tolerance and resistance in bacterial and fungal biofilms. **Trends Microbiol,** v. 22, n. 6, p. 326-33, 2014.

VENTOLA, C. L. The antibiotic resistance crisis: part 1: causes and threats. **Pharmacol Therapeut,** v. 40, n. 4, p. 277-83, 2015.

WAGHU, F. H. et al. CAMPR3: a database on sequences, structures and signatures of antimicrobial peptides. **Nucleic Acids Res,** v. 44, n. D1, p. D1094-7, 2016.

WANG, G.; LI, X.; WANG, Z. APD2: the updated antimicrobial peptide database and its application in peptide design. **Nucleic Acids Res,** v. 37, p. D933-7, 2009.

WELLINGTON, E. M. et al. The role of the natural environment in the emergence of antibiotic resistance in gram-negative bacteria. **Lancet Infect Dis,** v. 13, n. 2, p. 155-65, 2013.

WESSMAN, M. et al. Mucosal biofilm detection in chronic otitis media: a study of middle ear biopsies from Greenlandic patients. **Eur Arch Otorhinolaryngol,** v. 272, n. 5, p. 1079-85, 2015.

WHITE, S. H.; WIMLEY, W. C. Membrane protein folding and stability: physical principles. **Annu Rev Biophys Biomol Struct,** v. 28, p. 319-65, 1999.

WHITESIDE, S. A. et al. *Enterococcus faecalis* persistence in pediatric patients treated with antibiotic prophylaxis for recurrent urinary tract infections. **Future Microbiol,** v. 13, p. 1095-1115, 2018.

WHO. Global priority list of antibiotic-resistant bacteria to guide research, discovery, and development of new antibiotics. **World Health Organization**. 2017.

WU, X. et al. PSN-PC: A novel antimicrobial and anti-biofilm peptide from the skin secretion of *Phyllomedusa camba* with cytotoxicity on human lung cancer cell. **Molecules,** v. 22, n. 11, 2017.

YANDEK, L. E. et al. Mechanism of the cell-penetrating peptide transportan 10 permeation of lipid bilayers. **Biophys J,** v. 92, n. 7, p. 2434-44, 2007.

YOUNT, N. Y.; YEAMAN, M. R. Multidimensional signatures in antimicrobial peptides. **Proc Natl Acad Sci USA,** v. 101, n. 19, p. 7363-8, 2004.